1-1-2008

Palaeoproterozoic and Archaean gneiss complexes in northern Greenland: Palaeoproterozoic terrane assembly in the High Arctic

Allen Phillip Nutman
University of Wollongong, anutman@uow.edu.au

Peter Dawes

Feiko Kalsbeek

Mike Hamilton

Palaeoproterozoic and Archaean gneiss complexes in northern Greenland: Palaeoproterozoic terrane assembly in the High Arctic

Abstract

The Precambrian shield of northern Greenland has been investigated by SHRIMP U-Pb zircon dating of 14 orthogneisses and granitoids plus 5 metasediments, integrated with mapping by the Geological Survey of Denmark and Greenland and whole-rock Nd isotopic studies. The Inglefield Mobile Belt is a tract of Palaeoproterozoic sedimentation, plutonism, polyphase deformation and high-grade metamorphism that underlies Inglefield Land and northern Prudhoe Land. In the southern part of the belt at 78 degrees 30'N, the E-W-trending Sunrise Pynt Straight Belt is a high-grade, but structurally late, shear zone with contrasts in the geology on either side. South of the Sunrise Pynt Straight Belt, ca. 1980 Ma diorites and tonalites were emplaced into older orthogneisses and metasediments. Detrital zircons from two metaquartzites (deposited on Archaean basement?) yielded complex age spectra from ca. 3250 Ma to 2350 Ma, with 2600-2450 Ma grains dominant. In associated mica schist, low Th/U, 1923 +/- 8 Ma zircons date high-grade metamorphism. The most southern orthogneiss investigated (77 degrees 45'N) is Neoarchaean (ca. 2600 Ma), in agreement with previously published isotopic data. North of the Sunrise Pynt Straight Belt to 79 degrees 10'N an amphibolite-granulite-facies complex with extensive pelitic to psammitic paragneisses are the oldest rocks recognised. Two psammitic paragneisses yielded unrounded zircons with a unimodal detrital age population centred on 2000-1980 Ma. Their source could be ca. 1980Ma orthogneisses from south of the Sunrise Pynt Straight Belt, or from basement inliers in the North-East Greenland Caledonian fold belt. The metasediments were intruded by tonalites and diorites with dates of 1949 +/- 13 Ma and 1943 +/- 11 Ma, and then by granitoids (free of zircon inherited from older rocks) with ages of 1924 +/- 29 Ma to 1915 +/- 19 Ma. The metasediments show development of low Th/U zircon overgrowths at ca. 1920 Ma, coeval with the granitoids. Finally, other granites, some locally transformed into gneisses, have ages of 1783 +/- 22 Ma to 1741 +/- 15 Ma. Inherited zircons in the latter are up to 2650 Ma old. A granite dyke with a zircon age of 1783 Ma has an T(DM) age of 2981 Ma and a strongly negative epsilon(Nd) at 1.78 Ga, indicating derivation by melting or reworking of Archaean crust. Thus, by 1800 Ma this juvenile Palaeoproterozoic, terrane had probably over-ridden crust with Archaean components. North of Inglefield Land, Precambrian crystalline rocks are obscured until Victoria Fjord (81 degrees 30'N). One reconnaissance orthogneiss sample from there contains ca. 3400 Ma oscillatory-zoned zircons, which probably date the rock, rather than being a xenocrystic component in a younger rock. Thus, from north to south there is an assemblage of Archaean, Palaeoproterozoic and Archaean to early Palaeoproterozoic gneiss terranes. The Inglefield Mobile Belt is dominated by juvenile Palaeoproterozoic arc crust trapped between two unrelated blocks of Archaean crust of contrasting age. The collision, and probably thrusting of a Palaeoproterozoic arc over a southern Archaean foreland, occurred at ca. 1920Ma-dated by metamorphic zircon. The new isotopic results consolidate the regional mapping of Archaean and Palaeoproterozoic complexes across northern Baffin Bay that show continuity from Canada into Greenland, without displacement across the Nares Strait.

Keywords

northern, complexes, gneiss, archaean, palaeoproterozoic, greenland, terrane, assembly, arctic, high, GeoQUEST

Disciplines

Life Sciences | Physical Sciences and Mathematics | Social and Behavioral Sciences

Publication Details

Nutman, A. Phillip., Dawes, P., Kalsbeek, F. & Hamilton, M. (2008). Palaeoproterozoic and Archaean gneiss

Palaeoproterozoic and Archaean gneiss complexes in northern Greenland: a terrane constellation for the High Arctic

Allen P. Nutman[a,b*], Peter R. Dawes[c], Feiko Kalsbeek[c], Mike A. Hamilton[d]

[a] Institute of Geology, Chinese Academy of Geological Sciences, 26 Baiwanzhuang Road, Beijing 100037, China
[b] Research School of Earth Sciences, Australian National University, Canberra, A.C.T. 0200, Australia
[c] Geological Survey of Denmark and Greenland, Geocenter Copenhagen, Øster Voldgade 10, 1350 Copenhagen K, Denmark
[d] Department of Geology, Earth Sciences Centre, University of Toronto, 22 Russell Street, Toronto, Ontario M5S 3B1, Canada

*corresponding author: A. Nutman - email: Nutman@bjshrimp.cn

Abstract (=481 words)
The Precambrian shield of northern Greenland has been investigated by SHRIMP U–Pb zircon dating of fourteen orthogneisses and granitoids plus five metasediments, integrated with geological mapping by the Geological Survey of Denmark and Greenland and whole-rock Nd isotopic studies. The Inglefield Mobile Belt is a tract of Palaeoproterozoic sedimentation, plutonism, polyphase deformation and high-grade metamorphism that underlies Inglefield Land. In the southern part of the belt at 78°30°N, the E–W-trending *Sunrise Pynt Straight Belt* is a high-grade, but structurally late, shear zone with contrasts in the geology on either side.

In southern Inglefield Land and northern Prudhoe Land, south of the Sunrise Pynt Straight Belt, ca. 1980 Ma diorites and tonalites were emplaced into older orthogneisses and metasediments. Detrital zircons from two metaquartzites (deposited on Archaean basement?) yielded complex age spectra from ca. 3250 to 2350 Ma, with 2600–2450 Ma grains dominant. In associated mica schist, low Th/U, 1923±8 Ma zircons date high-grade metamorphism. The most southern orthogneiss investigated (77°45°N) is Neoarchaean (ca. 2600 Ma), in agreement with previously published isotopic data.

North of the Sunrise Pynt Straight Belt to 79°10°N, Inglefield Land is composed of an amphibolite–granulite-facies complex, where extensive pelitic to psammitic paragneisses are the oldest rocks recognised. Two psammitic paragneisses yielded unrounded zircons with a unimodal detrital age population centred on 2000–1980 Ma. Their source could be ca. 1980 Ma orthogneisses from south of Sunrise Pynt Straight Belt, or from basement inliers in the North-East Greenland Caledonian fold belt. The metasediments were intruded by tonalites and diorites with dates of 1949±13 Ma and 1943±11 Ma, and then by granitoids (free of zircon inherited from older rocks) with ages of 1924±29 Ma to 1915±19 Ma. The metasediments show development of low Th/U zircon overgrowths at ca. 1920 Ma, coeval with the granitoids. Finally, other granites, some locally transformed into gneisses, have ages of 1783±22 Ma to 1741±15 Ma. Inherited zircons in the latter are up to 2650 Ma old. A granite dyke with a zircon age of 1783 Ma has an T_{DM} age of 2981 Ma and a strongly negative ε_{Nd} at 1.78 Ga, indicating derivation by melting or reworking of Archaean crust. Thus by 1800 Ma this juvenile Palaeoproterozoic terrane might have overridden crust with Archaean components.

North of Inglefield Land, Precambrian crystalline rocks are obscured until Victoria Fjord (81°30′N) is reached. One reconnaissance orthogneiss sample from there contains ca. 3400 Ma oscillatory-zoned zircons, which probably dates the rock, rather than being a xenocrystic component in a Neoarchaean rock.

Thus, from north to south there is a constellation of Archaean, Palaeoproterozoic and then Neoarchaean – earliest Palaeoproterozoic gneiss terranes. The Inglefield Mobile Belt is dominated by juvenile Palaeoproterozoic arc crust trapped between two unrelated blocks of Archaean crust of contrasting age. The collision, and probably thrusting of a Palaeoproterozoic arc over a southern Archaean foreland, occurred at ca. 1920 Ma – dated by metamorphic zircon.

Keywords: SHRIMP U–Pb zircon dating, Sm–Nd model ages, Inglefield Mobile Belt, early Precambrian terranes, Northern Greenland, Metasediments, Plutonic rocks, Magmatic arc

1. Introduction

Archaean and Palaeoproterozoic rocks of the Precambrian shield form about 60% of the exposed bedrock of Greenland, with the northernmost exposures at 81º30′N (Henriksen et al., 2000). Much less geochronological data exist from northern Greenland than further south, where numerous conventional and SHRIMP U–Pb age determinations have been published. These come from both Archaean domains (e.g. Nutman et al., 1996; Friend and Nutman, 1994, 2001; Friend et al., 1996; Rosing et al., 2001; Crowley, 2002, 2003; Crowley et al., 2002) and Proterozoic mobile belts, viz. the Nagssugtoqidian (e.g. Kalsbeek and Nutman, 1996; Whitehouse et al., 1998; Nutman et al., 1999; Connelly and Mengel, 2000; Connelly et al., 2000) and the Ketilidian (e.g. Hamilton et al., 1999; Garde et al., 2002) (inset, Fig. 1). However, progress has been made in recent years to unravel the tectono-magmatic history of Greenland's northern shield exposures through isotope geology. Kalsbeek et al. (1993, 1999) and Nutman and Kalsbeek (1994) reported on the geochronology of the Precambrian crystalline rocks of North-East Greenland, that form reworked basement inliers within the Caledonian mobile belt (inset, Fig. 1). Even less isotopic age information has been available from North-West Greenland, a region that was not affected by Phanerozoic orogenesis. The last geochronological papers from that region and neighbouring Canada across Baffin Bay are those of Dawes et al. (1988), Frisch and Hunt (1988) and Jackson et al. (1990).

The purpose of this paper is to report on the geochronology of the Precambrian shield in North-West Greenland, including the northernmost exposures at 81°30′N, by presenting the results of a comprehensive SHRIMP U–Pb zircon dating together with new Sm-Nd whole-rock isotopic analyses, combined with earlier Sm-Nd whole-rock and U–Pb zircon IDTIMS isotopic data. This information is integrated with recently compiled mapping of the region between 75° and 81°N by the Geological Survey of Denmark and Greenland (Dawes, 2004, 2006). The results allow further insight into Palaeoproterozoic collisional orogenesis in the region, with further evidence that there is a block of juvenile Palaeoproterozoic crust – in the Inglefield Mobile belt - sandwiched between two blocks/terranes with Archaean crust.

2. Geological setting of North-West Greenland

North-West Greenland is the region between 75° and 79°N bordered on the east by the Inland Ice and seawards by the Kane Basin, Smith Sound and northern Baffin Bay (Fig. 1). The main focus of the paper is Inglefield Land and northern Prudhoe Land (ca. 77°45′–79°N), from where 18 out of the 19 SHRIMP zircon dating samples and 14 Nd isotope samples of the present study were derived (Fig. 2). The other SHRIMP sample is from a window into the shield at Victoria Fjord, which is 400 km to the northeast, a locality isolated from Inglefield Land by the Inland Ice and extensive Palaeozoic rocks (Fig. 1). Previously determined isotopic ages – four Sm–Nd and two IDTIMS bulk zircon U–Pb ages, as well as three Rb–Sr errorchron suites – are scattered throughout the region (see Figs. 1 and 2).

Inglefield Land and northern Prudhoe Land are dominated by the Palaeoproterozoic *Inglefield Mobile Belt* (IMB), - a region which has been investigated by geological, geochemical and geophysical mapping (Schjøth et al., 1996; Steenfelt and Dam, 1996; Thomassen and Dawes, 1996; Dawes et al., 2000; Thomassen et al., 2002). In a broader context, the IMB is the eastern part of the 'Ellesmere Island –Inglefield Land Belt' of Dawes (1988) which in turn is likely an extension of the

'Thelon Tectonic Zone' which borders the northern flank of the Archaean Rae Province of northern Canada (Hoffman, 1988).The Victoria Fjord basement exposures were last visited in the mid-1980s and on the basis of strongly discordant bulk zircon dates on two samples were interpreted to be Archaean (Hansen et al., 1987). The region to the south of the IMB is mainly reworked Archaean, with subordinate Palaeoproterozoic supracrustal sequences (Dawes and Frisch, 1981; Nutman, 1984; Thomassen et al., 2002; Dawes, 2006). These Archaean rocks were variably reworked in the Palaeoproterozoic, and forms much of North-West Greenland. The counterpart of this in Canada is the Committee Orogen, the nearest outcrops of which are on Devon Island (Fig. 1; Frisch, 1988; Jackson, 2000; Harrison et al., 2006). The Sunrise Pynt Straight Belt is an approximately E-W trending, structurally late, but still high metamorphic grade ductile shear zone at approximately 78°30'N, which marks the boundary between the terrane to the south containing Archaean rocks and one to the north of entirely Palaeoproterozoic rocks (Figs. 1and 2). An emphasis in this paper is the meaning of the geological contrast on either side of the straight belt.

In northern Greenland and adjacent Canada, the crystalline basement is overlain by homoclinal sequences of the Thule (Proterozoic) and Franklinian (Palaeozoic) Basins of the Arctic Platform (Trettin, 1991). In our study region these sequences are prominent along the coasts, hampering in many cases the regional correlation of units in the basement (Fig. 2). In Prudhoe Land, the cover sequences are preserved in down-faulted coastal blocks, so that apart from steep coastal exposures in Sonntag Bugt and at the heads of some fjords, rocks of the shield form nunataks and semi-nunataks. This stands in stark contrast to the topography of Inglefield Land, where a well-developed Mesoproterozoic (Calymmian) peneplain corresponds to the present-day low-altitude land surface (see Dawes, 1997, fig. 5). This gently undulating plateau is covered by abundant Quaternary deposits, which means that by Greenland standards, the basement rocks of Inglefield Land is very poorly exposed. In many inland areas, geological mapping relies on isolated exposures surrounded by extensive drift (Dawes & Garde, 2004). In these situations, aeromagnetic coverage is particularly useful in the distinction of metasedimentary rocks and derived paragneisses from plutonic rocks and orthogneisses. In coastal sections, particularly in the southwest, excellent exposures reveal important geological relationships between regional lithologies (Fig. 3).

3. Previous work

A comprehensive review of geological exploration in the Kane Basin – Smith Sound region can be found in Dawes (1999). More recent work is covered in the descriptive text to the Humboldt Gletscher map sheet (78°–81°N; Dawes, 2004). For the southern part of the region (75°–78°N), a summary of previous work is found in Dawes (2006).

3.1. Geology and geophysics

3.1.1. Inglefield Land and Prudhoe Land

Reconnaissance work in the 1970s by the Geological Survey of Greenland established the main geological provinces of the study region: in Prudhoe Land, a orthogneiss complex (basement?) structurally overlain by supracrustal rocks (Fig. 3a), and in western Inglefield Land, highly-deformed belts of supracrustal rocks characterised by marble (Etah Group) are intruded by the Etah meta-igneous complex. A third group of variable gneisses was defined as derived from these two complexes (Dawes, 1972, 1976, 1979). In the 1980s when isotopic data for samples became available from eastern Inglefield Land, the entire shield from 78°N to 79°10′N where it disappears under the ice of Humboldt Gletscher was interpreted to be Palaeoproterozoic in age (Dawes, 1988).

Following commercial assessment in the early 1990s (e.g. Sharp, 1991), an electromagnetic and magnetic survey was flown in 1994 over all but the southwestern part of Inglefield Land (Fig. 4; Stemp and Thorning, 1995). In 1995 and 1999 the region was covered by 1:500 000 geological and geochemical mapping (Schjøth et al., 1996; Steenfelt & Dam, 1996; Thomassen & Dawes, 1996; Schjøth and Thorning, 1998; Dawes et al., 2000), with additional field work in Prudhoe Land in 2001 (Steenfelt et al., 2002; Thomassen et al., 2002).

3.1.2. Victoria Fjord

In the late 1950s, nunataks on the northern fringe of the Inland Ice at the head Victoria Fjord (Fig. 3b) were noted from aerial photographs as 'anomalous' in appearance compared with neighbouring nunataks and were interpreted on early maps as the basement to the extensive Arctic Platform sequence (Haller, 1961; GGU, 1970). This remote area was subsequently found to consist of high-grade granitic gneisses and amphibolites (Dawes, 1976, 1978; Hurst and Peel, 1979). In the mid-1980s it was mapped systematically and reconnaissance radiometric-dating was undertaken (Henriksen and Jepsen, 1985; Hansen et al., 1987).

3.2. Geochronology

3.2.1. Inglefield Land and Prudhoe Land

Early studies using K–Ar and Rb–Sr whole-rock dating on random samples provided the first estimates of the ages of events in North-West Greenland (Larsen and Dawes, 1974; Kalsbeek and Dawes, 1980). These studies showed that Inglefield Land and Prudhoe Land had undergone strong 'Hudsonian' reactivation accompanying high-grade metamorphism around 1950 Ma, with closure ages down to about 1650 Ma. Subsequent, targeted Rb–Sr whole-rock age determinations on three complexes between 75° and 78°N – including the Etah meta-igneous complex of this study (Fig. 2) provided a first-order distinction between Proterozoic versus Archaean terranes (Dawes et al., 1988). The "isochrons" from all sample suites showed appreciable scatter, that was interpreted to indicate strong disturbance of the Rb–Sr systems in these rocks. However, within these limitations the Etah meta-igneous complex was determined to be Palaeoproterozoic (Dawes et al., 1988). The two other suites dated from the Melville Bugt area (76°N) at Kap York and Kivioq Havn are both Archaean, yielding Rb–Sr errorchron ages of *ca.* 2700 Ma (Fig. 1).

Whole-rock Nd model ages (T_{DM}; DePaolo, 1981) for four rocks from North-West Greenland were obtained in the 1980s, with the isotopic data suggesting the presence of both Neoarchaean and Palaeoproterozoic crust (P.N. Taylor, personal communication 1990). Two of these model ages are from our study region (Fig. 2). Conventional, early IDTIMS (isotope dilution – thermal ionisation mass spectrometry) bulk U–Pb zircon ages were also determined from three localities in Melville Bugt, and confirmed the Neoarchaean age of the southern gneiss terrane; these are included on Fig. 1 (R.T. Pidgeon, personal communication 1983, 1984; Kalsbeek, 1986).

3.2.2. Victoria Fjord

Conventional ID-TIMS U–Pb multigrain zircon analyses (2 samples), Rb–Sr whole-rock isotopic measurements, as well as K–Ar analyses on hornblende, were carried out on rocks from the Victoria Fjord inlier (Hansen et al., 1987). The zircon samples contained considerable common Pb and yielded discordant results, but nonetheless indicated that the examined rocks are Archaean.

Amphibole K–Ar analyses gave ages of ca. 1850 Ma interpreted to reflect closure to Ar diffusion after a Palaeoproterozoic thermal event (Hansen et al., 1987).

4. Regional geology and sampled lithologies

4.1. Inglefield Land and Prudhoe Land

The study region can be divided into six main map units (Dawes, 1991; Dawes and Garde, 2004), which are listed here broadly from south to north (Fig. 2). In Prudhoe Land: (1) Thule mixed-gneiss complex, (2) Prudhoe Land supracrustal complex and (3) Prudhoe Land granulite complex; then in Inglefield Land: (4) Etah Group, (5) Etah meta-igneous complex and (6) Late granitoids. See Dawes (2004, 2006) for description of units 4–6 and 1–3, respectively.

4.1.1. Thule mixed-gneiss complex: Neoarchaean (SHRIMP U-Pb zircon samples: 243495, 470214)

This unit is composed of tightly folded, packages of high-grade paragneiss and orthogneiss (see Dawes, 2006, figs. 2 and 10). Orthogneisses are clearly multiphase, with both gneissified mafic and felsic intrusions. Main orthogneiss types carry biotite ± hornblende ± orthopyroxene and they vary from homogeneous to veined and banded, with some augen varieties. Paragneiss generally carries garnet. The rocks have passed through both Archaean and Palaeoproterozoic tectonothermal events. The two samples of orthogneiss dated are both granulite-facies rocks: 243495 (Morris Jesup Gletscher) is a melanocratic variety, crudely banded and 470214 (Bowdoin Gletscher) is a more homogeneous rock characterised by a strong hornblende foliation. The former rock was collected as a possible ‘basement gneiss’ to the supracrustal rocks described in section 4.1.2 (that at the sample site structurally overlie the orthogneiss). The eastern sample (470214) is from a nunatak in the area designated as the boundary zone between Archaean and Palaeoproterozoic crustal provinces (Dawes, 1991; Fig. 2).

4.1.2. Prudhoe Land supracrustal complex: Palaeoproterozoic (SHRIMP U-Pb zircon samples 243506, 243510, 425507)

These supracrustal rocks generally form light brown- to rusty-weathering sequences interleaved with orthogneiss of the units described in sections 4.1.1 and 4.1.3. The most extensive occurrence is north of Morris Jesup Gletscher (the Morris Jesup Gletscher supracrustals of Dawes, 1979). Here, the supracrustal rocks are several hundred metres thick and probably lie in the core of a major recumbent isocline. They are thinly layered, garnetiferous mica schists (some of which carry sillimanite), granitic garnet paragneiss, siliceous schists, pale homogenous quartzites (Fig. 3c), thin marble units and occasional pyribolite and ultramafic layers (see Dawes, 2006, fig. 29). Samples 243506 and 243510 are from this locality; the former is from an intensely folded quartzite layer; the latter is a garnet-mica-sillimanite schist. The third supracrustal sample 425507, an isoclinally folded quartzite, is from southern Inglefield Land south of the Sunrise Pynt Straight Belt (assigned previously to the Etah Group by Dawes & Garde, 2004; Fig. 2). As pointed out by Dawes et al. (2000), this locality and others in the immediate area, are noteworthy because pure quartzites have not been located further north in Inglefield Land (see description of the Etah Group below). This field observation is particularly significant in light of the detrital zircon SHRIMP data presented in this paper.

4.1.3. Prudhoe Land granulite complex: Palaeoproterozoic (SHRIMP U-Pb zircon samples 140944, 243459)

This complex is characterised by brown to greenish-grey homogeneous hypersthene orthogneisses, frequently with blue quartz. The unit also contains less homogeneous gneiss packages that are paler in colour, veined and migmatitic, as well as pyribolite units. The dated samples come from Sonntag Bugt. Both samples are foliated, with 243459 being the more gneissic. This comes from the upper limb of a spectacular recumbent fold with a paragneiss core (see Dawes 2004, Fig. 7) and was collected on the plateau surface at ca. 750 m above Bamse Gletscher. Sample 140944 comes from sea level west of Bu Gletscher where it is associated with isoclinally folded, pale quartzite preserved as thin layers and inclusions in the gneiss. Although no clear cross-cutting relationships have been encountered due to strong deformation, finding apparent rafts of sediment within gneiss is permissive that the protoliths of the orthogneiss were intruded into the supracrustal rocks.

4.1.4. Etah Group: Palaeoproterozoic supracrustal rocks (SHRIMP U-Pb zircon samples 440314, 440321; Sm–Nd samples 425727, 425748)

The Etah Group of supracrustal rocks has been described by Dawes (1976, 1988, 2004), Schjøth et al. (1996) and Dawes et al. (2000). The Group forms a sedimentary pile that initially must have been many kilometres thick. It represents the oldest rocks known in Inglefield Land. The supracrustal rocks appear generally as lows on the aeromagnetic map shown in Fig. 4, apart from minor units where magnetite is present, particularly in mafic rocks. Intrusive sheets of meta-igneous rocks are commonly present.

The Group comprises granulite-grade metasediments, with minor units of mafic and ultramafic rocks that are assumed to be an integral part of the supracrustal package. The diagnostic lithological association of the Group is (i) pelitic, semi-pelitic and quartzo-feldspathic paragneisses with garnet + sillimanite ± cordierite (see Dawes, 2004, fig. 8), (ii) marble and calc-silicate rocks and (iii) only rare quartzites. There is a gradation to migmatitic varieties with several generations of anatectic melt components. Most lithologies have a distinct foliation and show variable banding but more homogeneous to massive rocks occur. Thus large areas of pale, leucocratic rocks, particularly in central and eastern Inglefield Land can easily be mistaken for granitoids instead of supracrustal rocks. These represent the grey gneisses of Koch (1933) and the garnet granulites of Sharp (1991). The two samples U-Pb dated by SHRIMP are typical quartzo-feldspathic, garnet-bearing paragneisses.

4.1.5. Etah meta-igneous complex: Palaeoproterozoic (SHRIMP U-Pb zircon samples 425522, 425542, 425562, 425571, 425623; Sm–Nd samples 425536, 425542, 425571, 425574, 425579, 425594, 425623)

The Etah meta-igneous complex is a high-grade, gneissose, polyphase plutonic complex dominated by dioritic to granodioritic rocks with minor gabbro that intrudes the Etah Group. On the aeromagnetic map, its main components appear generally as highs – of which a large syenite–granite body (the Minturn intrusive complex) in south-central Inglefield Land is particularly conspicuous. Gradations from homogeneous rocks to foliated and strongly deformed layered gneiss are commonplace and seen in outcrop-scale, and pervasive foliation and gneissic fabrics are typically developed along the margins of intrusions. Intrusive relationships between different phases and inclusions of supracrustal rocks within them can still be recognised locally.

The samples used for SHRIMP U-Pb zircon dating vary from a homogeneous orthogneiss (452522) to rocks that appear on outcrop scale little or non-deformed, although one of the latter (425571), a coarse-grained syenite from the horseshoe-shaped Wulff structure, has certainly passed through at least two periods of tight folding (Dawes, 1976, fig. 230; 1988, fig. 6). Sample 425542, a hypersthene quartz diorite from the Hiawatha pluton and represents a widespread and characteristic lithology in Inglefield Land first described by Bugge (1910). Sample 425562 is a monzogranite from the major pluton bordering the Inland Ice, and sample 425623 is a pale, apparently undeformed, radioactive granite.

4.1.6. Late granitic rocks: late Palaeoproterozoic (SHRIMP U-Pb zircon samples 425583, 425627, 425793, 425794; Sm–Nd samples 425530, 425552, 425558, 425583, 425738)*

Included here are a number of bodies of mostly granite that can be distinguished from the main lithologies of the Etah meta-igneous complex because they cut foliation and gneissic fabrics developed in those rocks. Three broad groups are recognised. Groups (1) and (2) are present throughout the mobile belt and locally may show foliation whereas the dykes of (3), only recorded in northeastern Inglefield Land east of 68°N, are undeformed.

(1) Granites of several generations – predominantly pink to red but locally grey – form bodies of varying size from outcrop-scale veins and sheets to units large enough to be mapped at a scale of 1:100,000. Transitions from paragneiss with few leucosome segregations, to veined gneiss with abundant pink granite components, to homogeneous granite carrying garnet are common in some areas, and indicates that they were derived at least partly from melting of the paragneisses. Sample 425627 is a weakly foliated grey, albite-rich granitoid that cuts paragneiss with red migmatitic veins.

(2) Pale grey to white leucocratic masses and sheets that generally are undeformed and non-foliated but locally may show a gneissic fabric. Later cross-cutting pegmatitic varieties occur and these are more conspicuous in north-eastern Inglefield Land. Sample 425583, collected as a grey gneissic rock within the Minturn Elv intrusive complex, is a deformed late granite. Sample 425794 is from an undeformed sheet cutting quartzo-feldspathic paragneiss.

(3) The youngest granitoid rocks are cross-cutting aplitic dykes up to 10 m thick that cut all other lithologies. They are mainly fine- to medium-grained, some with subordinate pegmatitic varieties, and they are conspicuous in the terrain because of their salmon to brick red colour. The dykes are anomalously radioactive, a reflection of high thorium content, for example with 130 ppm (Steenfelt and Dam, 1996, Table 6, sample 425624). Sample 425793 represents a fine-grained biotite-bearing granitic dyke that cuts the leucocratic mass represented by sample 425794.

4.1.7 Tectono-thermal history

The tectono-thermal history of the IMB is complex, with the Palaeoproterozoic rocks having been repeatedly deformed under high-grade metamorphic conditions with several episodes of anatectic melting (Dawes et al., 2000; Dawes, 2004). The presence of sillimanite and cordierite in metasediments, as well as widespread hypersthene, indicates low- to medium-pressure granulite facies conditions. Retrogression is seen in the form of local reddening of the rocks, and is in places associated with shear zones.

The majority of the rocks have pronounced foliation or gneissic layering. These have been deformed at least twice around structures, some of which form map-scale fold interference patterns, such as the horseshoe-shaped Wulff structure in north-eastern Inglefield Land, that involves rocks of the Etah meta-igneous complex (Dawes, 1988, fig. 6; Fig. 2). This structure is visible on the aeromagnetic map (Fig. 4). Although three fold generations can be documented in outcrop-scale, it is very probable that more phases are present. At least two major episodes of isoclinal folding affected the Etah Group, with at least one of these post-dating the Etah meta-igneous complex (Dawes, 1988).

A conspicuous feature of the Inglefield Land geological and geophysical maps is the E–W-trending Sunrise Point Straight Belt composed of steeply dipping to vertical rocks stretching from the coast at Sunrise Pynt to the Inland Ice margin (Figs. 2 and 3). Within it, rocks of the Etah Group and Etah meta-igneous complex are intricately interleaved and intensely deformed in tight, upright to slightly overturned folds with westerly plunging lineations (Fig. 3d). Thus late in the deformational history, all pre-existing structures were transposed into the common steeply-dipping linear trend.

4.2. Victoria Fjord (SHRIMP U/Pb zircon sample 312632)

Amphibolite-facies gneisses occur over about 250 km^2 in southeastern Wulff Land (Figs. 1, 3a). They crop out in lower reaches of valleys and on six nunataks at the head of Victoria Fjord (Henriksen, 1989; Fig. 1). Although not all outcrops have been studied and the available samples come from only a few localities, there appear to be no major lithological differences across the inlier. Henriksen & Jepsen (1985) describe the crystalline complex to be dominated by pale weathering, homogeneous leucocratic orthogneisses, with variations both to foliated granites and, with increased leucosome fractions, into migmatitic rocks. This granitoid suite is cut by pegmatites, both as subconcordant veins and sharply cross-cutting bodies. A pale, late-kinematic quartz diorite body has sharply discordant as well as gradational contacts to the orthogneisses. The dated sample, 312632, is a homogenous granitic gneiss intruded by the quartz diorite. Thin supracrustal packages of dominantly metasedimentary origin are concordantly interleaved with the gneisses; it is unknown whether the orthogneisses or the metasediments are the oldest rocks. The metasedimentary units consist of mica schists, marble, siliceous schists, quartzites and amphibolite, and commonly carry garnet. Sharp-bordered, amphibolite sheets are common and these can reach 30 m thick. These are locally discordant to the foliation in their country rocks and represent deformed and metamorphosed mafic dykes.

5. SHRIMP zircon geochronology

5.1. Data acquisition and interpretation

Nineteen zircon samples were dated using the SHRIMP 1 and SHRIMP RG instruments of the Research School of Earth Sciences, Australian National University (Table 1). The $^{238}U/^{206}Pb$ ratio in the unknowns was referenced to the standard AS3 with an age of 1099 Ma (Paces and Miller, 1993). U was calibrated against fragments of the standard crystal SL13, with 238 ppm U. Analytical protocols, calibration of data and calculation of analytical errors are summarised by Stern (1998) and Williams (1998). Data assessment via Terra-Wasserburg $^{238}U/^{206}Pb$ versus $^{207}Pb/^{206}Pb$ concordia plots, cumulative probability plus histogram figures for detrital provenance and weighted mean ages (reported in the text with 95% confidence limits) were facilitated via the Program ISOPLOT/EX (Ludwig, 1997). Chemical analyses and molecular norms of all SHRIMP dated plutonic rocks are given in Table 2.

5.2. Orthogneisses south of the Sunrise Pynt Straight Belt

Four orthogneisses from south of the Sunrise Pynt Straight Belt were examined. Two samples (243495 and 470214) come from the Thule mixed-gneiss complex in the south of the study area and two are from the Prudhoe Land granulite complex at Sonntag Bugt (140944 and 243459) in Prudhoe Land (Fig. 2).

Orthogneiss 243495 is from the northern side of Morris Jesup Gletscher (Fig. 2). The rock is a brownish-weathering, grey gneiss with cm-thick darker pyribolite bands that have transitional contacts to the mesocratic ‘host’ but that may well represent a separate intrusive phase (Table 2). The sample yielded somewhat rounded prismatic zircons 200–400 µm long. In CL images most grains are dominated by variably recrystallised oscillatory-zoned zircon (Fig. 5). This is mantled by shells of, and traversed by, thin recrystallisation veins of homogeneous bright zircon. Analyses concentrated on the best-preserved domains of oscillatory-zoned zircon. Only one site (2.1 with a $^{207}Pb/^{206}Pb$ date of 2506 ± 46 Ma 2σ) yielded an Archaean age. This site appears to be the best candidate from the selected grains for an (older) rounded core of possible inherited origin. The remaining sites on oscillatory-zoned zircon yielded early Palaeoproterozoic ages. These seem to consist of more than one age, possibly ca. 2400 and 2250 Ma. The complicated zircon geochronology has only been touched upon in this study. One interpretation is that this sample contains more than one Neoarchaean to early Palaeoproterozoic igneous components. This would be in keeping with the polyphase-banded nature of the rock. Another interpretation, based on the few data, is that the rock has a single age of ca. 2500 Ma, with data spread along a discordia to ca. 1900 Ma due to variable loss of radiogenic Pb.

Orthogneiss 470214 of dioritic composition is from a nunatak to the north of Bowdoin Gletscher (Fig. 2). It is a reddish weathering, rather homogeneous, greenish grey gneiss with a pronounced hypersthene foliation. The sample yielded somewhat rounded 200–300 µm long prismatic zircons. In CL images these contain centres of partly recrystallised oscillatory-zoned zircon replaced and mantled by (low-U) homogeneous bright domains (Fig. 5). Analyses were undertaken on both the oscillatory-zoned and homogeneous bright domains, with all sites yielding concordant dates (Fig. 6; Table 1). Most of these sites yielded $^{207}Pb/^{206}Pb$ dates between 2500–2600 Ma. Statistical analysis could not find any significant age difference between the two types of domains, and it was also not possible to calculate a pooled date on subsets of the oscillatory-zoned zircon analyses with a low MSWD. The results suggest the rock is Neoarchaean in age (probably 2600–2580 Ma), with the zircons experiencing penecontemporaneous recrystallisation (see e.g. Pidgeon, 1992 for a well-documented example of this). One site (8.1, Fig. 5) on the homogeneous bright exteriors of the grains, which looks no different in the CL images yielded a Palaeoproterozoic age, indicating further recrystallisation during later orogenic events.

Orthogneiss 140944 of the Prudhoe Land granulite complex is a tonalitic, grey to mauve homogeneous gneiss from coastal outcrops west of Bu Gletscher, Sonntag Bugt (Fig. 2). The rock is characterised by blue quartz and a foliation of hypersthene and biotite. The sample yielded slightly rounded prismatic zircons, 200–400 µm long. In CL images the grains appear rather dull, but oscillatory zoning, parallel to grain exteriors is present in all grains (Fig. 7). However, small overgrowths and recrystallisation domains are present. The grains have rather high U (ca. 1000 ppm) in keeping with their dull appearance in CL images. Ten analyses of oscillatory-zoned domains were undertaken on ten grains. These appear to be slightly reverse discordant (Fig. 6; Table 1). This is thought to be due slight overestimation of $^{206}Pb/^{238}U$ due to a matrix difference between the unknowns in this sample and the reference standard AS3 used for $^{206}Pb/^{238}U$ calibration. This was shown by the unknowns all having $^{238}U^{16}O/^{238}U$ values of ca. 6.7, whereas $^{238}U^{16}O/^{238}U$ in the standards was ca. 5.7. This calibration problem in no way affects the $^{207}Pb/^{206}Pb$ measurements, upon which age assessment is based in this case. The chosen sites show a spread in $^{207}Pb/^{206}Pb$ apparent age from ca. 2000 to 1600 Ma, which is interpreted to be the result of ancient loss of radiogenic Pb from these high U zircons. Accepting this interpretation, three sites with the 'oldest' $^{207}Pb/^{206}Pb$ dates give a pooled age of 1984 ± 8 Ma. Given the disturbed nature of these zircons, ca. 1985 Ma is proposed as the minimum (but probably close to the true age of) the igneous protolith of the rock.

Orthogneiss 243459 of the Prudhoe Land granulite complex (Fig. 7 in Dawes 2004) is from the plateau surface north of Bamse Gletscher, Sonntag Bugt (Fig. 2). It is a rock of similar appearance to the previous sample (140944) but it is dioritic in composition with a stronger mafic foliation. The sample yielded 200–500 µm long prismatic zircons. Some of these are entirely brown and turbid, others are largely translucent, whereas others have translucent margins and turbid centres. These features are displayed in CL images (Fig. 7). Turbid whole grains and centres consist of dull, low contrast oscillatory-zoned zircon, whereas translucent domains consist of brighter (lower-U) zircon with sector zoning dominant over oscillatory zoning. In some cases it is clear that the bright domains are replacing the dull oscillatory-zoned zircon (bottom right grain in Fig. 7). The bright homogeneous to sector-zoned zircon is interpreted to have developed during metamorphic recrystallisation. Analyses were undertaken on both types of domains. The dull oscillatory-zoned zircon yielded a spread of $^{207}Pb/^{206}Pb$ dates from ca. 2000 Ma down to ca. 1890 Ma. The homogeneous to sector zoned bright domains show a similar spread of $^{207}Pb/^{206}Pb$ dates. However, the three youngest out of five of these sites yielded a pooled $^{207}Pb/^{206}Pb$ date of 1886 ± 25 Ma (MSWD=0.04). From field relationships this sample is regarded as equivalent to orthogneiss 140944, with an age of ca. 1980 Ma. However, its zircons appear to have been severely affected by recrystallisation in an event at ca. 1890 Ma.

5.3. Metasediments south of the Sunrise Pynt Straight Belt

Three metasediments from south of the Sunrise Pynt Straight Belt are included in this study. One (425507) is from Inglefield Land and two (243506, 243510) are from the thickest pile of supracrustal rocks preserved in northern Prudhoe Land on the northern side of Morris Jesup Gletscher (Fig. 2). This sequence was referred to as the Prudhoe Land supracrustal complex by Dawes (1991).

Metaquartzite 425507 is a pale-weathering, homogeneous rock (ca. 90% $Si0_2$) from a thin unit within paragneisses in southernmost Inglefield Land (Fig. 2). The massive, bluish grey, isoclinally folded rock, has pelitic schlieren with appreciable secondary muscovite. It is interpreted as a recrystallised mature quartzite. The associated paragneisses carry garnet and sillimanite with partial melt segregations, indicating that the rock package experienced upper amphibolite- to granulite-facies metamorphism. The sample yielded abundant large to medium (300–100 µm) ovoid to rounded prismatic zircons. CL imaging shows that in many grains oscillatory zoning is truncated at the grain boundaries. This suggests lengthy residence in a sedimentary system, in accordance with interpretation of the rock as a mature quartzite. Detrital zircons yielded earliest Palaeoproterozoic to Archaean ages. Repeat analyses were undertaken on grains giving initially the youngest dates (e.g. grain 3, Fig. 8). These results suggest the youngest detrital grains in the population are ca. 2350 Ma – domains giving younger dates appear to have undergone partial loss of radiogenic Pb in ancient events. Thus ca. 2350 Ma is taken as the maximum age of deposition. The population is dominated by ca. 2450–2600 Ma grains but some older grains as old as ca. 3250 were encountered (Fig. 9).

Metaquartzite 243506 is very similar in lithology to the previous sample (425507), is likewise interpreted as a mature quartzite. It is from the thick supracrustal package north of Morris Jesup Gletscher (Fig. 2; see Dawes 2006, fig. 29). The sample is grey, brownish striped, massive garnetiferous quartzite from a unit that shows highly distorted, paper-thin pelitic seams (see Dawes, 2006, fig. 30B). Assemblages in associated pelitic rocks such as sample 243510 (below) indicate that the supracrustals experienced upper amphibolite- to granulite-facies metamorphism. The zircons in 243506 are morphologically similar to those in sample 425507. However, during analysis, many of grains were found to contain appreciable amounts of common Pb (higher measured $^{204}Pb/^{206}Pb$), indicating disturbance. In connection with this, sample 243506 originates not far below the Mesoproterozoic (Calymmian) unconformity under the Thule Supergroup and this could be the source of weathering/disturbance in these zircons (for regolith development in Prudhoe Land, see Dawes, 2006, fig. 34). Nonetheless, the detrital age spectrum is similar to that in 425507, with components between 2350–3200 Ma (Fig. 9).

Mica schist 243510 is a rusty, garnet-biotite-muscovite-sillimanite schist, collected close to metaquartzite 243506 (Fig. 2). The rock is interpreted as a pelite interlayered with quartzites represented by 243506. Sample 243510 yielded large oval (200–300 µm), equant to multifaceted zircons, dull and homogeneous in CL images. A minority may have small cores in them, only a few µm across. These inclusions are too small to analyse. Analyses of the dominant homogeneous zircon showed rather high U and low Th/U; all 8 analyses yielded a date of 1923 ± 8 Ma (95% confidence, MSWD=1.1). These are interpreted to have grown during metamorphism. The lack of datable detrital zircon within the schist is not surprising. If the original detrital zircons in a pelite are only a few µm across, they are readily dissolved, because of their small size and also the more 'reactive' composition of the rock (pelite versus quartzite) and a lesser grains have grown in their place.

5.4. Etah Group paragneiss north of the Sunrise Pynt Straight Belt

Detrital zircons from paragneisses 440314 and 440321 from the Etah Group north of the Sunrise Pynt Straight Belt, from northeastern and central Inglefield Land, have been dated. The samples come from localities about 50 km apart (Fig. 2), yet they are lithologically similar and thus described together.

The rocks are pinkish weathering, pale quartzo-feldspathic garnet-biotite gneisses: 440321 contains more magnetite, graphite and biotite than 440314. They are interpreted as impure semipelitic to psammitic sediments, thus contrasting lithologically with the cleaner, quartz arenite composition of 243506 and 425507 discussed above. Both samples yielded abundant medium (100–200 µm) zircons. The zircons in these samples are not as rounded, and oscillatory zoning is generally parallel to the grain boundaries (Fig. 8). Also a few prisms of large aspect ratio have survived. Both samples gave an essentially unimodal age spectrum, with the age of the detrital grains centred on 1980–2000 Ma (Fig. 9). A few older detrital grains back to only ca. 2150 Ma were found. Thus, after analysing about 60 detrital grains, *no* Archaean detritus was found and we are 95% confident that Archaean grains form <5% of the detrital population. This is in stark contrast to the metaquartzites to the south, where Archaean detrital grains are common. The almost unimodal age population and the unabraded/unrounded grain morphology suggests that the sediments represented by 440314 and 440321 are dominated by material with short residence time in the sedimentary system, and were derived from ca. 1980–2000 Ma magmatic complexes. Two rim analyses of low Th/U, higher U homogeneous zircon in one of these samples (analyses 14.2 and 14.3 of sample 440321) gave a date of ca. 1920 Ma. These rims are interpreted as metamorphic in origin, and constrain the age of deposition to between ca. 1980 and 1920 Ma.

5.5. Etah meta-igneous complex north of the Sunrise Pynt Straight Belt

Five Etah meta-igneous complex orthogneisses and metagranitoids of different strain state, composition and relative age from field relationships were dated (Fig. 2). Broadly, the samples fall into two main categories: (1) early, calc-alkaline diorites and quartz diorites, and their gneissic equivalents from higher strain zones (samples 425522 and 425542) and (2) variably deformed granites and quartz-poor granitoids of monzonitic–syenitic affinity (samples 425623, 425562 and 425571).

Orthogneiss 425522 is a finely banded, foliated, melanocratic, orthopyroxene-bearing dioritic rock that lies structurally below a thick sequence of calc-silicate gneisses and marble in northeastern Inglefield Land, in a unit too small to depict in Figure 2. It was collected as a possible 'basement' to the supracrustal rocks, although elsewhere it is known that dioritic rocks cut the supracrustal rocks. Zircons from 425522 are 150–200 µm long prisms. In CL images (not reproduced here) oscillatory zoning parallel to grain exteriors dominates the grains, but it is disrupted by partial shells and discordant patches of homogeneous, bright (low-U) zircon. Oscillatory-zoned zircon in six grains was dated, and gave mostly close to concordant dates (Fig. 11a, Table 1). If the one discordant analysis is rejected, then a weighted mean $^{207}Pb/^{206}Pb$ date of 1943 ± 11 (MSWD=0.22) is obtained. This age is interpreted as the time of intrusion of the protolith of gneiss.

Quartz diorite 425542 is a massive, melanocratic, greenish hypersthene-bearing rock from the Hiawatha pluton, an up to 2 km thick unit intercalated within paragneisses northeast of Hiawatha Gletscher (Fig. 2; Dawes, 2004). Traced into higher strain zones, these igneous-looking rocks are transformed into orthopyroxene-bearing orthogneiss indicating that the orthopyroxene is metamorphic in origin (see Dawes et al., 2000, fig. 4B). Sample 425542 yielded 200–300 µm long prismatic zircons. In CL images the zircons are dominated by central domains of oscillatory-zoned zircon, with the exterior of the grains consisting of shells of low-U structureless zircon appearing bright in the images (Fig. 10). Choice of sites concentrated on obtaining the age of the igneous oscillatory-zoned zircon. Thus ten analyses were undertaken on oscillatory-zoned zircon and none on the homogeneous shells. All sites yielded close to concordant ages (Fig. 11b, Table 1). Nine analyses give a weighted mean $^{207}Pb/^{206}Pb$ age of 1949 ± 13 Ma (95% confidence, MSWD=0.37) that is interpreted as the age of intrusion. A tenth site was clearly disturbed, with lower $^{207}Pb/^{206}Pb$ date and high common Pb.

Granite 425623 is a grey, radioactive, medium-grained, heterogeneous rock from south of Hiawatha Gletscher (Fig. 2). It contains biotite + garnet, has low Zr (18 ppm) and could represent an S-type granite (Table 1). It was chosen for this study as a ‘late’ granite phase since it forms veins in paragneiss that had previously been invaded by diorite. The sample yielded whole prismatic grains 200–300 µm across plus fragments of larger prisms, >500 µm across. In CL images (not reproduced here) the grains show dull oscillatory zoning parallel to the grain margins. The grains display no obvious inherited components. Eight analyses of oscillatory-zoned zircon yielded concordant dates and have rather high U (300–400 ppm) (Fig. 11c, Table 1). All analyses give a weighted mean $^{207}Pb/^{206}Pb$ date of 1915 ± 10 Ma (MSWD=0.89) that is interpreted as the age of granite intrusion.

Sample 425562 is a reddish-brown weathered, quartz-poor biotite-bearing granitic rock that contains K-feldspar megacrysts up to 4 cm long. It is typical of the Humboldt pluton in northeastern Inglefield Land (Fig. 2). It was initially considered a post-tectonic body and thus younger than the main magmatic pulses of the Etah meta-igneous complex (Thomassen & Dawes, 1996). However, the body has foliated margins, associated with interleaving of deformed monzogranite and host-rock paragneiss. Zircons from 425562 are 200–500 µm long, subeuhedral to corroded prisms. In CL images (not reproduced here) oscillatory zoning parallel to grain exteriors is common, but is disrupted by partial shells and abundant discordant patches of homogeneous zircon. Oscillatory-zoned zircon in ten grains was targeted, avoiding as much as possible the recrystallisation domains. These gave mostly close to concordant dates (Fig. 11d, Table 1). The zircons have rather high U, which is probably responsible for the more extensive disruption of primary oscillatory-zoned material. Eight analyses gave a weighted mean $^{207}Pb/^{206}Pb$ age of 1924 ± 20 Ma (MSWD=0.24). The other two sites were disturbed with lower $^{207}Pb/^{206}Pb$ ages, and were not considered. 1924 ± 20 Ma is interpreted as the age of granite intrusion.

Sample 425571 is a pale, coarse-grained monzonitic rock from the western part of the horseshoe-shaped Wulff fold structure in northeastern Inglefield Land (Fig. 2). The rock yielded large, 300–500 µm, prismatic grains and fragments. In CL images (not reproduced here) the zircons show a very weak oscillatory zoning parallel to grain margins and locally disrupted by discordant recrystallisation domains. Our reconnaissance study dated weakly oscillatory-zoned zircon in four grains. The sites have rather high U (650–1500 ppm) and yielded close to concordant ages (Fig. 11, Table 1). Rejecting 4.1, which is interpreted to have lost some radiogenic Pb, the remaining sites give a weighted mean $^{207}Pb/^{206}Pb$ age of 1920 ± 16 Ma (MSWD=0.38), which is interpreted to be close to the age of intrusion.

5.6. Late granitic rocks north of the Sunrise Pynt Straight Belt

Four granitoid samples, 425583, 425627, 425793 and 425794, from Inglefield Land were dated. Three of these rocks were considered in the field to be ‘late’ intrusions on account of rock relationships and undeformed appearance and nondirectional textures, but 425583 was collected as an orthogneiss. Sample 425794 is from an alaskite sheet-like body that is cut by felsic dyke 425793. This sample gave but a small yield of very high U, disturbed, high $^{204}Pb/^{206}Pb$ zircons with only highly discordant ages. The U/Pb zircon data for 425794 are included in Table 1 but not discussed further because the analyses do not provide any useful age constraint on the sample.

Orthogneiss 425583 from central Inglefield Land is granodioritic and represents the pale grey, palaeosome of a homogeneous to veined gneiss. It occurs within the syenitic Minturn intrusive complex (Dawes, 2004; Fig. 2). The sample was collected as part of the possible host rocks to the syenites making up much of the Minturn intrusive complex. The sample yielded whole prismatic and fragments of prismatic grains, mostly 200–300 µm long. In CL images these display oscillatory zoning parallel to the grain boundaries (Fig. 10). Also present are a few smaller, rounded prismatic grains, which consist of a core and a thin overgrowth. Most analyses gave close to concordant dates (Fig. 11, Table 1). Ignoring a strongly discordant analysis, eight analyses of the prisms and fragments yielded a weighted mean $^{207}Pb/^{206}Pb$ age of 1752 ± 25 Ma (MSWD=0.18). This is interpreted as the age of intrusion of the granite. An analysis of rounded grain 2.1 gave an age of ca. 2650 Ma, indicating the presence of considerably older crustal material in the rock. Thus, its SHRIMP zircon age shows that it is a late granitoid and indicative of late high strain zones within the IMB.

Sample 425627 is from a small, weakly sinuous, sheet-like leucodioritic body cutting migmatitic paragneiss from coastal exposures at Force Bugt (Fig. 2). The rock is biotite-bearing, pink weathered but grey on fresh surfaces, with a coarse-grained to feldspar-phyric texture. The sample yielded zircons of diverse morphology. Dominant grains are rounded 150–250 µm prisms but rare fragments of larger >400 µm prisms are also present. In CL images (not reproduced here) the rounded prisms appear dull but show vestiges of oscillatory zoning. In some grains homogeneous recrystallisation domains dominate. Despite the poor luminescence, some of these grains appear to have new sheaths <10 µm thick of new growth. Fragments of larger oscillatory-zoned zircon luminescence slightly better, with weak oscillatory zoning parallel to grain margins. Five analyses were undertaken on a fragment of a large homogeneous to oscillatory-zoned prism. Four are concordant within error, with a weighted mean $^{207}Pb/^{206}Pb$ age of 1741 ± 15 Ma (MSWD=0.42). Three analyses were undertaken on a rounded grain with vestiges of oscillatory zoning, and gave concordant dates, with a weighted mean $^{207}Pb/^{206}Pb$ age of 2198 ± 15 Ma (MSWD=0.12). A single analysis of another rounded grain gave discordant dates, with the $^{207}Pb/^{206}Pb$ date being ca. 2420 Ma (with large uncertainty). Analyses of three other rounded grains gave a weighted mean $^{207}Pb/^{206}Pb$ age of 1886 ± 37 Ma (MSWD=2.1). Provisionally, the large fragment of a 1741 ± 15 Ma zircon is interpreted to be igneous in origin, giving the age of intrusion. The rounded grains are interpreted to be inherited Palaeoproterozoic or Archaean grains.

Granite 425793 (Fig. 2) is from a NW–SE-trending, linear to sinuous dyke up to 8 m thick of brick-red, fine-grained, quartz-poor granite that post-dates the gneiss fabric and migmatitic veins of the host paragneiss, as well as cross-cutting a large mass of leucogranite (sample 425794, see above). The zircons are rather turbid euhedral to subhedral prisms and have relatively muted CL response (not reproduced here). Locally, however, hints of oscillatory zoning can be seen. They have high to locally very high U and Th (>1000 ppm) and consistently high Th/U (mostly 1.3 - 2). The grains are generally isotopically disturbed and discordant (Fig. 12). All ten analyses yield a model 1 concordia intercept of 1833 ± 56 Ma (MSWD=0.64). Whereas eight of the analyses (rejecting two with the lowest $^{207}Pb/^{206}Pb$) give a weighted mean $^{207}Pb/^{206}Pb$ age of 1783 ± 22 Ma (MSWD=0.60). Although not entirely satisfactory results, they do indicate this granite is a relatively young intrusion.

5.7. Victoria Fjord

Zircons from the sample 312632 used by Hansen et al. (1987) were analysed with SHRIMP (Table 1). 312632 is a pink, leucocratic, medium-grained, homogeneous granitic orthogneiss (Table 1) collected from eastern exposures (co-ordinates, Fig. 2).

The zircons obtained are slightly corroded 250–400 µm long prisms, buff/cloudy in appearance. In transmitted light, the grains are translucent to slightly clouded, with no obvious internal structure; in

CL images, the zircons show spectacular recrystallisation textures (Fig. 13). Although there are rare vestiges of oscillatory zoning preserved in the grains (e.g. oscillatory domains (osc.) within grains 1 and 2 in Fig. 13), the grains are dominated by discordant homogeneous bright and homogeneous dark domains (hb-rex and hd-rex domains in Fig. 13). The remnants of oscillatory zircon are interpreted to be igneous in origin. Four analyses were undertaken on the best-preserved vestiges of oscillatory-zoned zircon. These gave close to concordant dates, with the oldest having a $^{207}Pb/^{206}Pb$ age of 3380 ± 4 Ma (2σ). Regression of these four determinations yielded a model 1 upper concordia intercept age of 3401 ± 12 Ma (MSWD=0.10) (Fig. 14). Two determinations were undertaken on homogeneous bright recrystallisation domains. These yielded close to concordant ages at ca. 3270 Ma (Fig. 14), and they indicate first recrystallisation of oscillatory zoned zircon in an event ca. 100 million years after the zircons formed. Two analyses were undertaken on homogeneous dull recrystallisation domains in grain 3. These yielded discordant ages, younger than the bulk analyses of Hansen et al. (1987). These analyses indicate major recrystallisation/replacement in the zircons in the late Neoproterozoic to the early Palaeozoic (Fig. 14). Recrystallisation in these zircons is probably so advanced for the combined reason that the zircons have rather high U + Th (Table 2) and that the sample was taken just below the Palaeozoic unconformity.

On the basis of size fraction multigrain analyses which yielded discordant ages, Hansen et al. (1987) obtained an upper concordia intercept age of 2863^{+32}_{-30} Ma for zircons from 312632. All apart from one size fraction formed a tight cluster, hence the one remaining point strongly controlled the upper intercept age (Fig. 14). On the other hand, we obtained an age of ca. 3400 Ma from remnant oscillatory zoned zircon by SHRIMP, about 500 million years older. Furthermore, the imaging of the zircons together with the SHRIMP analyses of different types of recrystallisation domains demonstrate that the original bulk IDTIMS analyses must have been dominated by recrystallised/disturbed zircon. Our preferred interpretation based on the small amount of SHRIMP U-Pb data and the zircon petrography is that the rock is approximately 3400 Ma old, as given by the age determinations on the vestiges of oscillatory-zoned zircon. However the present data set cannot entirely exclude the possibility that the rock is somewhat younger but still Archaean, but carries ca. 3400 Ma xenocrystic zircon. Even with this interpretation, this sample demonstrates the presence of Palaeoarchaean crustal material in northernmost Greenland.

6. Sm–Nd isotope data

6.1. Analytical method and sample suite

Sm–Nd isotope data have been obtained for 14 samples, all of which are from Inglefield Land (Fig. 2, Table 3). Radiogenic isotope compositions for Sm and Nd were determined at the Geological Survey of Canada in Ottawa. Analytical determinations for all samples were made on single 200 mg aliquots of powder after spiking with mixed ^{87}Rb-^{84}Sr and ^{149}Sm-^{148}Nd tracers and dissolution in an HF-HNO3 mixture. All samples were dissolved in TFE Teflon bombs in steel jackets at 200°C for 100 hours. Following conventional cation-exchange chromatography, Sm and Nd were further separated using a modified version of the HDEHP-Teflon® powder method described by Richard et al. (1976). Procedural blanks were <100 pg for Nd and <50 pg for Sm. All isotopic analyses were performed using a MAT-261 mass spectrometer in multicollector mode. Measured Nd isotopic compositions reported in Table 2 were corrected for mass fractionation by normalization to $^{146}Nd/^{144}Nd$ = 0.7219, and corrected to La Jolla $^{143}Nd/^{144}Nd$ = 0.511860. Samples were analysed for neodymium using a static multicollector cup configuration; replicate analyses of an Ames Nd metal solution measured during this period yielded a mean $^{143}Nd/^{144}Nd$ = 0.512160 (equivalent to La Jolla $^{143}Nd/^{144}Nd$ = 0.511875). Initial $^{143}Nd/^{144}Nd$ ratios were calculated assuming $^{147}Sm/^{144}Nd$ = 0.1967 and $^{143}Nd/^{144}Nd$ = 0.512638 for present-day CHUR. External precisions on isotopic ratio measurements are better than ± 2.5×10^{-5} for Nd. Based on replicate analyses, $^{147}Sm/^{144}Nd$ ratios are reproducible to 0.3%.

Thirteen samples come from rocks north of the Sunrise Pynt Straight Belt, with one sample (425748), a garnet-biotite schist, from a package of Etah Group metasediments and paragneiss caught up in the actual shear belt. Four of these samples (425542, 425571, 425583, 425623) have ages determined directly using SHRIMP U-Pb zircon geochronology, while another (425738) comes from the same cross-cutting granite dyke as SHRIMP sample 425793. The new data are represented on a time versus ε_{Nd} plot (Fig. 15).

In addition, four unpublished Sm-Nd isotopic data have been supplied by Paul N. Taylor (personal communication 1990). Three of these are from the southern terrane, and the fourth is from the northeast of the Inglefield Mobile Belt. T_{DM} ages of these are summarised on Figures 1 and 2.

6.1. Results

Sample 425748 of paragneiss within the Sunrise Pynt Straight Belt yields Neoarchaean depleted mantle model ages, which demonstrates that sedimentary material of Archaean provenance is caught-up within the straight belt. On the other hand metasediment 425727 from central Inglefield Land has Palaeoproterozoic depleted mantle model ages, in accord with other sediments north of the Sunrise Pynt Straight Belt only contain Palaeoproterozoic detrital zircons (samples 440314 and 440321 of this study).

Etah metaigneous complex samples with likely protolith ages of 1950-1900 Ma (e.g. zircon geochronology on samples 525542, 425571 and 425623 – this paper) all yield a narrow age range of Palaeoproterozoic depleted mantle model ages, no more than a few hundred million years older than their igneous emplacement ages obtained by zircon dating. This shows these rocks are “juvenile” crustal additions, probably in a volcanic (island?) arc. It is generally found that depleted mantle model ages are somewhat older than the emplacement age of arc rocks, as first shown by DePaolo (1981) for the Phanerozoic Sierra Nevada Batholith. This is because juvenile magma can be contaminated by a variety of older crustal sources, for example continental basement in an Andean arc or subducted far-travelled turbiditic sediment in an island arc setting.

Inglefield Land Mobile Belt late granite sheets and orthogneisses derived from them give a range of depleted mantle model ages from Palaeoproterozoic to Mesoarchaean (sample 425793). This is in accord with the SHRIMP U/Pb zircon study, which found Palaeoproterozoic to Neoarchaean xenocrystic zircons in these rocks. Thus, it appears that by 1800 Ma, there was a source at depth of crust with Archaean components, not present at depth during the generation and emplacement of the 1950-1900 Ma arc rocks in the Inglefield Mobile Belt.

7. Discussion

The SHRIMP zircon dating integrated with mapping and whole-rock Nd isotopic data allows the definition of three terranes, each with a characteristic age and isotopic signature: (1) An area of poorly-known Archaean rocks north of the Inglefield Mobile Belt (IMB), comprising the Victoria Fjord inlier, but almost completely covered by younger deposits; (2) The IMB, composed entirely of Palaeoproterozoic rocks, and (3) a southern terrane consisting of Neoarchaean to earliest Palaeoproterozoic rocks.

7.1.A northern terrane with Archaean rocks

The northern terrane named here the *Victoria Fjord Complex*, might contain Palaeoarchaean orthogneisses, although further confirmation of this finding is needed. The ages of other components such as intercalated supracrustal rock units and metamorphosed basic intrusions are unknown. Due to the remote location of this terrane, information on its evolution is so far only of a preliminary nature. Because of its occurrence as isolated inliers within an area of Palaeozoic platform sediments, and extensive ice cover to the south and west, the boundary with the IMB (if such a boundary exists) is concealed and the nature is unknown (Fig. 1). The Archaean rocks at Victoria Fjord represent the northernmost exposures of the North American craton. Nowhere else in Greenland have ca. 3400 Ma rocks been proposed, and a literature review has failed to reveal the existence of rocks of this age in lands around the eastern Arctic Basin (e.g. Grantz et al., 1990)

7.2. The Inglefield Land Mobile Belt

The southern boundary of the IMB is now the Sunrise Pynt Straight Belt, which although late kinematic, still has a high metamorphic grade. The IMB thus occupies most of Inglefield Land, and it contains major packages of quartzo-feldspathic metasediments that have zircons showing little sedimentary transport and an essentially unimodal Palaeoproterozoic age distribution (ca. 2020–1980 Ma; Fig. 16). These rocks of likely volcano-sedimentary origin were intruded by marginally younger (1950–1920 Ma) diorites, granodiorites and syenites, with only slightly older Nd T_{DM} (DePaulo, 1981) model ages of 2180-2080 Ma. Together, these volcano-sedimentary rocks and intrusions are interpreted to represent a juvenile Palaeoproterozoic arc complex. They suffered high-grade (up to granulite facies) metamorphism at ca. 1930–1920 Ma, as demonstrated by dating of metamorphic overgrowths on zircons in the metasediments. Late kinematic granites intruded between 1800–1740 Ma into this juvenile Palaeoproterozoic assemblage, occasionally have older Nd T_{DM} model ages (up to at least 2748 Ma) and rare Archaean inherited zircons have been detected within them (Fig. 16).

7.3. A southern terrane with Archaean and earliest Palaeoproterozoic orthogneisses

Within the Sunrise Pynt Straight Belt (SSPB) and to the south of it in Prudhoe Land, there are packages of metapelites and marbles with metaquartzites. The metaquartzites increase in abundance towards the south and the zircons obtained from them are commonly strongly abraded, indicating long transport history. They show a spectrum of ages from earliest Palaeoproterozoic to Archaean (Fig. 16). In the nunataks of Prudhoe Land, these metasediments are found with both Palaeoproterozoic (1990–1980 Ma) and Neoarchaean orthogneisses. The northern edge of the southern terrane is interpreted to contain an Archaean basement with Palaeoproterozoic platformal carbonate and detrital quartzitic sediments that were intruded by a suite of Palaeoproterozoic granites, diorites and tonalites marginally older than those in the IMB. As these rocks appear to have an age of ca. 2000 Ma, they might represent an (Andean?) arc complex that is marginally older than that exposed in the IMB to the north of the Sunrise Pynt Strait Belt. These granites, diorites and tonalites match in age ones that occur in the Caledonian basement of North East Greenland (Kalsbeek et al., 1993). Southwards, the southern terrane appears to be dominated by Archaean rocks, including a large anorthosite complex (Nutman, 1984).

7.4. Palaeoproterozoic tectonothermal evolution, North-West Greenland

The Palaeoproterozoic rocks of the IMB underwent early (1930-1920 Ma) metamorphism up to granulite facies and a complex folding history. There was high-grade metamorphism and deformation until as late as 1800–1740 Ma, because granite intrusions of that age in the IMB carry amphibolite-facies assemblages and are variably deformed. Another important constraint on the tectonothermal evolution of the IMB is that the older suite of 1950–1920 Ma intrusions have Palaeoproterozoic Nd T_{DM} model ages and the sediments contain no Archaean zircon, whereas the younger granites have older model ages and may contain inherited Archaean zircons. Together, this indicates that the IMB developed and evolved isolated from Archaean crust up to ca. 1930 Ma, but thereafter it was juxtaposed with and probably tectonically underlain by a terrane containing Archaean material.

In the southern terrane, Archaean and Palaeoproterozoic orthogneisses and paragneisses, with prominent Palaeoproterozoic quartzite packages, are interleaved and folded, excellent exposures being present along Inglefield Bredning (Fig. 2; see Dawes, 2006, fig. 7). Together these rocks underwent high-grade metamorphism at ca. 1930–1920 Ma (Fig. 16). At the head of Inglefield Bredning, fieldwork and detailed metamorphic studies indicate a complex metamorphic history. Thus, amphibolitised mafic dykes that cut Archaean basement rocks carry garnet, now widely replaced by plagioclase + hornblende symplectites (Nutman, 1984). Host rocks to the dykes locally contain complex coronas where early orthopyroxene is first mantled by garnet and then by orthopyroxene + plagioclase (Garde et al., 1984). Although originally interpreted as fluctuation in oxygen fugacity during a single metamorphism, another interpretation is that these textures could indicate polybaric metamorphism, whereby the first garnet coronas indicate pressure increase followed by the outer coronas indicating lower pressures again. Thus, the interleaving of rocks of different age and origin at the northern edge of the southern terrane and the complex metamorphic textures, may indicate Palaeoproterozoic tectonic stacking followed by exhumation and decompression.

An interpretation proposed here for the IMB and the southern terrane, is that the former represents a juvenile arc that collided and was thrust over the edge of the latter, which contains an Archaean basement overlain by Palaeoproterozoic platform sediments. This probably occurred at ca. 1930–1920 Ma, as recorded by coeval growth of zircon during high-grade metamorphism in both terranes. This relationship would explain that a source of Archaean material was present at depth under the IMB by the time of post-collisional tectonothermal events, as evidenced by the inherited Archaean detrital zircons in the 1800–1740 Ma late kinematic granitic intrusions. The Sunrise Pynt Straight Belt is a late structure (<1800 Ma) in the Palaeoproterozoic tectonothermal evolution of the region. Presently, it is unknown if it contains a deformed earlier (1920-1930 Ma) suture between the unrelated terranes on either side, or if it has excised the earlier suture. K–Ar ages on hornblende and mica suggest elevated temperatures as late as ca. 1650 (Larsen and Dawes, 1974), after which the uplifted crust was subjected to continental-scale intrusion of basic dykes at ca. 1630 (Denyszyn et al., 2005; Dawes 2006).

At Victoria Fjord, the impact of Palaeoproterozoic tectonothermal processes, perhaps related to that in the southern terranes, is demonstrated by K–Ar hornblende dating and the resetting of Rb-Sr whole rock isotope systems (Hansen et al., 1987). Presently no further information is available on the Palaeoproterozoic evolution of this terrane. However, it is noteworthy that the detailed studies of strongly recrystallised zircons from the single gneiss sample from this terrane show no evidence of Palaeoproterozoic zircon growth. Thus this terrane may not have been tectonically buried with high-grade metamorphism when it was juxtaposed with the other terranes.

7.5. Disposition of Precambrian provinces around northern Baffin Bay

North-West Greenland and southeastern Ellesmere Island share the same chronostratigraphic and tectono-magmatic history (Frisch and Dawes, 1982; Frisch, 1988). The boundary in Prudhoe Land (Greenland) between Archaean gneisses of the southern terrane and Palaeoproterozoic gneisses to the north (Fig. 2) is taken from the most recent geological map (Dawes 1991). In neighbouring Canada, the boundary between Archaean and Palaeoproterozoic domains lies essentially between Ellesmere and Devon islands (Frisch, 1988; Fig. 1). On Devon Island, U–Pb and Sm–Nd isotopic data show that the gneissic protoliths are late Neoarchaean with a strong Palaeoproterozoic metamorphic overprint (Frisch and Hunt, 1988; Schärer and Deutsch, 1990). For example, in addition to the ages from Canada shown on our map (Fig. 1), the latter authors report a U–Pb age on monazite of 1903 Ma and a Nd T_{DM} model age on the whole rock of 2570 Ma from a gneiss positioned just off the map near the northern coast of Devon Island. Unpublished T_{DM} Nd model ages of granitoid rocks obtained by E. Hegner (pers. comm., 2007) support the notion that the shield terrane on Ellesmere Island is Palaeoproterozoic in age whereas that on Devon and Coburg islands is in part Archaean. Model ages of 16 samples from Ellesmere cluster tightly in the range 2300-2100 Ma; two rocks from Coburg Island yielded ages of 2800 and 2200 Ma; five samples from Devon Island range from 2800 to 2200 Ma. This matches the history of the gneisses of the Thule mixed-gneiss complex in Prudhoe Land, exemplified by our samples 243495 and 470214 (Fig. 16). On a broader scale, the IMB of Greenland (Escher and Pulvertaft, 1995; Dawes and Garde, 2004) maybe part of the ‘Thelon Tectonic Zone’ of Canada (Dawes, 1988; Hoffman, 1988, 1989, 1990; Fig. 1). Farther to the south, another obvious correlation involves the extensive Neoarchaean iron deposits of the Mary River Group of Baffin Island with Greenland’s largest iron province (Jackson, 1966, 2000, fig. 114) that occurs within supracrustal sequences interleaved with gneisses of the Melville Bugt orthogneiss complex (southern part of the southern terrane; Dawes, 1991, 2006).

Four decades of mapping by the geological surveys of Canada and Greenland/Denmark, supported by isotopic studies, has shown that the Precambrian crystalline shield around northern Baffin Bay constitutes a litho-tectonically coherent block. The recognition of the continuous Precambrian geology around northern Baffin Bay is confirmed by the available isotopic ages (Dawes et al., 1988; Frisch and Hunt, 1988; Hegner and Jackson, 1990; Jackson et al., 1990; Schärer and Deutsch, 1990, Jackson and Hegner, 1991; Henderson and van Breemen, 1992; Jackson, 2000). This unity also characterises the later Precambrian geology, as shown by the overlying Mesoproterozoic cover sequence (Thule Supergroup) and the Neoproterozoic dyke swarms that pierce it (Dawes, 1997, 2006; Oakey, 2005). The main Precambrian elements of this crustal block show no apparent displacement between Greenland and Canada across Nares Strait (Frisch and Dawes, 1982, 1994; Frisch, 1988; Dawes, 1988, 1997; Jackson, 2000). This aspect is important to stress, because there are some reconstructions of the Arctic and North Atlantic regions that show North-West Greenland displaced hundreds of kilometres from neighbouring Canada. Such reconstructions – for example those figured by Roest and Srivastava (1989), Eide (2002), Ketchum et al. (2002). Wardle et al. (2002), Piper and Darabi (2005) and Tessensohn et al. (in press) do not explain the lack of displacement in the Precambrian rock units across the Nares Strait. Offshore geophysical work confirms the coherent crustal nature of the Smith Sound – northern Baffin Bay region, and fails to recognise major transcurrent dislocation in Nares Strait that could be interpreted as the plate boundary between Greenland and Canada (Damaske and Oakey, 2005; Oakey, 2005; Harrison et al., 2006).

8. Conclusions

• Integrated geological mapping, whole-rock geochemistry, zircon geochronology and Nd isotopic studies provide a fundamental division of the early Precambrian basement geology of North-West Greenland with the recognition of three early Precambrian crustal provinces: (1) the poorly-known northern terrane of the Victoria Fjord Complex with Archaean rocks in Victoria Fjord, (2) the central juvenile Palaeoproterozoic IMB of metasediments and magmatic rocks regarded as a magmatic arc, and (3) the southern terrane that contains Neoarchaean basement gneisses, Palaeoproterozoic mixed-provenance detrital quartzites, pelites and carbonates and some Palaeoproterozoic intrusions.

• These terranes evolved separately until juxtaposition in the Palaeoproterozoic (certainly by 1800 Ma and probably at ca. 1930–1920 Ma). This juxtaposition might have involved tectonic emplacement of the IMB terrane juvenile Palaeoproterozoic arc complex over the northern edge of the southern terrane, with its Archaean basement and platformal sediments. This original tectonic relationship has been modified by the Sunrise Pynt Straight Belt – the major late kinematic shear zone that now forms the boundary between the two terranes. Tectonic emplacement of the IMB over the northern edge of the southern terrane would explain why late kinematic granites in the former carry inherited Archaean zircons (Fig. 16).

• Zircon dating of a gneiss from the northern terrane in Victoria Fjord has documented ca. 3400 Ma zircon. Our preferred interpretation is that ca. 3400 Ma is the age of the rock, but on the basis of present knowledge, it cannot be entirely discounted that the 3400 Ma zircon is xenocrystic in a younger (but still Archaean) rock.

• The new isotopic results in this paper confirm the position of the boundary between Palaeoproterozoic and Neoarchaean basement domains in North-West Greenland initially determined by geological mapping. This correlates with a similar boundary in the Canadian Arctic. The congruence of the Archaean–Palaeoproterozoic basement geology – as well as the younger Precambrian rocks – strongly militates against the presence of a major wrench fault separating Greenland and Canada in the Smith Sound –northern Baffin Bay region.

Acknowledgements

The six digit sample numbers, in official archives with the prefix ‘GGU’, refer to material in the files of the Geological Survey of Denmark and Greenland (GEUS), Copenhagen. Twenty-eight of the samples for which analytical data are presented were collected by one of us (PRD): thanks to Adam A. Garde, Jeroen A.M. van Gool, Hans F. Jepsen and Agnete Steenfelt (GEUS) for supplying the remaining five. We are grateful to Paul N. Taylor, E. Hegner and Robert (Bob) T. Pidgeon for permission to quote unpublished isotopic ages and to Peter Venslev, University of Copenhagen, Geocenter Copenhagen, for separating the zircons used in the SHRIMP analysis. Tom Frisch is thanked for his comments on the final draft manuscript. Zircon geochronology by APN whilst at the Research School of Earth Sciences (ANU) was undertaken to recover salary from external sources. MAH thanks technical support staff of the Geological Survey of Canada for assistance while collecting Sm-Nd isotopic data. The paper is published with the permission of the Geological Survey of Denmark and Greenland.

References

Bugge, C., 1910. Petrographische Resultate der 2ten Fram-Expedition. Rep. of the 2nd Norwegian Arctic Expedition 'Fram' 1898–1902, 3(22), 38 pp. Videnskabs-Selskabet, Kristiana.

Connelly, J.N., Mengel, F.C., 2000. Evolution of Archean components in the Paleoproterozoic Nagssugtoqidian orogen, West Greenland. Geol. Soc. Amer. Bull. 112(5), 747–763.

Connelly, J.N., van Gool, J.A.M., Mengel, F.C., 2000. Temporal evolution of a deeply eroded orogen; the Nagssugtoqidian Orogen, West Greenland. Canadian Journal of Earth Sciences 37, 1121–1142.

Crowley, J.L., 2002. Testing the model of late Archean terrane accretion in southern West Greenland: a comparison of timing of geological events across the Qarliit nunaat fault, Buksefjorden region. Precambrian Res. 116, 57–79.

Crowley, J.L., 2003. U-Pb geochronology of 3810–3630 Ma granitoid rocks south of the Isua greenstone belt, southern West Greenland. Precambrian Res. 126, 235–257.

Crowley, J.L., Myers, J.S., Dunning, G.R., 2002. Timing and nature of multiple 3700–3600 Ma tectonic events in intrusive rocks north of the Isua greenstone belt, southern West Greenland. Geol. Soc. Amer. Bull. 114, 1311–1325.

Damaske, D., Oakey, G.S., 2005. Basement structures and dykes: aeromagnetic anomalies over southern Kane Basin. Proceedings of the 4th International Conference on Arctic margins, Abstract volume 67–68.

Dawes, P.R., 1972. Precambrian crystalline rocks and younger sediments of the Thule district, North Greenland. Rapport Grønlands Geologiske Undersøgelse 45, 10–15.

Dawes, P.R., 1976. Precambrian to Tertiary of northern Greenland. In: Escher, A., Watt, W.S. (Eds.), Geology of Greenland, 248–303. Geological Survey of Greenland, Copenhagen, Denmark.

Dawes, P.R., 1978. Crystalline basement complex of the Victoria Fjord arch. Unpublished report, Geological Survey of Greenland, Copenhagen, Denmark, 6 pp.

Dawes, P.R., 1979. Field investigations in the Precambrian terrain of the Thule district, North-West Greenland. Rapport Grønlands Geologiske Undersøgelse 95, 14–22.

Dawes, P.R., 1988. Etah meta-igneous complex and the Wulff structure: Proterozoic magmatism and deformation in Inglefield Land, North-West Greenland. Rapport Grønlands Geologiske Undersøgelse 139, 24 pp.

Dawes, P.R., 1991. Geological map of Greenland 1:500 000, Thule, sheet 5. Geological Survey of Greenland, Copenhagen, Denmark.

Dawes, P.R., 1997. The Proterozoic Thule Supergroup, Greenland and Canada: history, lithostratigraphy and development. Geology of Greenland Survey Bulletin 174, 150 pp.

Dawes, P.R., 1999. A review of geoscientific exploration and geology in the Kane Basin region of Greenland, central Nares Strait. Danmarks og Grønlands Geologiske Undersøgelse Rapport 1999/32, 58 pp. + 6 maps

Dawes, P.R., 2004. Explanatory notes to the geological map of Greenland, 1:500 000, Humboldt Gletscher, Sheet 6. Geological Survey of Denmark and Greenland Map Series 1, 48 pp.

Dawes, P.R., 2006. Explanatory notes to the geological map of Greenland, 1:500 000, Thule, Sheet 5. Geological Survey of Denmark and Greenland Map Series 2, 97 pp.

Dawes, P.R., Frisch, T., 1981. Geological reconnaissance of the Greenland Shield in Melville Bugt, North-West Greenland. Rapport Grønlands Geologiske Undersøgelse 105, 18–26.

Dawes, P.R., Garde, A.A., 2004. Geological map of Greenland 1:500 000, Humboldt Gletscher, sheet 6. Geological Survey of Denmark and Greenland, Copenhagen, Denmark.

Dawes, P.R., Larsen, O., Kalsbeek, F., 1988. Archean and Proterozoic crust in North-West Greenland: evidence from Rb–Sr whole-rock age determinations. Canadian Journal of Earth Sciences 25, 1365–1373.

Dawes, P.R., Frisch, T., Garde, A.A., Iannelli, T.R., Ineson, J.R., Jensen, S.M., Pirajno, F., Sønderholm, M., Stemmerik, L., Stouge, S., Thomassen, B., van Gool, J.A.M., 2000. Kane Basin 1999: mapping, stratigraphic studies and economic assessment of Precambrian and Lower Palaeozoic provinces in north-western Greenland. Geology of Greenland Survey Bulletin 186, 11–28.

Denyszyn, S.W., Halls, H.C., Davis, D.W., 2005. Paleomagnetism and U–Pb geochronology of the Melville Bugt dyke swarm, northwestern Greenland, and implications for the Laurentia-Baltica reconstructions in the late Paleoproterozoic. Geophysical Research Abstracts 7, 09597.

DePaolo, D.J., 1981. A neodymium and strontium isotopic study of the Mesozoic calc-alkaline granitic batholiths of the Sierra Nevada and Peninsular Ranges, California. J Geophys Res. 86, 10470-10488

Eide, E.A. (coordinator), 2002. BATLAS – Mid Norway plate reconstruction atlas with global and Atlantic perspectives. Geological Survey of Norway, Trondheim, 150 pp.

Escher, J.C., Pulvertaft, T.C.R., 1995. Geological map of Greenland 1:2 500 000. Geological Survey of Greenland, Copenhagen, Denmark.

Friend, C.R.L., Nutman, A.P., 1994. Two Archaean granulite-facies metamorphic events in the Nuuk-Maniitsoq region, southern West Greenland: correlation with the Saglek block, Labrador. J. Geol. Soc. Lond. 151, 421–424.

Friend, C.R.L., Nutman, A.P., 2001. U-Pb zircon study of tectonically-bounded blocks of 2940–2840 Ma crust with different metamorphic histories, Paamiut region, South-West Greenland: Implications for the tectonic assembly of the North Atlantic craton. Precambrian Res. 105, 143–164.

Friend, C.R.L., Nutman, A.P., Baadsgaard, H., Kinny, P.D., McGregor, V.R., 1996. Timing of late Archaean terrane assembly, crustal thickening and granite emplacement in the Nuuk region, southern West Greenland. Earth Plan. Sci. Lett. 124, 353–365.

Frisch, T., 1988. Reconnaissance geology of the Precambrian Shield of Ellesmere, Devon and Coburg islands, Canadian Arctic Archipelago. Geological Survey of Canada Memoir 409, 102 pp. + 4 maps.

Frisch, T., Dawes, P.R., 1982. The Precambrian Shield of northernmost Baffin Bay: correlation across Nares Strait. In: Dawes, P.R., Kerr, J.W. (Eds.), Nares Strait and the drift of Greenland: a conflict in plate tectonics. Meddelelser om Grønland Geoscience 8, 79–88.

Frisch, T., Dawes, P.R., 1994: A seismic reflection study of northern Baffin Bay: implication for tectonic evolution: Discussion. Canadian Journal of Earth Sciences 31, 219–221.

Frisch, T., Hunt, P.A., 1988. U–Pb zircon and monazite ages from the Precambrian Shield of Ellesmere and Devon islands, Arctic Archipelago. Geological Survey of Canada Paper 88-2, 117–125.

Garde, A.A., Glassley, W.E., Nutman, A.P., 1984. Two-stage corona growth during Precambrian granulite facies metamorphism of Smithson Bjerge, north-west Greenland. J. Metamorphic Geol. 2, 237–247.

Garde, A.A., Hamilton, M.A., Chadwick, B., Grocott, J., McCaffrey, K.J.W., 2002. The Ketilidian orogen of South Greenland: geochronology, tectonics, magmatism, and fore-arc accretion during Palaeoproterozoic oblique convergence. Canadian Journal of Earth Sciences 39, 765–793.

GGU, 1970. Tectonic/geological map of Greenland, 1:2 500 000. Geological Survey of Greenland, Copenhagen, Denmark.

Grantz, A., Johnson, L., Sweeney, J.F. (Eds), 1990. The Arctic Ocean Region. The Geology of North America, L. Geological Society of America, Boulder, Colorado, 644 pp.

Haller, J., 1961. An account of Caledonian orogeny in Greenland. In Raasch, G.O. (Ed.), Geology of the Arctic 1, 170–187. University Press, Toronto.

Hamilton, M.A., Garde, A.A., Chadwick, B., Grocott, J., McCaffrey, K. [J.W.], 1999. Temporal evolution of the Palaeoproterozoic Ketilidian orogen, South Greenland: a synopsis of results from conventional and SHRIMP U–Pb geochronology. European Union of Geosciences, 10th Annual meeting, Journal of Conference Abstracts 4(1), 129.

Hansen, B.T., Kalsbeek, F., Holm, P.M., 1987. Archaean age and Proterozoic metamorphic overprinting of the crystalline basement at Victoria Fjord, North Greenland. Rapport Grønlands Geologiske Undersøgelse 133, 159–168.

Harrison, J.C., Brent, T.A., Oakey, G.N., 2006. Bedrock geology of the Nares Strait region of Arctic Canada and Greenland, with explanatory text and GIS content. Geological Survey of Canada Open File 5278, scale 1:1 000 000, 1 CD–ROM .

Hegner, E., Jackson, G.D., 1990. Nd isotopic constraints on late Archean and early Proterozoic crust formation in Baffin and Ellesmere Islands, northern Labrador and Ungava Peninsula, eastern Canada. Eos, Transactions American Geophysical Union 71, p. 1689.

Henderson, J.B., van Breemen, O., 1992. U–Pb zircon ages from an Archaean orthogneiss and a Proterozoic metasedimentary gneiss of the Thelon Tectonic Zone, District of Mackenzie, Northwest Territories. Geological Survey of Canada Paper 91–2, 25–33.

Henriksen, N., 1989. Geological map of Greenland 1:500 000, Nyeboe Land, sheet 7. Geological Survey of Greenland, Copenhagen, Denmark.

Henriksen, N., Jepsen, H.F., 1985. Precambrian crystalline basement at the head of Victoria Fjord, North Greenland. Rapport Grønlands Geologiske Undersøgelse 126, 11–16.

Henriksen, N., Higgins, A.K., Kalsbeek, F., Pulvertaft, T.C.R., 2000. Greenland from Archaean to Quaternary. Descriptive text to the Geological map of Greenland 1:2 500 000. Geology of Greenland Survey Bulletin 186, 93 pp.

Hoffman, P.F., 1988. United plates of America, the birth of a craton: Early Proterozoic assembly and growth of Laurentia. Annual Review of Earth and Planetary Science 16, 543–603.

Hoffman, P.F., 1989. Precambrian geology and tectonic history of North America. In: Bally, A.W., Palmer, A.R. (Eds.), The Geology of North America; an overview. The geology of North America A, 447–512. Geological Society of America, Boulder, Colorado.

Hoffman, P.F., 1990. Dynamics of the tectonic assembly of northeast Laurentia in geon 18 (1.9–1.8 Ga). Geoscience Canada 17, 222–226.

Hurst, J.M., Peel, J.S., 1979. Late Proterozoic(?) to Silurian stratigraphy of southern Wulff Land, North Greenland. Rapport Grønlands Geologiske Undersøgelse 91, 37–56.

Jackson, G.D., 1966. Geology and mineral possibilities of the Mary River region, northern Baffin Island. Canadian Mining Journal 87(6), 57–61.

Jackson, G.D., 2000. Geology of the Clyde-Cockburn Land map area, north-central Baffin Island, Nunavut. Geological Survey of Canada Memoir 440, 303 pp.

Jackson, G.D., Hegner, E., 1991. Evolution of Late Archean to Early Proterozoic crust based on Nd isotopic data for Baffin Island and northern Quebec and Labrador. Geological Association of Canada Annual Meeting Toronto, Program with abstracts 16, p. A59.

Jackson, G.D., Hunt, P.A., Loveridge, W.D., Parrish, R.R., 1990. Reconnaissance geochronology of Baffin Island, N.W.T. Geological Survey of Canada Paper 89–2, 123–148.

Kalsbeek, F., 1981. The northward extent of the Archaean basement of Greenland – a review of Rb–Sr whole-rock ages. Precambrian Res. 14, 203–219.

Kalsbeek, F., 1986. The tectonic framework of the Precambrian shield of Greenland. A review of new isotopic evidence. In: Kalsbeek, F., Watt, W.S. (Eds.), Developments in Greenland geology. Rapport Grønlands Geologiske Undersøgelse 128, 55–64.

Kalsbeek, F., Dawes, P.R., 1980. Rb–Sr whole-rock measurements of the Kap York meta-igneous complex, Thule district, North-West Greenland. Rapport Grønlands Geologiske Undersøgelse 100, 30–33.

Kalsbeek, F., Nutman, A.P., 1996. Anatomy of the Early Proterozoic Nagssugtoqidian orogen, West Greenland, explored by reconnaissance SHRIMP U–Pb zircon dating. Geology 24(6), 515–518.

Kalsbeek, F., Nutman, A.P., Taylor, P.N., 1993. Palaeoproterozoic basement province in the Caledonian fold belt of North-East Greenland. Precambrian Res. 63, 163–178.

Kalsbeek, F., Pulvertaft, T.C.R., Nutman, A.P., 1998. Geochemistry, age and origin of metagreywackes from the Palaeoproterozoic Karrat Group, Rinkian Belt, West Greenland. Precambrian Res. 91, 383–39.

Kalsbeek, F., Nutman, A.P., Escher, J.C., Friderichsen, J.D., Hull, J.M., Jones, K.A., Pedersen, S.A.S., 1999. Geochronology of granitic and supracrustal rocks from the northern part of the East Greenland Caledonides: ion microprobe U–Pb zircon ages. Geology of Greenland Survey Bulletin 184, 31–48.

Ketchum, J.W.F., Culshaw, N.G., Barr, S.M., 2002. Anatomy and orogenic history of a Paleoproterzoic accretionary belt: the Makkovik Province, Labrador, Canada. Canadian Journal of Earth Sciences 39(5), 711–730.

Koch, L., 1933. The geology of Inglefield Land. Meddelelser om Grønland 73, 1(2) 38 pp.

Larsen, O., Dawes, P.R., 1974. K/Ar and Rb/Sr age determinations on Precambrian crystalline rocks in the Inglefield Land – Inglefield Bredning region, Thule district, western North Greenland. Rapport Grønlands Geologiske Undersøgelse 66, 4–8.

Ludwig, K., 1997. Isoplot/Ex. Berkeley Geochronology Center, Publication 1. [Allen: publisher + number of pages?]

Nutman, A.P., 1984. Precambrian gneisses and intrusive anorthosite of Smithson Bjerge, Thule district, North-West Greenland. Rapport Grønlands Geologiske Undersøgelse 119, 31 pp.

Nutman, A.P., Kalsbeek, F., 1994. Search for Archaean basement in the Caledonian fold belt of North-East Greenland. In: Higgins, A.K. (Ed.), Geology of North-East Greenland. Rapport Grønlands Geologiske Undersøgelse 162, 129–133.

Nutman, A.P., McGregor, V.R., Friend, C.R.L., Bennett, V.C., Kinny, P.D., 1996. The Itsaq Gneiss Complex of southern West Greenland; the world's most extensive record of early crustal evolution (3900–3600 Ma). Precambrian Res. 78, 1–39.

Nutman, A.P., Kalsbeek, F., Marker, M, van Gool, J.A.M., Bridgwater, D., 1999. U–Pb zircon ages of Kangâmiut dykes and detrital zircons in metasediments in the Palaeoproterozoic Nagssugtoqidian Orogen (West Greenland). Clues to the pre-collisional history of the orogen. Precambrian Res. 93, 87–104.

Oakey, G.N., 2005. Cenozoic evolution and lithosphere dynamics of the Baffin Bay Nares Strait region of Arctic Canada and Greenland. Ph.D. thesis, Vrije University, Amsterdam, Netherlands, 233 pp.

Okulitch, A.V., 1991. Geology of the Canadian Arctic Archipelago, Northwest Territories and North Greenland, 1:2 000 000. In: Trettin, H.P. (Ed.), Geology of the Innuitian Orogen and the Arctic Platform of Canada and Greenland. Geology of Canada 3, Figure 2. Geological Survey of Canada, Ottawa, Ontario. (Also: The geology of North America vol. E, Geological Society of America, Boulder, Colorado.).

Paces, J.B., Miller, J.D. Jr., 1993. Precise U-Pb ages of Duluth Complex and related mafic intrusions, northeastern Minnesota: Geochronological insights to physical, petrogenetic, paleomagnetic, and tectonomagmatic processes associated with the 1.1 Ga midcontinent rift system. J. Geophys. Res. 98, 13997–140013.

Pidgeon, R.T., 1992. Recrystallisation of oscillatory-zoned zircon: some geochronological and petrological implications. Contributions to Mineralogy and Petrology 110, 463–472.

Piper, J.D.A., Darabi, M.H., 2005. Palaeomagnetic study of the (late Mesoproterozoic) Torridon Group, NW Scotland: age, magnetostratigraphy, tectonic setting and partial magnetic overprinting by Caledonian orogeny. Precambrian Res. 142(1–2), 45–81.

Richard, P., Shimizu, N., Allègre, C. J., 1976. $^{143}Nd/^{146}Nd$, a natural tracer: an application to oceanic basalts. Earth and Planetary Science Letters, 31, 269-278.

Roest, W.R., Srivastava, S.P., 1989. Sea-floor spreading in the Labrador Sea: a new reconstruction. Geology 17, 1000–1003.

Rosing, M.T., Nutman, A.P., Løfqvist, L., 2001. A new fragment of the early Earth crust: the Aasivik terrane of West Greenland. Precambrian Res. 105, 115–128.

Schärer, U., Deutsch, A., 1990. Isotope systematics and shock-wave metamorphism: II. U–Pb and Rb–Sr in naturally shocked rocks: the Haughton Impact Structure, Canada. Geochimica et Cosmochimica Acta 54, 3435–3447.

Schjøth, F., Thorning, L., 1998. GIS compilation of geoscience data: an ArcView GIS version of previously published thematic maps from Inglefield Land, North-West Greenland. Danmarks og Grønlands Geologiske Undersøgelse Rapport 1998/107, 59 pp. + CD-ROM with 51 maps.

Schjøth, F., Steenfelt, A., Thorning, L. (Eds.), 1996. Regional compilations of geoscience data from Inglefield Land, North-West Greenland. Thematic Map Series Grønlands Geologiske Undersøgelse 96/1, 35 pp. + 51 maps.

Sharp, G., 1991. Gossan search on Inglefield Land, North-West Greenland, 22 pp. Unpublished report, RTZ Mining and Exploration Limited, Bristol, UK (in archives of the Geological Survey of Denmark and Greenland, GEUS report file 21084).

Steenfelt, A., Dam, E., 1996. Reconnaissance geochemical mapping of Inglefield Land, North-West Greenland. Danmarks og Grønlands Geologiske Undersøgelse Rapport 1998/12, 27 pp. + 49 maps.

Steenfelt, A., Dawes, P.R., Krebs, J.D., Moberg, E., Thomassen, B., 2002. Geochemical mapping of the Qaanaaq region 77°10′ to 78°10′, North-West Greenland. Danmarks og Grønlands Geologiske Undersøgelse Rapport 2002/65, 29 pp.

Stemp, R.W., Thorning, L., 1995. Airborne electromagnetic and magnetic survey of Inglefield Land, North-West Greenland. Results from project AEM Greenland 1994. Open File Series Grønlands Geologiske Undersøgelse 95/1, 45 pp.

Stern, R.A., 1998. High-resolution SIMS determination of radiogenic trace-isotope ratios in minerals. In: Cabri, L.J., Vaughan, D.J. (Eds.), Modern approaches to ore and environmental mineralogy. Min. Assoc. Can. Short Course Series 27, 241–268.

Tessensohn, F., von Gosen, W., Piepjohn, K., Saalmann, K., Mayr, U., in press. Nares transform motion and Eurekan compression: evidence from structural work on the Ellesmere coast, Arctic Canada. Geological Survey of Canada Bulletin.

Thomassen, B., Dawes, P.R., 1996. Inglefield Land 1995: geological and economic reconnaissance in North-West Greenland. Bulletin Grønlands Geologiske Undersøgelse 172, 62–68.

Thomassen, B., Dawes, P.R., Steenfelt, A., Krebs, J.D., 2002. *Qaanaaq 2001*: mineral exploration reconnaissance in North-West Greenland. Geology of Greenland Survey Bulletin 191, 133–143.

Thrane, K., Baker, J., Connelly, J., Nutman, A., 2005. Age, petrogenesis and metamorphism of the syn-collisional Proven igneous complex, West Greenland. Contributions to Mineralogy and Petrology 149, 541–555.

Trettin, H.P. (Ed.), 1991. Geology of the Innuitian Orogen and the Arctic Platform of Canada and Greenland. Geology of Canada 3, 569 pp. + map vol. Geological Survey of Canada, Ottawa, Ontario. (Also: The geology of North America E, Geological Society of America, Boulder, Colorado.)

Wardle, R.J., James, D.T., Scott, D.J., Hall, J., 2002. The southeastern Churchill Province: synthesis of a Paleoproterozoic transpressional orogen. Canadian Journal of Earth Sciences 39(5), 639–663.

Whitehouse, M.J., Kalsbeek, F., Nutman, A.P., 1998. Crystal growth and crystal recycling in the Nagssugtoqidian orogen of West Greenland: constraints from radiogenetic isotopic systematics and U–Pb zircon geochronology. Precambrian Res. 91, 365–381.

Williams, I.S., 1998. U-Th-Pb geochronology by ion microprobe. In: Applications of microanalytical techniques to understanding mineralizing processes. In: McKibben, M.A., Shanks III, W.C.P., Ridley, W.I., (Eds.), Soc. Econ. Geol. Short Course vol. 7.

Table 1. SHRIMP U–Th-Pb zircon data.

Table 2. Chemical compositions of SHRIMP investigated orthogneiss and granitoid samples

Table 3. Sm–Nd analytical data

Captions to Figures

Figure 1. Northern Greenland and adjacent Canada showing the Precambrian shield divided into the Palaeoarchaean, Neoarchaean and Palaeoproterozoic domains, and the extensive Mesoproterozoic–Phanerozoic cover. All but one of the SHRIMP dates released in this paper are located within the region framed as Fig. 2, with the outstanding one being to the northeast at Victoria Fjord. SHRIMP age of the Proven igneous complex (1869 ± 9 Ma) is from Thrane et al. (2005), the Rb–Sr date (1860 ± 25 Ma) from the same complex is from Kalsbeek (1981). The two other Rb–Sr ages are from Dawes et al. (1988); isotopic ages from Canada are from Frisch and Hunt (1988). Other ages are from unpublished data supplied by R.T. Pidgeon (zircon U–Pb) and P.N. Taylor (whole-rock Sm–Nd). **Inset map** shows regional location and main geological provinces. **B,** Baffin Island; **P,** Peary Land.

Figure 2. Geological map of Inglefield Land and northern Prudhoe Land. Six-digit numbers refer to samples for which data are presented in Tables 1 and 2: SHRIMP samples in **bold**, Sm–Nd samples in **italics**. Rb–Sr errorchron age of ca. 1850 Ma from Dawes et al. (1988) is based on samples north and south of Sunrise Pynt; the two Sm–Nd model ages of 2570 Ma and 1990 Ma are supplied by P.N. Taylor. The Sunrise Pynt Straight Belt stretches from Sunrise Pynt eastwards to the Inland Ice and is characterised by thick marble units; cf. Fig. 3. Geology is simplified from 1:500 000 maps of Dawes (1991) and Dawes and Garde (2004); Quaternary that forms extensive areas in Inglefield Land is omitted. Regional location is shown in Fig. 1. **H**, Hiawatha pluton; **Hu**, Humboldt pluton; **M**, Minturn intrusive complex; **W**, Wulff structure. In light of the SHRIMP U-Pb zircon dating of detrital zircons from sample 425507 presented in this paper, the sedimentary rocks south of the Sunrise Pynt Straight Belt, designated as Etah Group in this Figure, are probably better assigned to the Prudhoe Land Supracrustal Complex. This has not been modified here, in order to maintain consistency with maps published by the Geological Survey of Denmark and Greenland.

Figure 3. (**a**) View across the largest nunatak exposing the Victoria Fjord Complex. The nunatak is capped by Neoproterozoic? and Cambrian homoclinal strata of the Arctic Platform sequence (“Phanerozoic”). In right foreground, a ca. 200 m high cliff comprises Victoria Fjord Complex orthogneisses (“og”) with a sub-concordant amphibolite layer/lens (“a”). The easternmost and smallest nunatak exposing the Victoria Fjord Complex is seen in the background. (**b**) Contact

between Neoarchaean orthogneisses of the Thule mixed-gneiss complex and overlying, more recessive (rusty-weathering) Palaeoproterozoic Prudhoe Land supracrustal complex. The compositional layering in both units are concordant, but the contact between them is interpreted as a tectonised unconformity. The supracrustal rocks are preserved in the core of a regional isocline. North coast of Inglefield Bredning with the foreground summit about 600 m a.s.l. (**c**) Metaquartzite showing highly deformed pelitic seams. Sample 243506 was taken from this unit. Location is northwest of Morris Jesup Gletscher. Notebook for scale is 17 cm long. (d) Central part of the steeply dipping Sunrise Pynt Straight Belt in the cliffs north of Sunrise Pynt. Marble ("marb") and pelitic schist ("pel") are invaded by dioritic and granitic rocks transformed into gneisses ("og"). Height of cliffs is ca. 300 m.

Figure 4. Total magnetic intensity map of Inglefield Land modified from Schjøth et al. (1996). The E–W-trending Sunrise Pynt Straight Belt is seen as a conspicuous as a linear feature up to 15 km wide separating the IMB from the southern terrane that stretches south into Prudhoe Land. Two syenitic masses – the Minturn intrusive complex in central Inglefield Land and the Humboldt pluton in the extreme northeast – are also outlined by the magnetic mapping, cf. Fig. 2.

Figure 5. CL images of zircons from two orthogneiss samples (470214 and 243495) from the Thule mixed-gneiss complex, Prudhoe Land.

Figure 6. U–Pb Tera-Wasserburg concordia diagrams for four orthogneiss samples from Prudhoe Land: 470214 and 242495 from the Thule mixed-gneiss complex; 140944 and 243459 from the Prudhoe Land granulite complex.

Figure 7. CL images of zircons from two orthogneiss samples (140944 and 243459) from northern outcrops of the Prudhoe Land granulite complex at Sonntag Bugt.

Figure 8. CL images of zircons from two metasediments from either side of the Sunrise Pynt Straight Belt: metaquartzite (425507) from southern Inglefield Land and paragneiss (440314) from northeastern Inglefield Land.

Figure 9. U–Pb Tera-Wasserburg concordia diagrams for four metasediments showing contrast in detrital zircon provenance in samples north and south of the Sunrise Pynt Straight Belt: metaquartzites (243506 and 425507) from the south, paragneisses (440314 and 440321) from the north.

Figure 10. CL images of zircons from two meta-igneous rocks of Inglefield Land: 425542 a greenish, hypersthene quartz diorite from the Hiawatha pluton and 425583, a grey orthogneiss or deformed late granite from within the Minturn intrusive complex.

Figure 11. U–Pb Tera-Wasserburg concordia diagram for five rocks from the Etah meta-igneous complex of Inglefield Land.

Figure 12. U–Pb Tera-Wasserburg concordia diagram for three late granitoid rocks from Inglefield Land.

Figure 13. CL and transmitted light images of zircons from granitic gneiss 312632 from Victoria Fjord.

Figure 14. U–Pb Tera-Wasserburg concordia diagram for analyses of zircons from sample 312632 from Victoria Fjord.

Figure 15. Time versus ε_{Nd} plot for Inglefield Mobile Belt samples

Figure 16. Diagram summarising the SHRIMP zircon geochronology of this study that leads to the recognition of three terranes from south to north in northern Greenland.

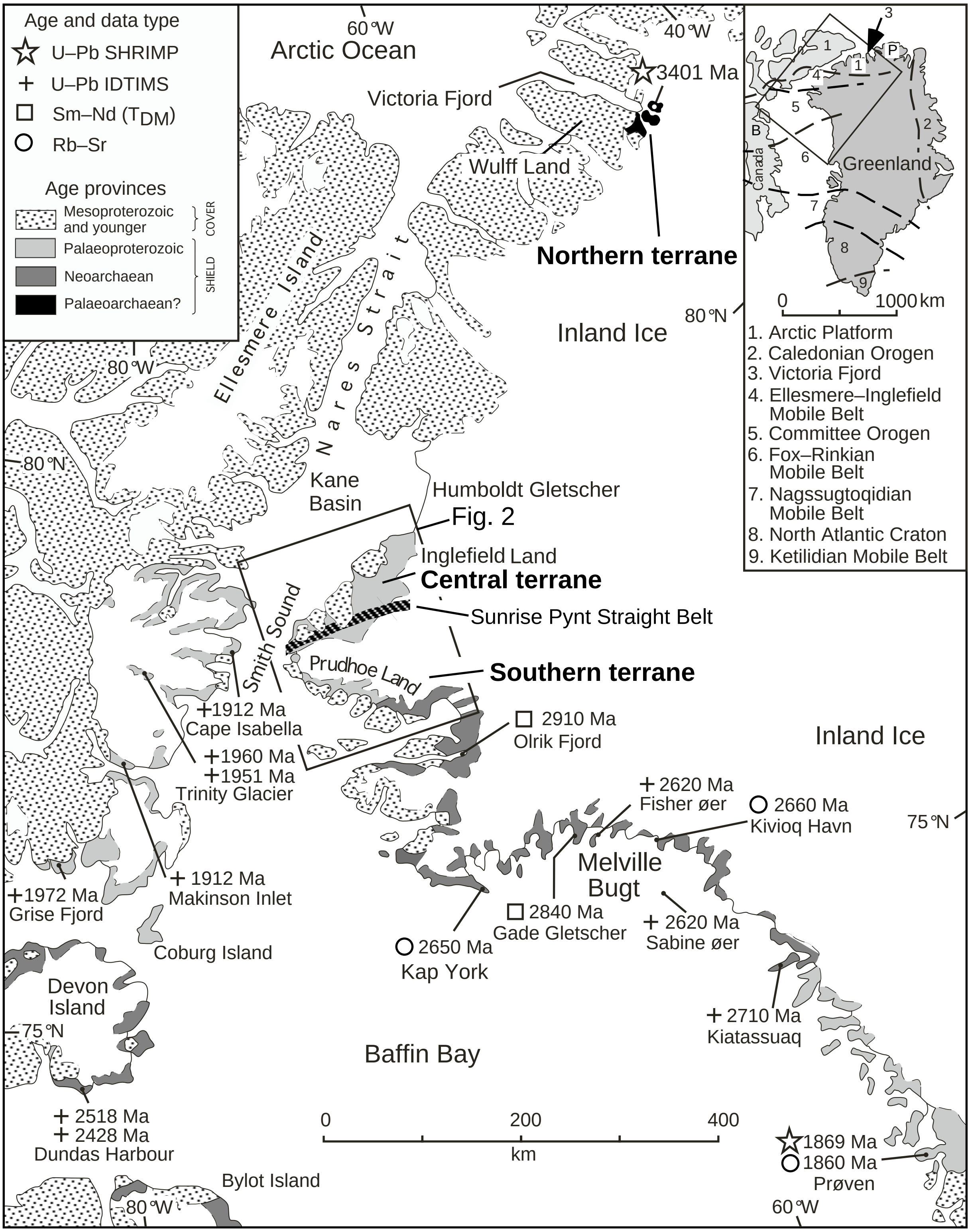

Age and data type
U–Pb SHRIMP
U–Pb IDTIMS
Sm–Nd (T_DM)
Rb–Sr
Age provinces
Mesoproterozoic and younger
Palaeoproterozoic
Neoarchaean
Palaeoarchaean?
COVER
SHIELD
Arctic Ocean
60°W
40°W
3401 Ma
Victoria Fjord
Wulff Land
Northern terrane
Ellesmere Island
Nares Strait
80°W
80°N
Inland Ice
Kane Basin
Humboldt Gletscher
Fig. 2
Inglefield Land
Central terrane
Sunrise Pynt Straight Belt
Smith Sound
Prudhoe Land
Southern terrane
1912 Ma
Cape Isabella
1960 Ma
1951 Ma
Trinity Glacier
2910 Ma
Olrik Fjord
Inland Ice
2620 Ma
Fisher øer
2660 Ma
Kivioq Havn
75°N
Melville Bugt
1912 Ma
Makinson Inlet
1972 Ma
Grise Fjord
2840 Ma
Gade Gletscher
2620 Ma
Sabine øer
Coburg Island
2650 Ma
Kap York
Devon Island
75°N
2710 Ma
Kiatassuaq
Baffin Bay
0
200
400
km
2518 Ma
2428 Ma
Dundas Harbour
1869 Ma
1860 Ma
Prøven
Bylot Island
80°W
60°W
3
P
B
Canada
Greenland
0
1000 km
1. Arctic Platform
2. Caledonian Orogen
3. Victoria Fjord
4. Ellesmere–Inglefield Mobile Belt
5. Committee Orogen
6. Fox–Rinkian Mobile Belt
7. Nagssugtoqidian Mobile Belt
8. North Atlantic Craton
9. Ketilidian Mobile Belt

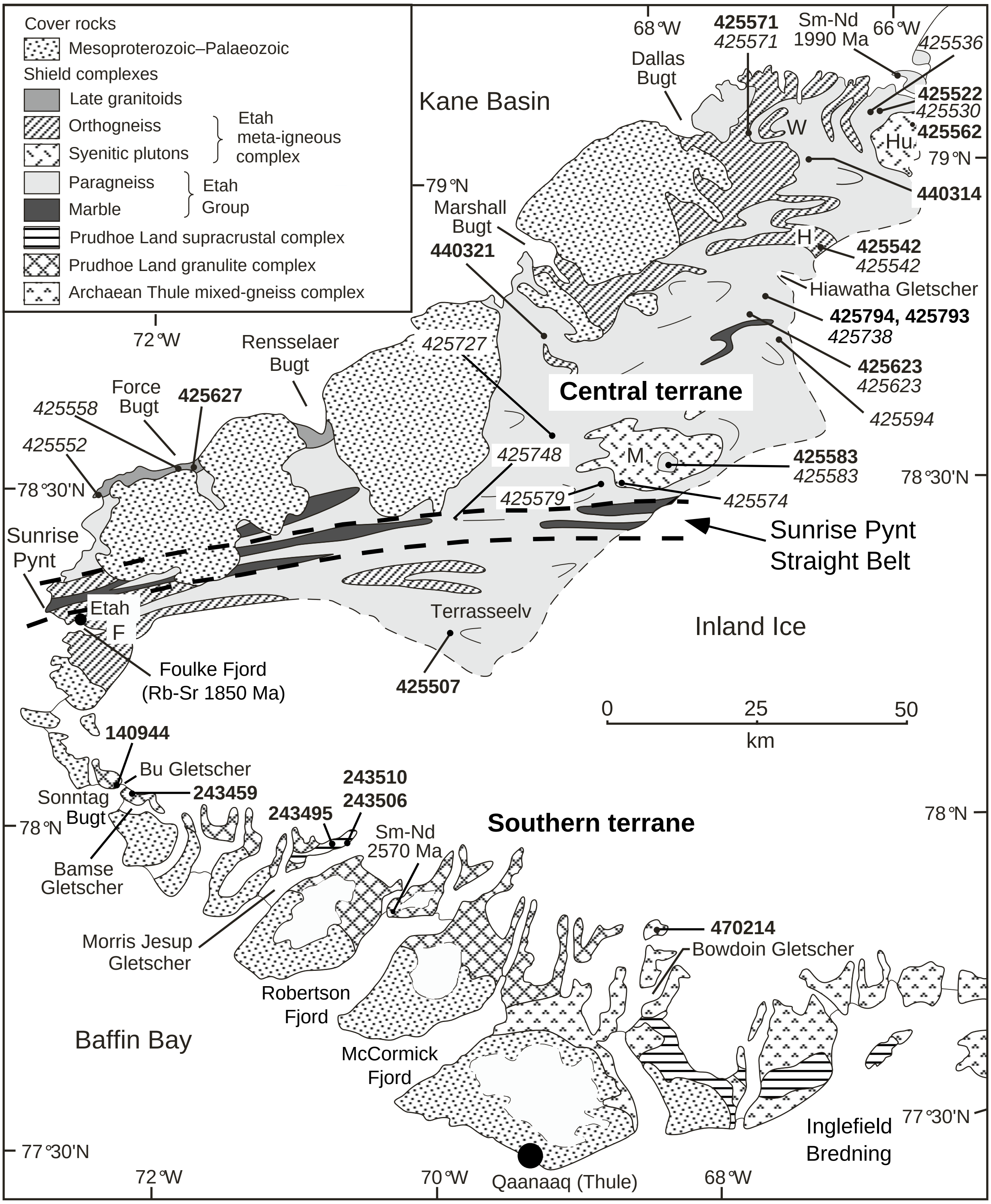
Cover rocks
Mesoproterozoic–Palaeozoic
Shield complexes
Late granitoids
Orthogneiss
Syenitic plutons
Etah meta-igneous complex
Paragneiss
Marble
Etah Group
Prudhoe Land supracrustal complex
Prudhoe Land granulite complex
Archaean Thule mixed-gneiss complex
Kane Basin
Central terrane
Southern terrane
Sunrise Pynt Straight Belt
Inland Ice
Baffin Bay
Dallas Bugt
Marshall Bugt
Rensselaer Bugt
Force Bugt
Sunrise Pynt
Etah
F
Foulke Fjord
(Rb-Sr 1850 Ma)
Sm-Nd
1990 Ma
Sm-Nd
2570 Ma
Hiawatha Gletscher
Terrasseelv
W
H
Hu
M
Bu Gletscher
Sonntag Bugt
Bamse Gletscher
Morris Jesup Gletscher
Robertson Fjord
McCormick Fjord
Bowdoin Gletscher
Inglefield Bredning
Qaanaaq (Thule)
425571
425571
425536
425522
425530
425562
440314
425542
425542
440321
425794, 425793
425738
425623
425623
425594
425727
425558
425627
425552
425748
425583
425583
425579
425574
425507
140944
243459
243510
243506
243495
470214
0
25
50
km
68°W
66°W
72°W
70°W
79°N
78°30'N
78°N
77°30'N

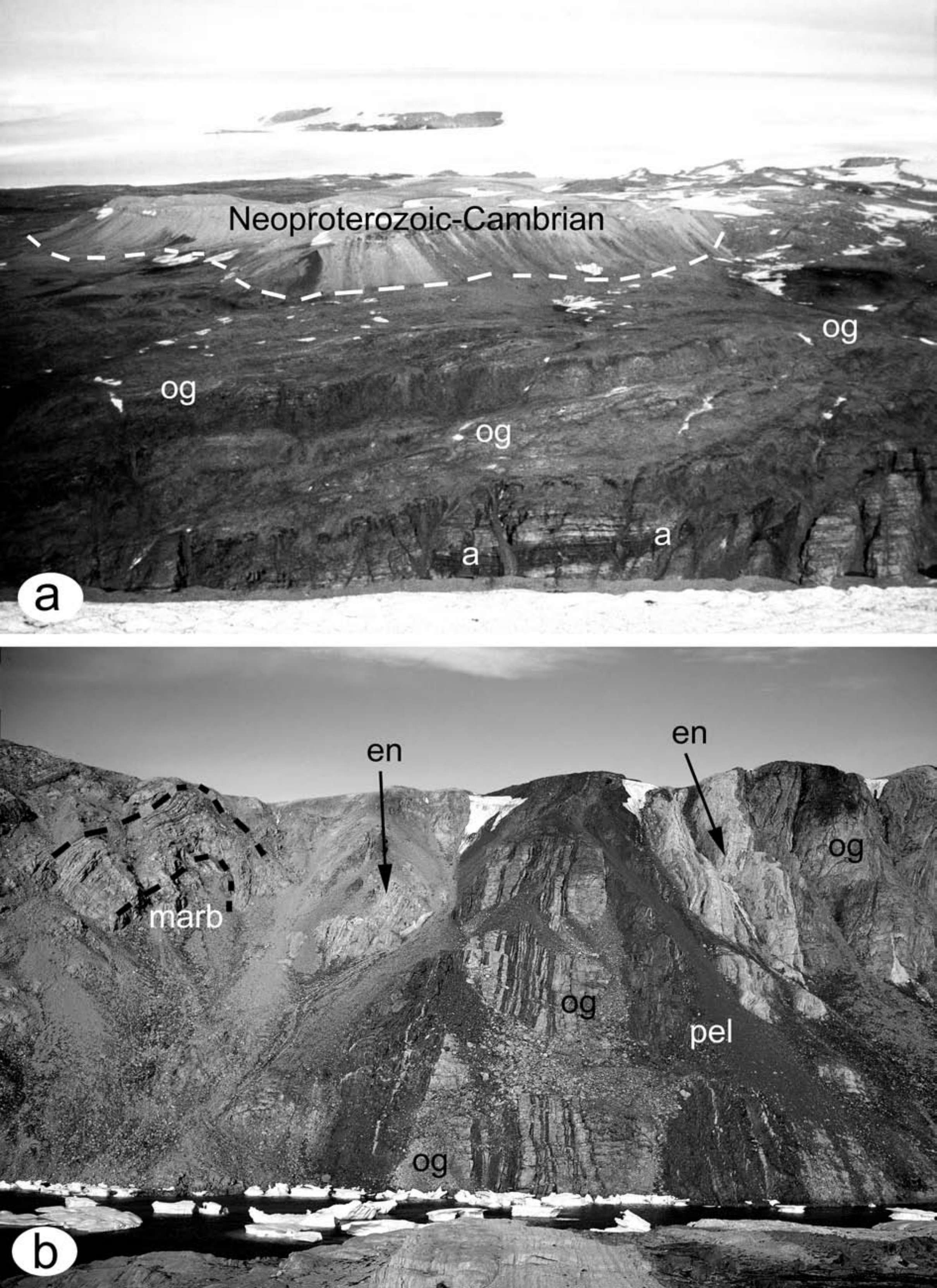

a
Neoproterozoic-Cambrian
og
og
og
a
a
b
en
en
marb
og
og
pel
og

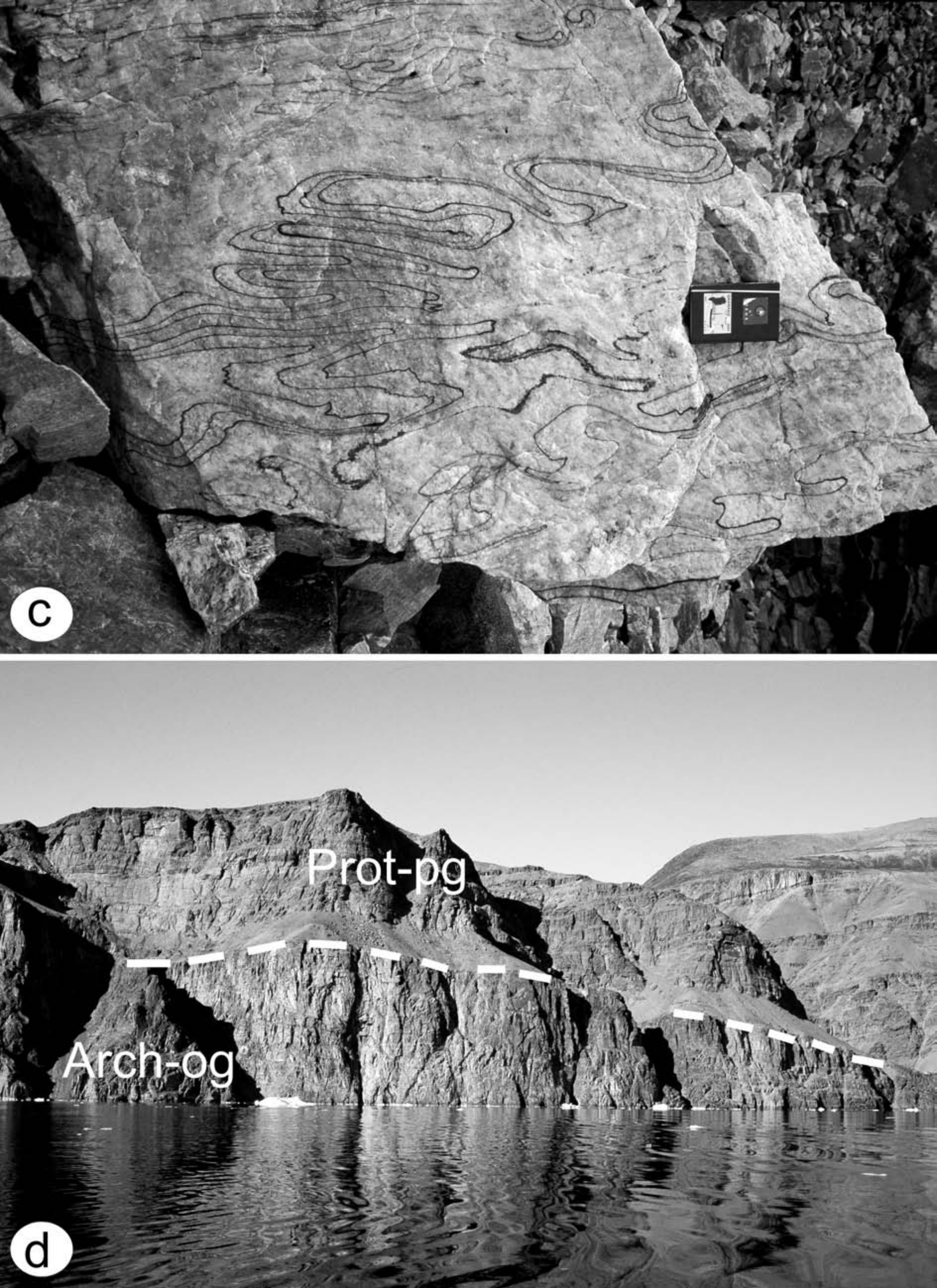
c
Prot-pg
Arch-og
d

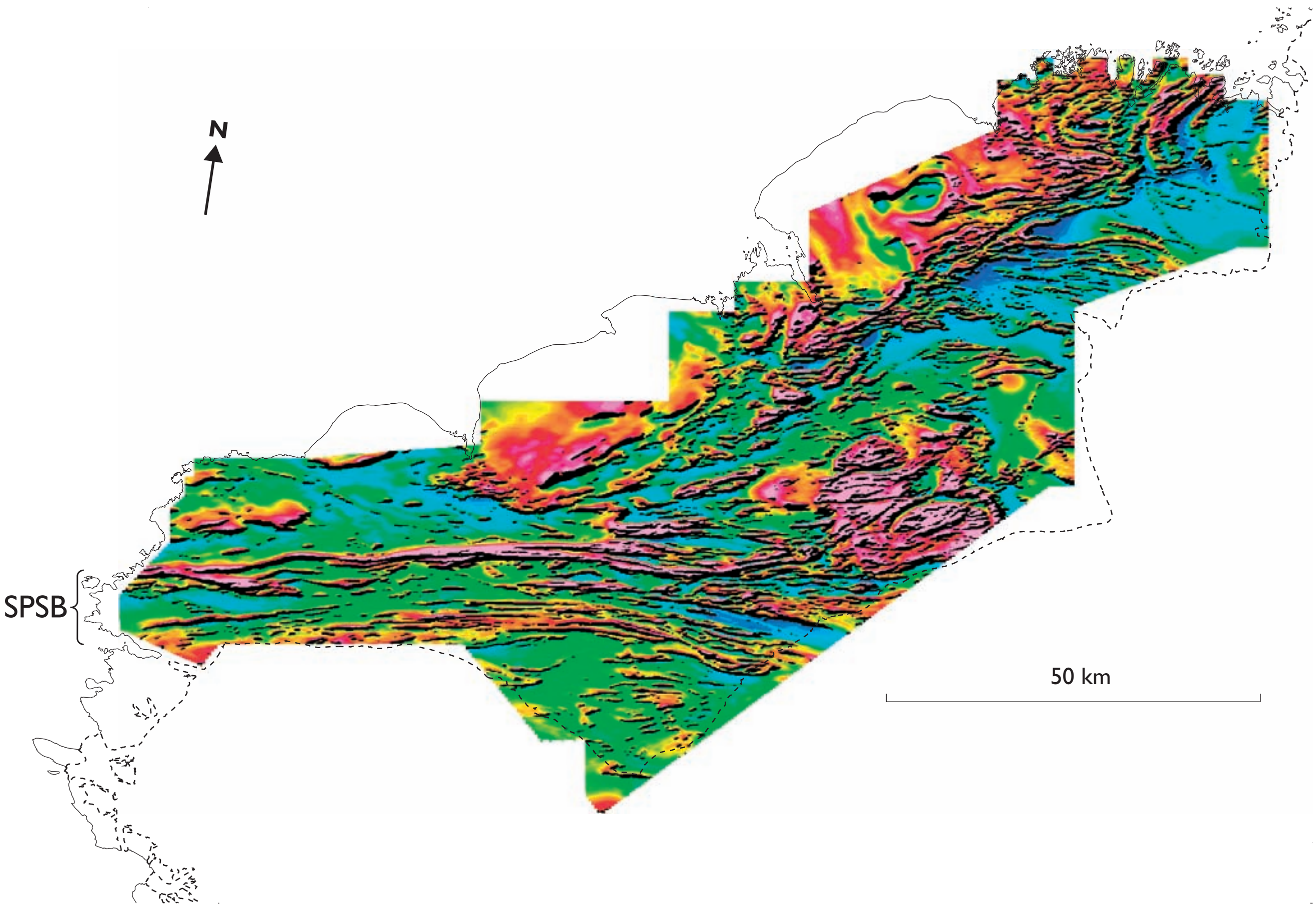
N
SPSB
50 km

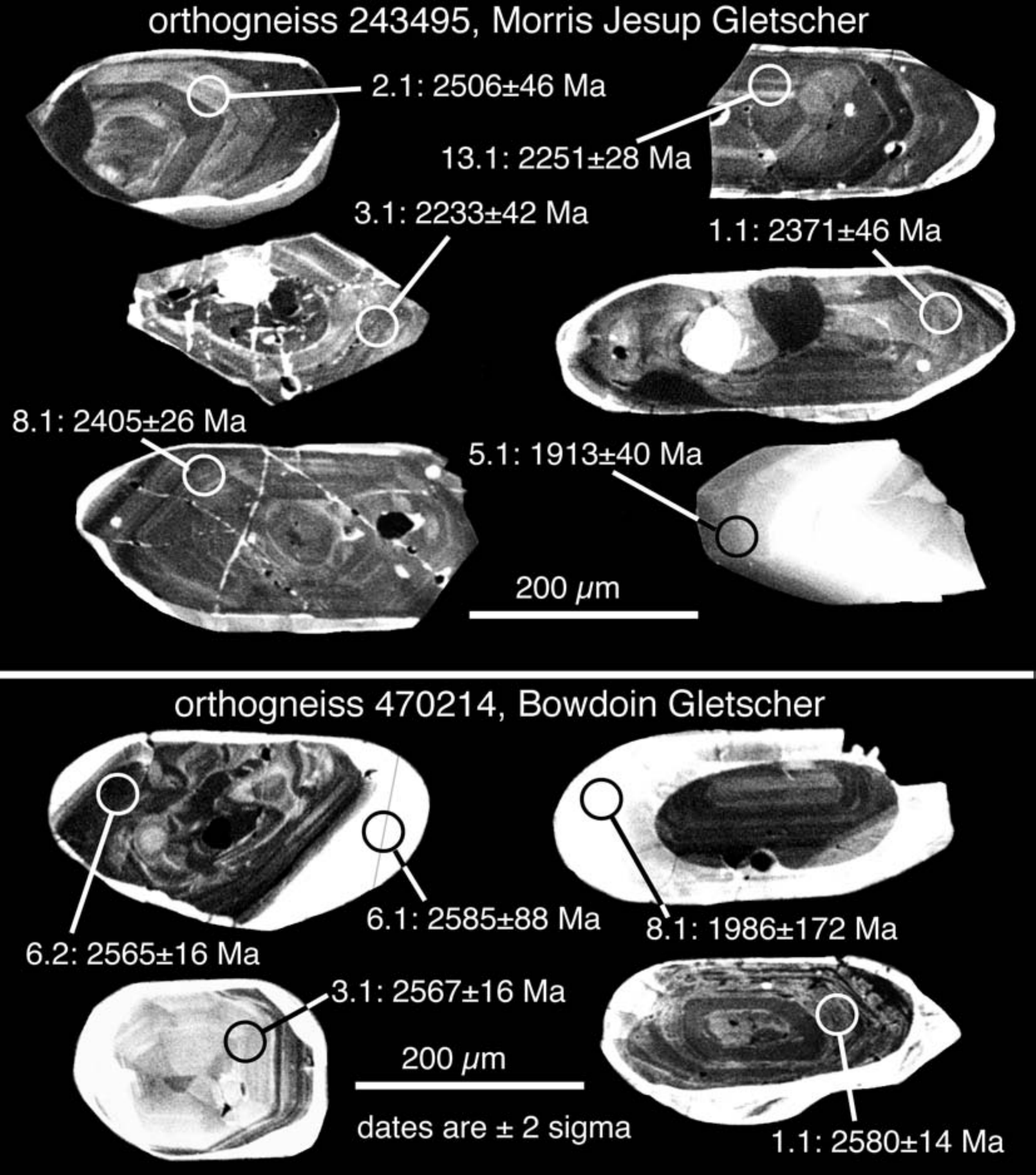
orthogneiss 243495, Morris Jesup Gletscher
2.1: 2506±46 Ma
13.1: 2251±28 Ma
3.1: 2233±42 Ma
1.1: 2371±46 Ma
8.1: 2405±26 Ma
5.1: 1913±40 Ma
200 μm
orthogneiss 470214, Bowdoin Gletscher
6.1: 2585±88 Ma
8.1: 1986±172 Ma
6.2: 2565±16 Ma
3.1: 2567±16 Ma
200 μm
dates are ± 2 sigma
1.1: 2580±14 Ma

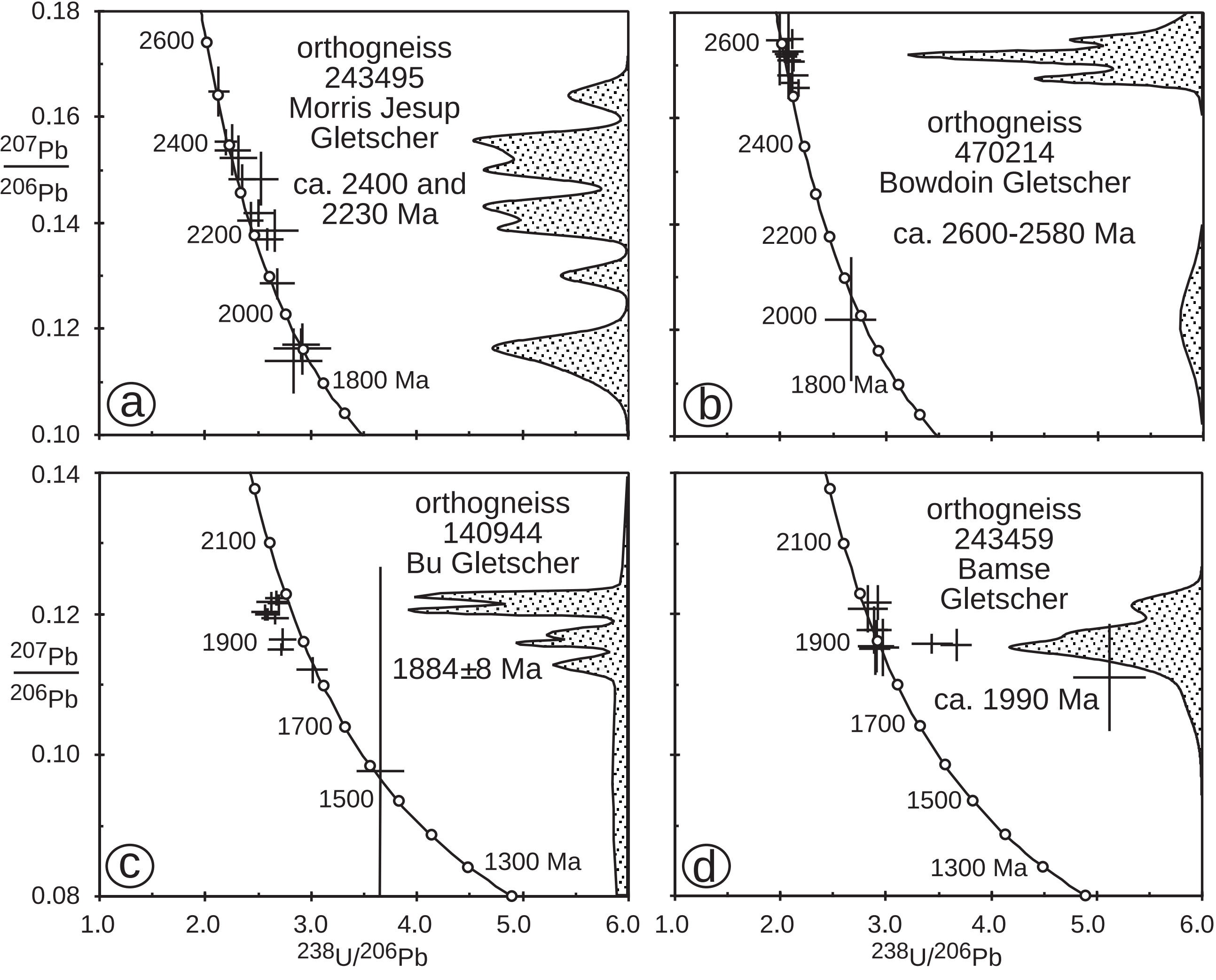

orthogneiss
243495
Morris Jesup
Gletscher
ca. 2400 and
2230 Ma
2600
2400
2200
2000
1800 Ma
a
orthogneiss
470214
Bowdoin Gletscher
ca. 2600-2580 Ma
2600
2400
2200
2000
1800 Ma
b
orthogneiss
140944
Bu Gletscher
1884±8 Ma
2100
1900
1700
1500
1300 Ma
c
orthogneiss
243459
Bamse
Gletscher
ca. 1990 Ma
2100
1900
1700
1500
1300 Ma
d
207Pb/206Pb
238U/206Pb
0.18
0.16
0.14
0.12
0.10
0.08
1.0
2.0
3.0
4.0
5.0
6.0

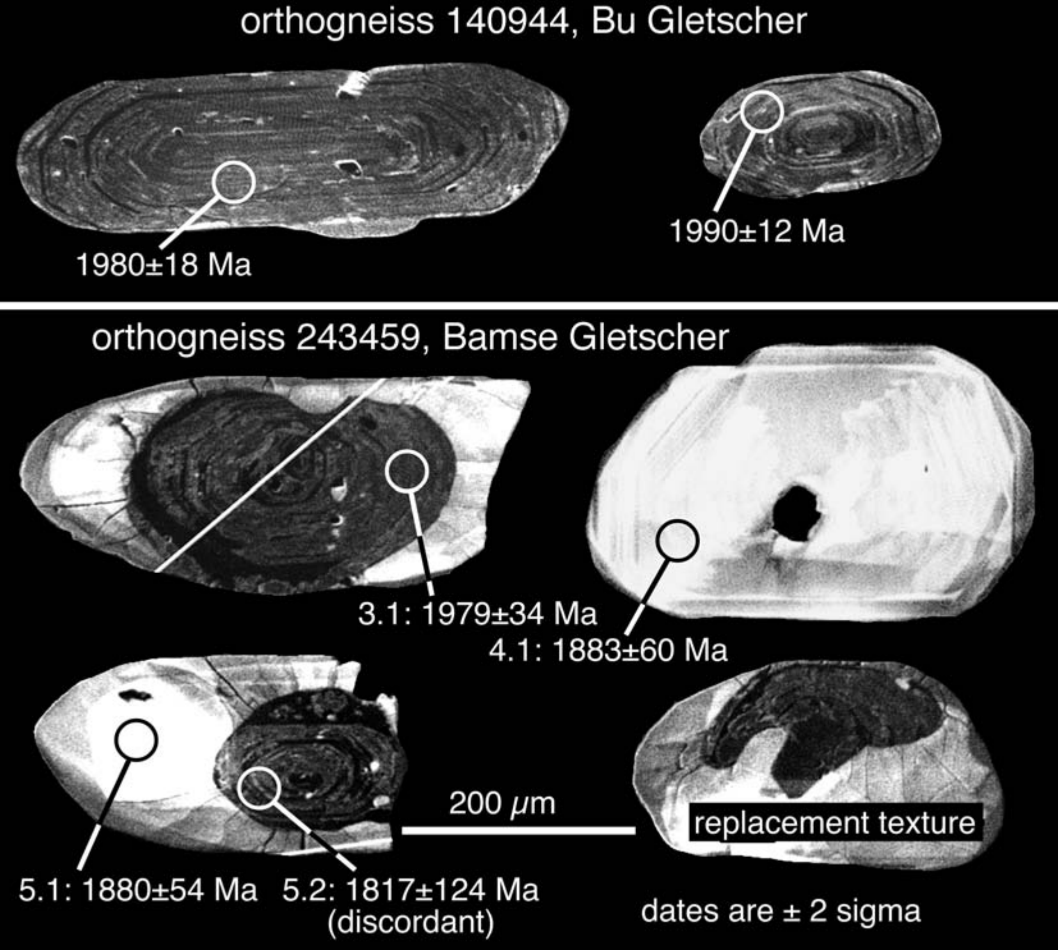
orthogneiss 140944, Bu Gletscher
1980±18 Ma
1990±12 Ma
orthogneiss 243459, Bamse Gletscher
3.1: 1979±34 Ma
4.1: 1883±60 Ma
5.1: 1880±54 Ma
5.2: 1817±124 Ma
(discordant)
200 μm
replacement texture
dates are ± 2 sigma

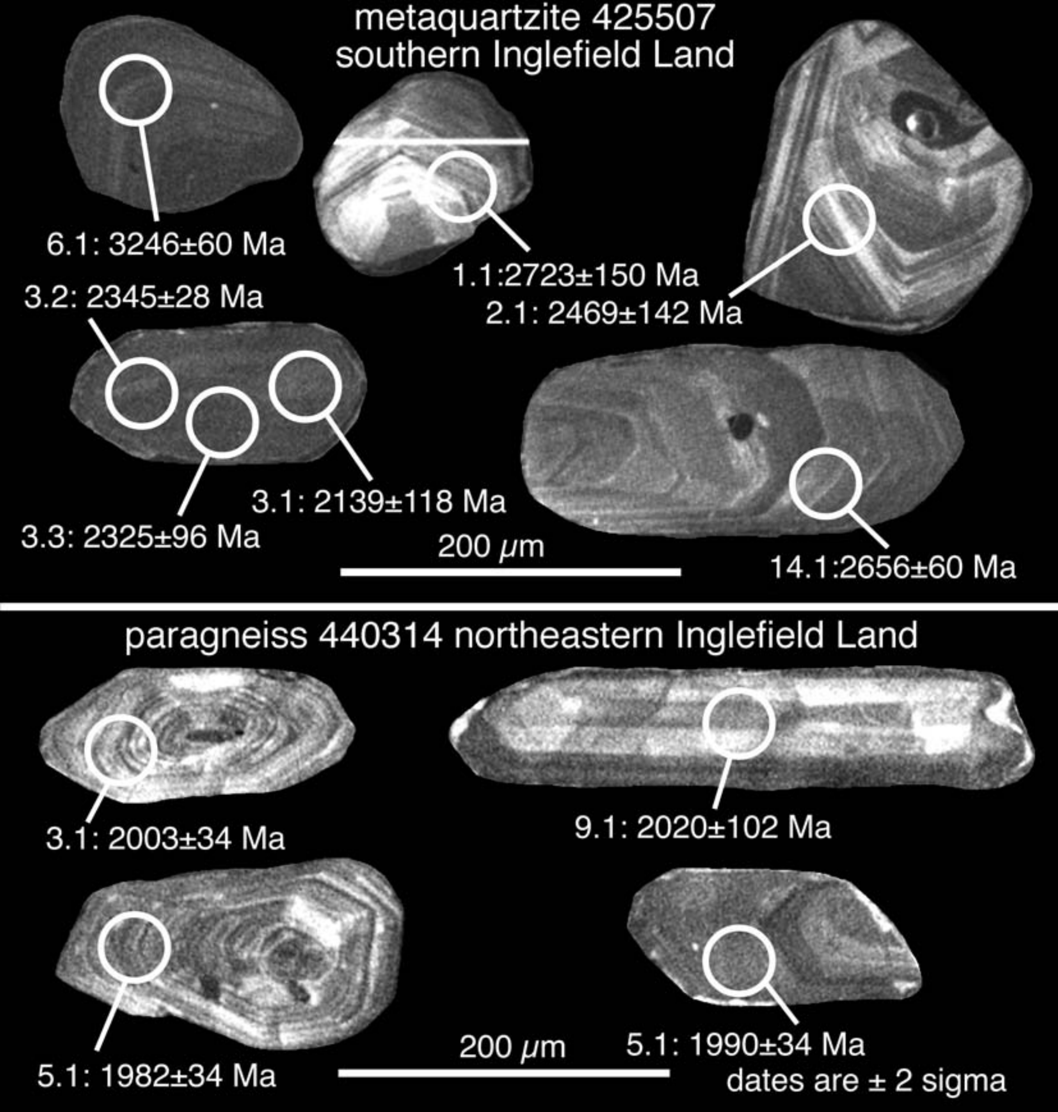
metaquartzite 425507
southern Inglefield Land
6.1: 3246±60 Ma
1.1:2723±150 Ma
2.1: 2469±142 Ma
3.2: 2345±28 Ma
3.1: 2139±118 Ma
3.3: 2325±96 Ma
200 μm
14.1:2656±60 Ma
paragneiss 440314 northeastern Inglefield Land
3.1: 2003±34 Ma
9.1: 2020±102 Ma
5.1: 1982±34 Ma
200 μm
5.1: 1990±34 Ma
dates are ± 2 sigma

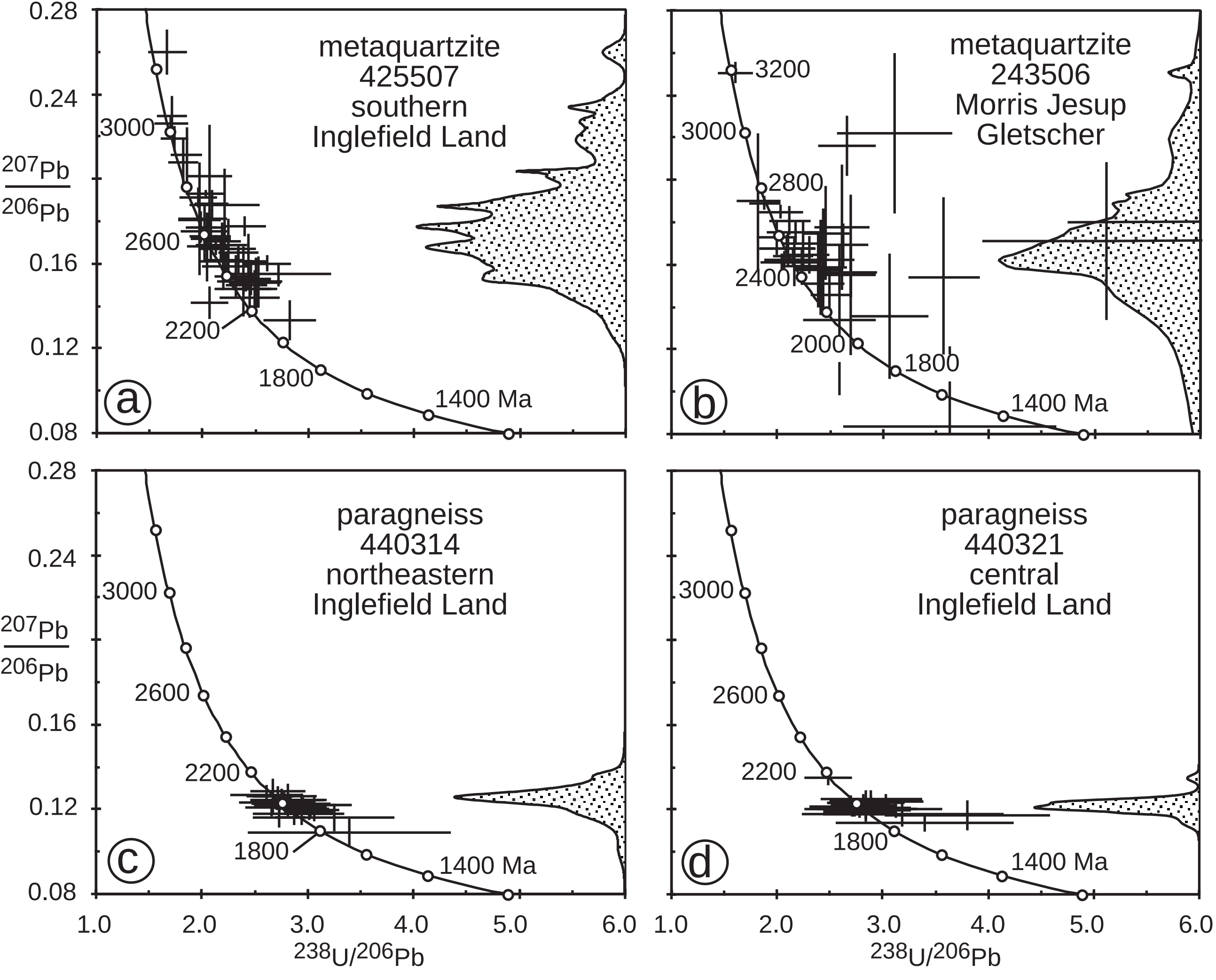
metaquartzite
425507
southern
Inglefield Land
metaquartzite
243506
Morris Jesup
Gletscher
paragneiss
440314
northeastern
Inglefield Land
paragneiss
440321
central
Inglefield Land
a
b
c
d
3200
3000
2800
2600
2400
2200
2000
1800
1400 Ma
0.28
0.24
0.16
0.12
0.08
1.0
2.0
3.0
4.0
5.0
6.0
207Pb/206Pb
238U/206Pb

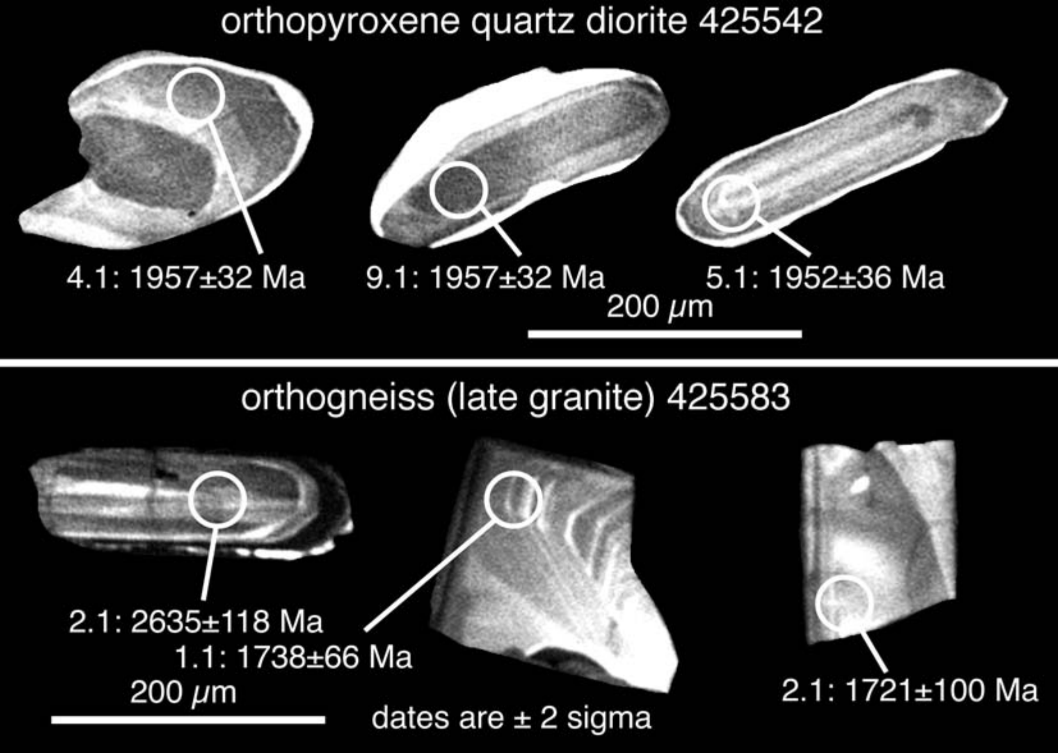
orthopyroxene quartz diorite 425542
4.1: 1957±32 Ma
9.1: 1957±32 Ma
5.1: 1952±36 Ma
200 μm
orthogneiss (late granite) 425583
2.1: 2635±118 Ma
1.1: 1738±66 Ma
200 μm
dates are ± 2 sigma
2.1: 1721±100 Ma

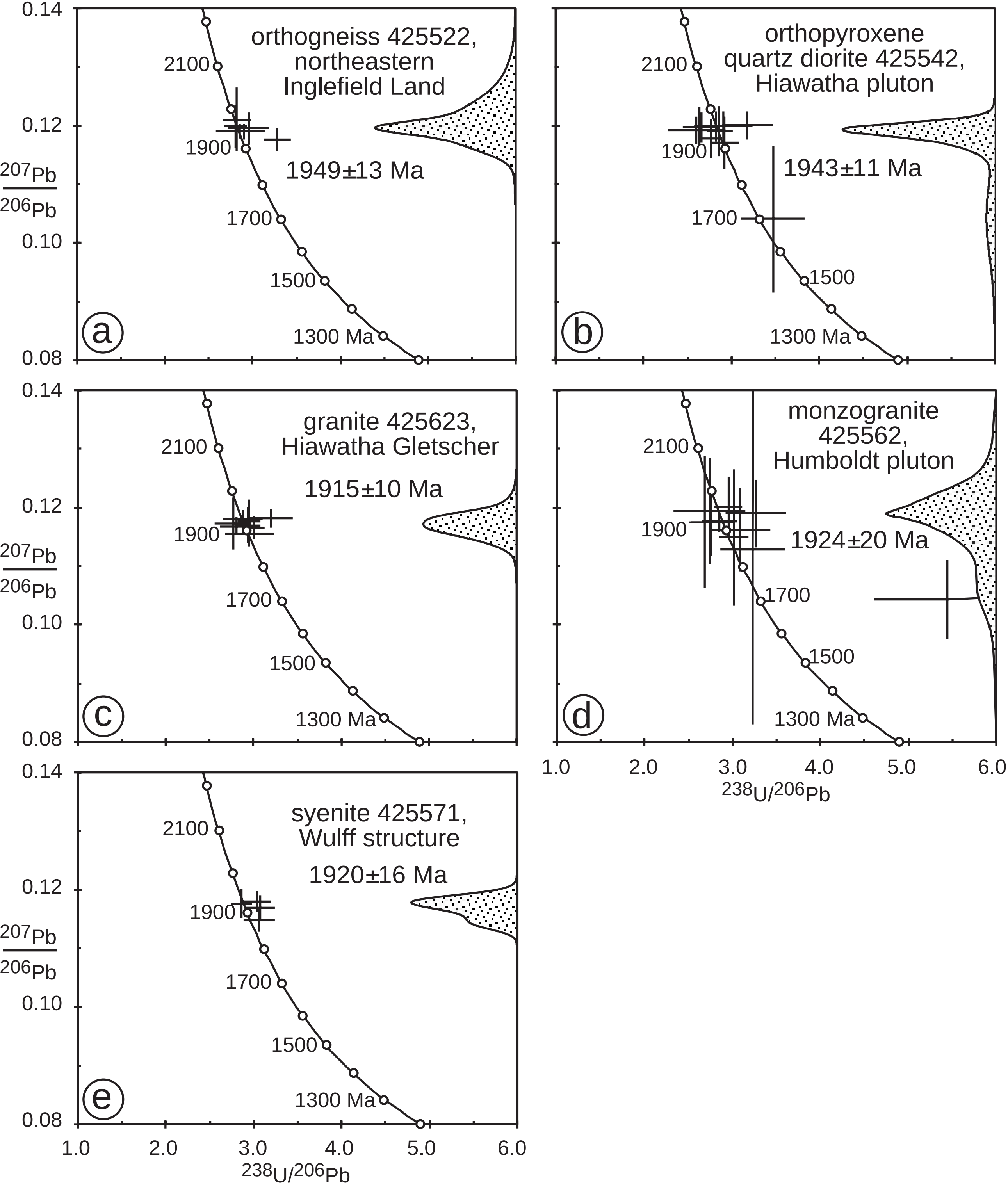
orthogneiss 425522, northeastern Inglefield Land
1949±13 Ma
orthopyroxene quartz diorite 425542, Hiawatha pluton
1943±11 Ma
granite 425623, Hiawatha Gletscher
1915±10 Ma
monzogranite 425562, Humboldt pluton
1924±20 Ma
syenite 425571, Wulff structure
1920±16 Ma
a
b
c
d
e
2100
1900
1700
1500
1300 Ma
0.14
0.12
0.10
0.08
207Pb/206Pb
1.0
2.0
3.0
4.0
5.0
6.0
238U/206Pb

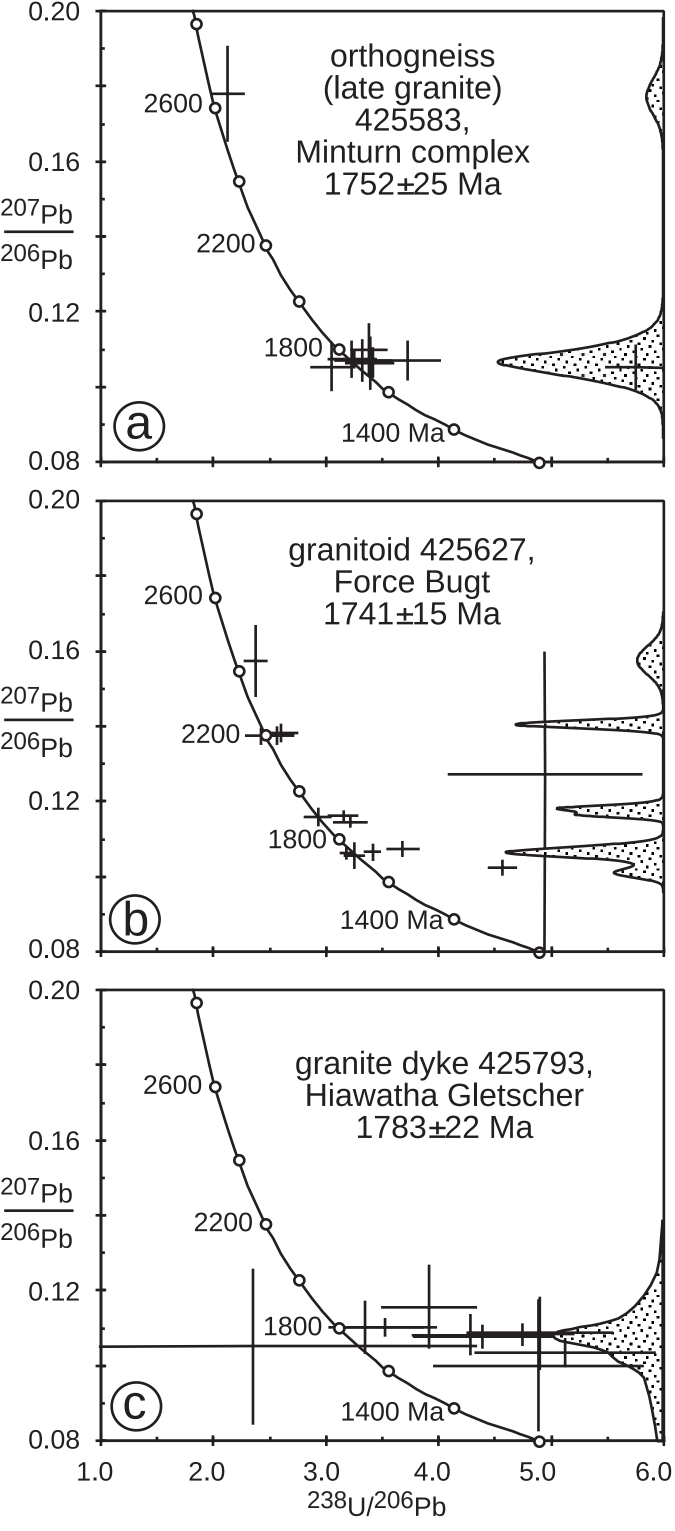
orthogneiss
(late granite)
425583,
Minturn complex
1752±25 Ma
a
granitoid 425627,
Force Bugt
1741±15 Ma
b
granite dyke 425793,
Hiawatha Gletscher
1783±22 Ma
c
2600
2200
1800
1400 Ma
0.20
0.16
0.12
0.08
207Pb/206Pb
1.0
2.0
3.0
4.0
5.0
6.0
238U/206Pb

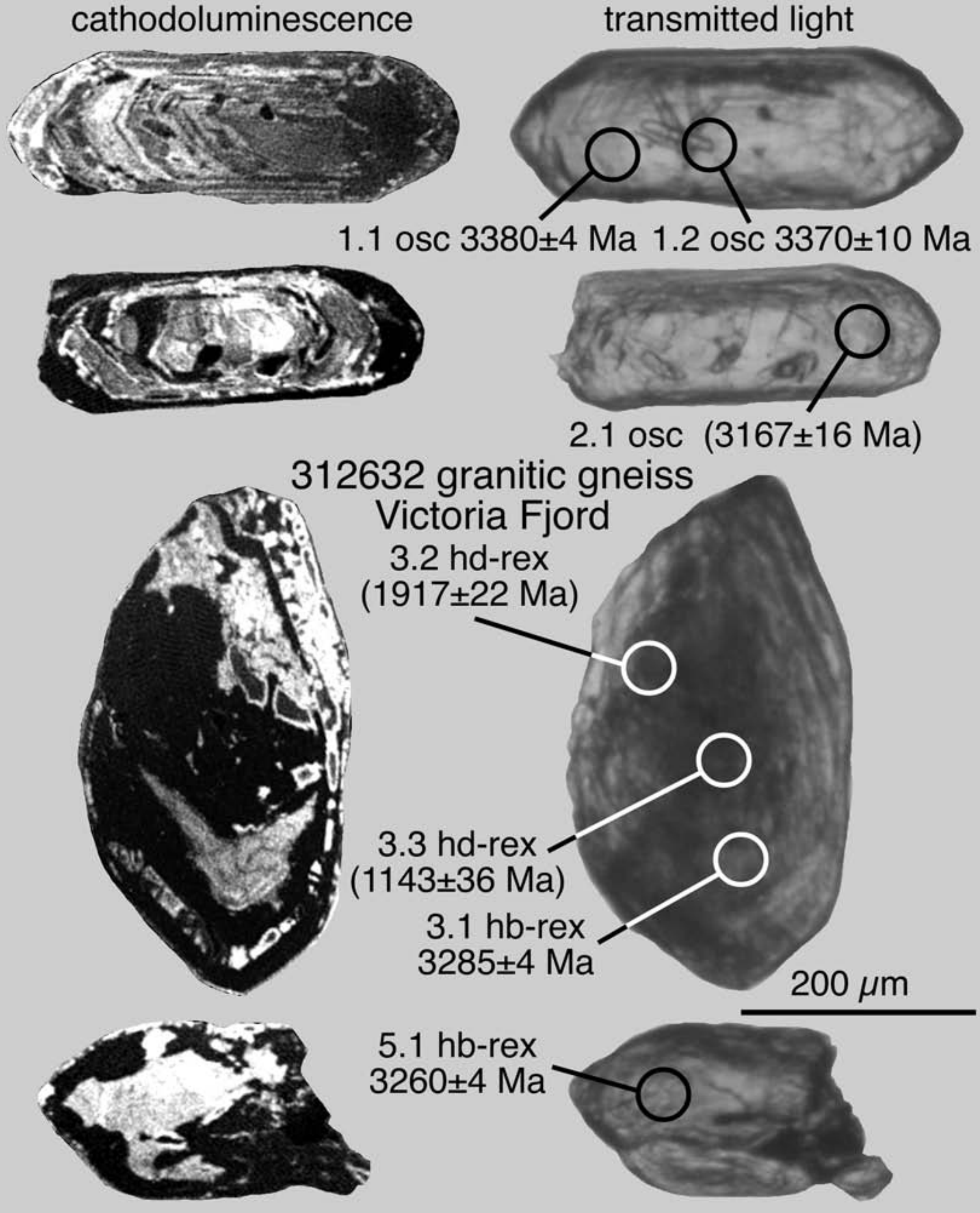

cathodoluminescence
transmitted light
1.1 osc 3380±4 Ma
1.2 osc 3370±10 Ma
2.1 osc (3167±16 Ma)
312632 granitic gneiss
Victoria Fjord
3.2 hd-rex
(1917±22 Ma)
3.3 hd-rex
(1143±36 Ma)
3.1 hb-rex
3285±4 Ma
200 μm
5.1 hb-rex
3260±4 Ma

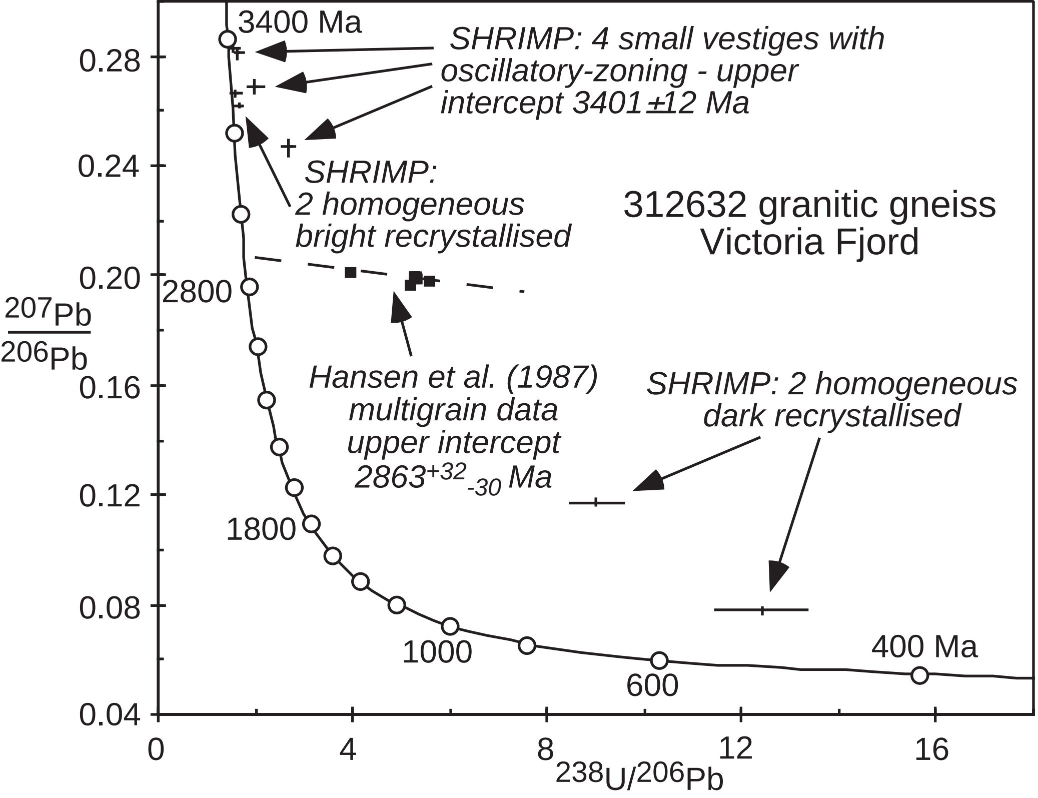

3400 Ma
SHRIMP: 4 small vestiges with oscillatory-zoning - upper intercept 3401±12 Ma
SHRIMP: 2 homogeneous bright recrystallised
312632 granitic gneiss
Victoria Fjord
2800
Hansen et al. (1987) multigrain data upper intercept 2863+32-30 Ma
SHRIMP: 2 homogeneous dark recrystallised
1800
1000
600
400 Ma
0.28
0.24
0.20
0.16
0.12
0.08
0.04
207Pb/206Pb
0
4
8
12
16
238U/206Pb

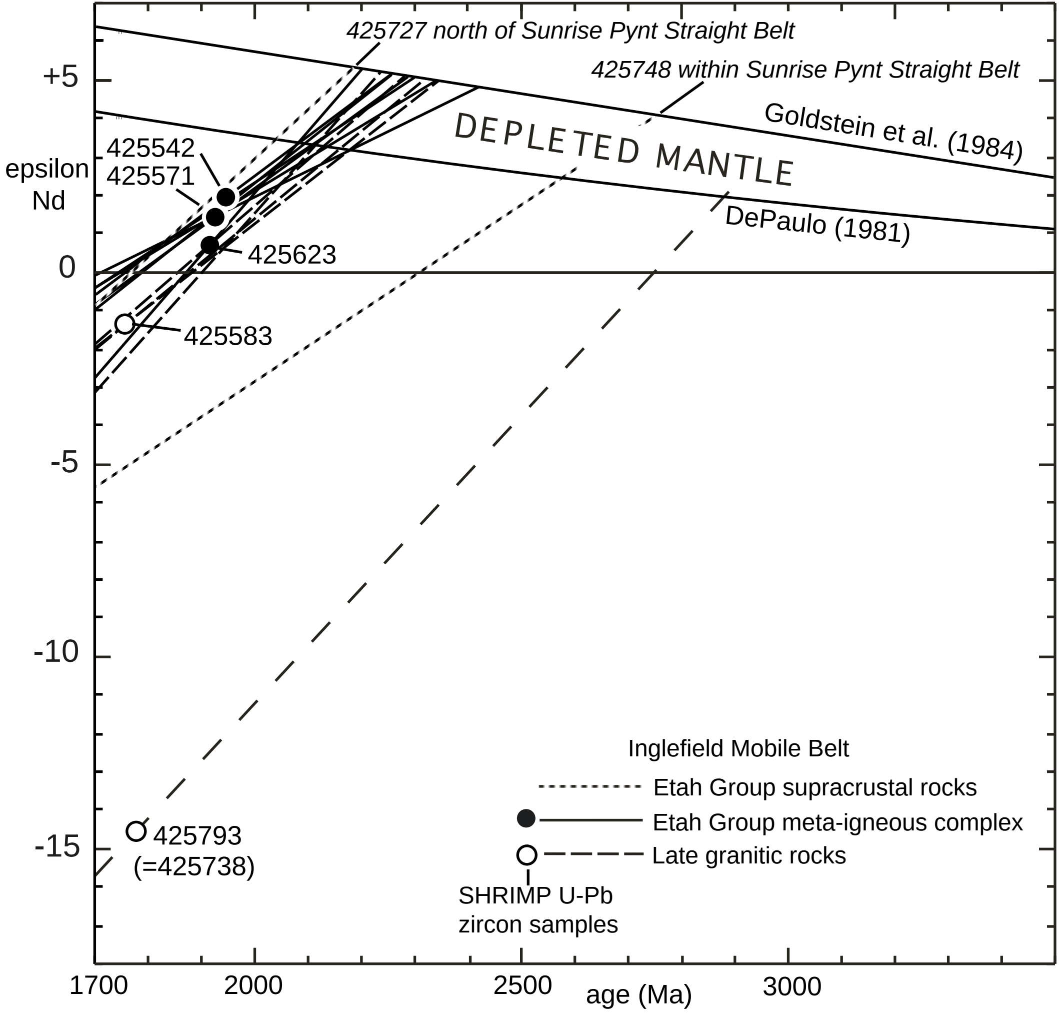

425727 north of Sunrise Pynt Straight Belt
425748 within Sunrise Pynt Straight Belt
Goldstein et al. (1984)
DEPLETED MANTLE
DePaulo (1981)
epsilon Nd
+5
0
-5
-10
-15
425542
425571
425623
425583
425793
(=425738)
Inglefield Mobile Belt
Etah Group supracrustal rocks
Etah Group meta-igneous complex
Late granitic rocks
SHRIMP U-Pb zircon samples
1700
2000
2500
3000
age (Ma)

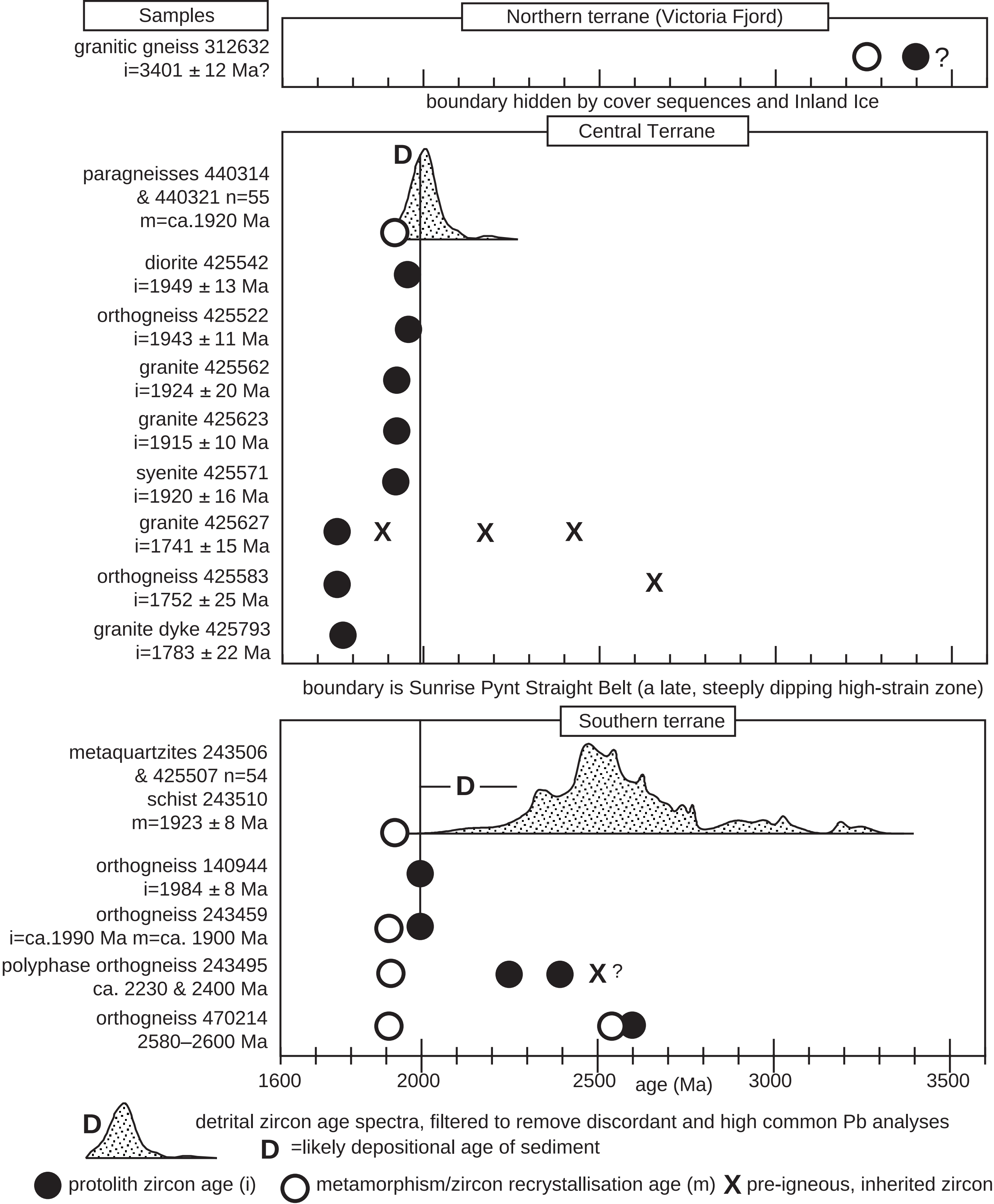

Samples
Northern terrane (Victoria Fjord)
granitic gneiss 312632
i=3401 ± 12 Ma?
?
boundary hidden by cover sequences and Inland Ice
Central Terrane
D
paragneisses 440314
& 440321 n=55
m=ca.1920 Ma
diorite 425542
i=1949 ± 13 Ma
orthogneiss 425522
i=1943 ± 11 Ma
granite 425562
i=1924 ± 20 Ma
granite 425623
i=1915 ± 10 Ma
syenite 425571
i=1920 ± 16 Ma
granite 425627
i=1741 ± 15 Ma
X
X
X
orthogneiss 425583
i=1752 ± 25 Ma
X
granite dyke 425793
i=1783 ± 22 Ma
boundary is Sunrise Pynt Straight Belt (a late, steeply dipping high-strain zone)
Southern terrane
metaquartzites 243506
& 425507 n=54
schist 243510
m=1923 ± 8 Ma
D
orthogneiss 140944
i=1984 ± 8 Ma
orthogneiss 243459
i=ca.1990 Ma m=ca. 1900 Ma
polyphase orthogneiss 243495
ca. 2230 & 2400 Ma
X ?
orthogneiss 470214
2580–2600 Ma
1600
2000
2500
3000
3500
age (Ma)
D
detrital zircon age spectra, filtered to remove discordant and high common Pb analyses
D =likely depositional age of sediment
protolith zircon age (i)
metamorphism/zircon recrystallisation age (m)
X pre-igneous, inherited zircon

Table 1. Chemical compositions of SHRIMP investigated orthogneiss and granitoid samples

	Victoria Fjord complex	Thule mixed gneiss complex			Prudhoe Land granulite complex		Etah meta-igneous complex					Late granitoids		
Sample no.	312632	243494*	243496*	470214	140944	243459	425522	425542	425623	425562	425571	425583	425627	425793
SiO_2	73.69	73.60	57.93	55.72	61.95	55.55	61.70	66.61	71.39	64.95	60.61	67.66	58.77	70.21
TiO_2	0.11	0.41	1.75	0.69	0.84	0.72	0.67	0.49	0.73	1.15	0.26	0.68	0.26	0.48
Al_2O_3	14.08	13.07	15.09	20.85	16.95	20.95	12.72	16.28	14.22	14.78	18.71	14.74	24.03	14.24
$Fe_2O_3^T$	0.96	2.27	10.47	7.02	6.16	5.88	5.53	3.68	0.95	6.05	5.17	5.71	1.28	2.58
MnO	0.02	0.04	0.16	0.08	0.08	0.07	0.10	0.05	0.00	0.07	0.11	0.05	0.01	0.03
MgO	0.22	0.72	4.07	2.46	3.30	3.08	4.37	2.14	1.09	1.52	0.42	2.92	0.78	0.64
CaO	1.17	2.49	6.74	6.02	5.56	6.61	9.77	4.41	0.68	3.09	2.56	1.97	5.36	1.10
Na_2O	4.19	2.64	1.64	5.12	3.43	4.79	2.99	4.49	2.96	3.03	4.02	2.99	6.80	3.56
K_2O	4.32	3.62	0.99	1.16	1.30	1.11	1.24	1.37	6.53	4.22	7.17	1.87	1.84	5.23
P_2O_5	0.03	0.09	0.21	0.25	0.22	0.27	0.15	0.14	0.09	0.46	0.08	0.10	0.10	0.11
LOI	0.42	0.46	1.28	0.52	0.54	0.97	0.40	0.15	0.60	0.02	0.23	0.65	0.40	0.96
Sum	99.21	99.41	100.33	99.89	100.33	100.00	99.63	99.82	99.24	99.33	99.34	99.35	99.63	99.16
Normative mineralogy (cation norms)														
Qz	27.74	35.46	19.15	1.74	16.52	2.23	15.14	19.76	24.85	19.69	0.91	30.35		24.00
Ol													2.10	
Or	25.89	22.04	6.09	6.83	7.74	6.54	7.44	8.11	39.30	25.51	42.51	11.36	10.59	31.68
Ab	38.17	24.43	15.33	45.79	31.06	42.88	27.26	40.41	27.08	27.84	36.22	27.60	59.46	32.77
An	5.69	12.13	32.17	28.12	26.37	30.94	17.90	20.27	2.84	12.61	11.88	9.38	25.26	4.86
Co	0,51	0.56		0.90	0.35	0.54			1.40	0.80		5.00	1.43	1.10
Di			0.98				24.26	0.59			0.28			
Hy	1.57	4.12	21.01	13.68	15.01	14.08	5.55	9.10	3.10	9.63	6.58	13.90	0.34	4.10
Il	0.16	0.59	2.54	0.96	1.18	1.00	0.95	0.68	1.04	1.64	0.36	0.97	0.35	0.69
Mt	0.20	0.49	2.28	1.46	1.30	1.23	1.17	0.77	0.20	1.29	1.08	1.23	0.26	0.55
Ap	0.06	0.19	0.46	0.52	0.46	0.56	0.32	0.29	0.19	0.99	0.17	0.22	0.20	0.24

Analysed at the Geological Survey of Denmark and Greenland (GEUS). Sample numbers according to the Survey's files. $Fe_2O_3^T$ is total iron reported as Fe_2O_3. LOI is the loss on ignition. Samples 243494* and 243496* represent the leucocratic and melanocratic components of polyphase orthogneiss 243495 that was investigated by SHRIMP.

Table 2

Labels	Morphology	U ppm	Th ppm	Th/U	204Pb/206Pb	f206	238U/206Pb corrected	207Pb/206Pb corrected	207Pb/206Pb date Ma (1σ)	conc.
Southern terrane										
243495 orthogneiss - Morris Jesup Gletscher (map 77°57'N 70°44'W - collected 1978)										
1.1	e,osc,p	162	80	0.49	0.00004 ± 0.00003	0.0006	2.316 ± 0.083	0.1522 ± 0.0020	2371 ± 23	98
2.1	c,osc,p	136	73	0.53	0.00008 ± 0.00003	0.0012	2.130 ± 0.045	0.1649 ± 0.0023	2506 ± 23	99
3.1	e,osc,p	151	86	0.57	0.00013 ± 0.00005	0.0018	2.429 ± 0.057	0.1405 ± 0.0017	2233 ± 21	100
4.1	e,osc,p	217	111	0.51	0.00007 ± 0.00003	0.0009	2.654 ± 0.108	0.1386 ± 0.0019	2210 ± 24	93
5.1	e,h,p	112	90	0.80	0.00012 ± 0.00005	0.0017	2.909 ± 0.082	0.1172 ± 0.0013	1913 ± 20	100
6.1	c,osc,p	215	113	0.52	0.00007 ± 0.00002	0.0010	2.354 ± 0.059	0.1484 ± 0.0012	2327 ± 14	98
7.1	e,osc,p	170	86	0.51	0.00003 ± 0.00002	0.0004	2.589 ± 0.069	0.1368 ± 0.0010	2187 ± 12	96
8.1	e,osc,p	157	93	0.59	0.00009 ± 0.00003	0.0013	2.198 ± 0.047	0.1553 ± 0.0011	2405 ± 13	101
9.1	e,osc,p	195	80	0.41	0.00014 ± 0.00005	0.0020	2.531 ± 0.074	0.1484 ± 0.0024	2327 ± 28	92
10.1	e,h,p	45	40	0.90	0.00027 ± 0.00013	0.0039	2.924 ± 0.130	0.1162 ± 0.0023	1899 ± 36	100
10.2	e,h,p	46	55	1.19	0.00062 ± 0.00017	0.0087	2.839 ± 0.129	0.1140 ± 0.0029	1864 ± 47	104
11.1	c,osc,p	122	71	0.58	0.00012 ± 0.00004	0.0017	2.261 ± 0.080	0.1538 ± 0.0023	2389 ± 26	99
12.1	c,osc,p	123	67	0.55	0.00006 ± 0.00004	0.0008	2.682 ± 0.078	0.1286 ± 0.0014	2079 ± 19	98
13.1	e,osc,p	198	113	0.57	0.00004 ± 0.00002	0.0006	2.507 ± 0.069	0.1420 ± 0.0012	2251 ± 14	96
470214 orthogneiss - Bowdoin Gletscher (GPS 77°49.44'N 68°24.36'W - collected 2001)										
1.1	e,osc,p	943	1102	1.17	0.00002 ± 0.00001	0.0003	2.060 ± 0.049	0.1723 ± 0.0008	2580 ± 7	99
2.1	m,osc,p	521	234	0.45	0.00003 ± 0.00001	0.0005	2.100 ± 0.038	0.1667 ± 0.0009	2524 ± 9	100
3.1	e,osc,p	231	80	0.35	0.00002 ± 0.00001	0.0002	2.084 ± 0.050	0.1709 ± 0.0008	2567 ± 8	98
4.1	e,osc,p	683	570	0.84	0.00000 ± 0.00001	0.0001	2.057 ± 0.045	0.1717 ± 0.0006	2574 ± 6	99
5.1	c,osc,p	339	136	0.40	0.00004 ± 0.00001	0.0005	2.112 ± 0.047	0.1751 ± 0.0009	2607 ± 8	96
6.1	r,hb,p	27	27	0.99	0.00017 ± 0.00019	0.0024	2.073 ± 0.068	0.1728 ± 0.0045	2585 ± 44	98
6.2	c,osc/rex,p	461	191	0.41	0.00037 ± 0.00003	0.0051	2.130 ± 0.046	0.1707 ± 0.0009	2565 ± 8	97
7.1	m,osc,p,f	307	455	1.48	0.00008 ± 0.00003	0.0012	2.175 ± 0.045	0.1658 ± 0.0007	2516 ± 7	97
7.2	e,hb,p,f	60	90	1.50	0.00018 ± 0.00010	0.0026	2.116 ± 0.069	0.1681 ± 0.0021	2539 ± 21	98
8.1	r,hb,p	20	18	0.90	0.00144 ± 0.00034	0.0199	2.666 ± 0.116	0.1221 ± 0.0058	1986 ± 86	103
9.1	r,hb,p	29	31	1.06	0.00050 ± 0.00023	0.0070	1.994 ± 0.061	0.1747 ± 0.0041	2603 ± 40	101
140944 orthogneiss - Bu Gletscher (map 78°03'N 72°17'W - collected 1971)										
1.1	e,osc,p	1019	310	0.30	0.00007 ± 0.00001	0.0010	2.726 ± 0.060	0.1164 ± 0.0007	1902 ± 10	106
2.1	e,osc,p	1256	415	0.33	0.00317 ± 0.00065	0.0483	3.650 ± 0.107	0.0978 ± 0.0144	1582 ± 304	99
3.1	e,osc,p	679	148	0.22	0.00009 ± 0.00002	0.0013	3.009 ± 0.066	0.1121 ± 0.0008	1834 ± 14	101
4.1	e,osc,p	836	202	0.24	0.00003 ± 0.00001	0.0005	2.566 ± 0.062	0.1203 ± 0.0005	1960 ± 7	108
5.1	e,osc,p	1198	286	0.24	0.00003 ± 0.00001	0.0005	2.659 ± 0.061	0.1194 ± 0.0004	1948 ± 6	106
6.1	e,osc,p	934	225	0.24	0.00008 ± 0.00001	0.0012	2.714 ± 0.056	0.1150 ± 0.0003	1879 ± 5	108
7.1	e,osc,p	861	163	0.19	0.00005 ± 0.00001	0.0008	2.626 ± 0.068	0.1216 ± 0.0006	1980 ± 9	105
8.1	e,osc,p,fr	1074	232	0.22	0.00002 ± 0.00000	0.0003	2.695 ± 0.049	0.1216 ± 0.0005	1980 ± 7	103
9.1	e,osc,p	857	158	0.18	0.00003 ± 0.00001	0.0005	2.588 ± 0.054	0.1200 ± 0.0004	1956 ± 5	108
10.1	e,osc,p	974	229	0.24	0.00010 ± 0.00001	0.0015	2.668 ± 0.048	0.1223 ± 0.0004	1990 ± 6	103
243459 orthogneiss - Bamse Gletscher (map 78°03'N 72°10'W - collected 1978)										
1.1	e,w-osc,p	78	27	0.34	0.00012 ± 0.00006	0.0019	2.828 ± 0.087	0.1208 ± 0.0016	1968 ± 24	99
2.1	c,osc,p	939	431	0.46	0.00072 ± 0.00005	0.0109	3.670 ± 0.069	0.1156 ± 0.0011	1889 ± 17	82
3.1	c,osc,p	747	216	0.29	0.00039 ± 0.00004	0.0059	2.921 ± 0.058	0.1216 ± 0.0011	1979 ± 17	96
4.1	e,w-osc,p	84	23	0.28	0.00017 ± 0.00010	0.0026	2.966 ± 0.076	0.1152 ± 0.0019	1883 ± 30	100
5.1	e,h,p	87	31	0.36	0.00024 ± 0.00009	0.0036	2.897 ± 0.067	0.1150 ± 0.0017	1880 ± 27	102
5.2	c,osc,p	1403	626	0.45	0.00064 ± 0.00011	0.0098	5.119 ± 0.168	0.1110 ± 0.0037	1817 ± 62	63
6.1	e,w-osc,p	93	25	0.27	0.00019 ± 0.00006	0.0030	2.907 ± 0.081	0.1154 ± 0.0018	1887 ± 28	101
7.1	e,w-osc,p	74	20	0.27	0.00005 ± 0.00004	0.0008	2.888 ± 0.077	0.1177 ± 0.0016	1921 ± 24	100
8.1	c,osc,p	776	109	0.14	0.00003 ± 0.00001	0.0004	2.908 ± 0.050	0.1176 ± 0.0007	1921 ± 10	99
9.1	c,osc,p	1112	553	0.50	0.00030 ± 0.00003	0.0046	3.439 ± 0.094	0.1157 ± 0.0006	1891 ± 9	87
425507 metaquartzite - Morris Jesup Gletscher (GPS 78°17.08'N 69°47.33'W - collected 1995)										
1.1	m,osc,ov	112	35	0.31	0.00000 ± 0.00012	0.0000	2.209 ± 0.162	0.1878 ± 0.0083	2723 ± 75	88
2.1	m,osc,ov	102	57	0.56	0.00015 ± 0.00005	0.0021	2.197 ± 0.106	0.1613 ± 0.0067	2469 ± 71	98
3.1	e,osc/hd,rp	387	78	0.20	0.00002 ± 0.00001	0.0003	2.824 ± 0.119	0.1331 ± 0.0044	2139 ± 59	91
3.2	e,osc/hd,rp	581	204	0.35	0.00002 ± 0.00001	0.0002	2.415 ± 0.092	0.1499 ± 0.0012	2345 ± 14	95
3.3	e,osc/hd,rp	462	105	0.23	0.00003 ± 0.00001	0.0005	2.499 ± 0.096	0.1482 ± 0.0041	2325 ± 48	93
4.1	e,osc,rp	77	52	0.67	0.00013 ± 0.00009	0.0019	2.123 ± 0.089	0.1688 ± 0.0020	2546 ± 20	98
5.1	m,osc,ov	332	267	0.81	0.00015 ± 0.00004	0.0021	2.088 ± 0.073	0.1881 ± 0.0031	2726 ± 28	93
6.1	m,osc,ov	541	247	0.46	0.00003 ± 0.00001	0.0005	1.667 ± 0.084	0.2599 ± 0.0050	3246 ± 30	93
7.1	e,osc,ov	173	87	0.50	0.00002 ± 0.00001	0.0003	2.211 ± 0.098	0.1686 ± 0.0009	2543 ± 9	95
8.1	e,osc,ov	185	96	0.52	0.00000 ± 0.00002	0.0001	2.077 ± 0.088	0.1718 ± 0.0046	2575 ± 45	98
9.1	e,hd,rp	338	98	0.29	0.00078 ± 0.00013	0.0110	2.446 ± 0.137	0.1441 ± 0.0047	2277 ± 57	97
9.2	e,hd,rp	502	133	0.26	0.00563 ± 0.00026	0.0792	2.043 ± 0.089	0.1680 ± 0.0078	2538 ± 80	101
10.1	e,osc,ov/rp	97	62	0.64	0.00005 ± 0.00005	0.0008	2.075 ± 0.092	0.1730 ± 0.0032	2586 ± 31	98
11.1	e,osc,ov	395	383	0.97	0.00025 ± 0.00004	0.0036	2.401 ± 0.094	0.1775 ± 0.0021	2630 ± 20	85
12.1	e,osc,rp	343	351	1.02	0.00000 ± 0.00001	0.0000	1.700 ± 0.074	0.2261 ± 0.0017	3024 ± 12	99
13.1	e/m,osc,ov	143	124	0.86	0.00005 ± 0.00002	0.0007	2.381 ± 0.116	0.1518 ± 0.0080	2366 ± 93	96
13.2	e,osc,ov	669	215	0.32	0.00008 ± 0.00003	0.0012	2.719 ± 0.244	0.1549 ± 0.0025	2400 ± 28	84
14.1	e,osc,rp	220	119	0.54	0.00007 ± 0.00003	0.0010	1.972 ± 0.094	0.1803 ± 0.0033	2656 ± 30	100
15.1	e,osc,ov	81	66	0.82	0.00012 ± 0.00004	0.0018	2.016 ± 0.104	0.1752 ± 0.0063	2608 ± 61	100

Labels	Morphology	U ppm	Th ppm	Th/U	204Pb/206Pb	f206	238U/206Pb corrected	207Pb/206Pb corrected	207Pb/206Pb date Ma (1σ)	conc.
16.1	m,osc,ov	319	247	0.77	0.00002 ± 0.00001	0.0003	2.051 ± 0.077	0.1769 ± 0.0008	2624 ± 7	98
17.1	m,osc,ov	105	102	0.97	0.00331 ± 0.00026	0.0466	2.194 ± 0.090	0.1618 ± 0.0052	2475 ± 55	98
18.1	e,osc,ov	796	202	0.25	0.00009 ± 0.00002	0.0013	2.615 ± 0.107	0.1601 ± 0.0017	2456 ± 18	85
18.2	m,osc,ov	481	224	0.47	0.00004 ± 0.00002	0.0006	2.170 ± 0.069	0.1671 ± 0.0021	2529 ± 22	97
19.1	m,hd,ov	301	135	0.45	0.00001 ± 0.00001	0.0002	2.211 ± 0.104	0.1590 ± 0.0028	2445 ± 30	98
20.1	e,osc,ov	129	169	1.32	0.00002 ± 0.00002	0.0003	2.237 ± 0.109	0.1609 ± 0.0016	2465 ± 16	97
21.1	e,osc,rp	156	133	0.85	0.00010 ± 0.00003	0.0014	1.961 ± 0.081	0.1912 ± 0.0020	2752 ± 17	97
22.1	m,osc,ov	251	91	0.36	0.00004 ± 0.00002	0.0006	2.430 ± 0.087	0.1611 ± 0.0063	2467 ± 67	90
23.1	e,osc,ov	171	101	0.59	0.00004 ± 0.00002	0.0005	2.188 ± 0.084	0.1707 ± 0.0040	2565 ± 40	95
24.1	m,osc,rp	128	124	0.97	0.00004 ± 0.00003	0.0006	2.340 ± 0.089	0.1653 ± 0.0019	2510 ± 19	91
25.1	m,osc,ov	340	34	0.10	0.00001 ± 0.00001	0.0001	1.712 ± 0.066	0.2297 ± 0.0046	3050 ± 32	97
26.1	e,osc,rp	117	46	0.39	0.00001 ± 0.00003	0.0002	2.241 ± 0.128	0.1672 ± 0.0068	2529 ± 70	94
27.1	e,osc,rp	305	126	0.41	0.00003 ± 0.00002	0.0005	2.315 ± 0.095	0.1541 ± 0.0047	2392 ± 53	97
28.1	m,osc,ov	129	93	0.72	0.00169 ± 0.00021	0.0238	1.848 ± 0.071	0.2111 ± 0.0062	2914 ± 49	96
29.1	m,osc,ov	391	117	0.30	0.00003 ± 0.00003	0.0004	2.455 ± 0.089	0.1531 ± 0.0038	2380 ± 43	93
30.1	e,osc,rp	288	237	0.82	0.00019 ± 0.00003	0.0026	2.066 ± 0.076	0.1812 ± 0.0022	2664 ± 20	96
31.1	m,osc,rp	338	148	0.44	0.00436 ± 0.00045	0.0613	2.067 ± 0.100	0.2010 ± 0.0119	2834 ± 100	90
32.1	e,osc,ov	402	323	0.80	0.00021 ± 0.00006	0.0030	2.067 ± 0.084	0.1416 ± 0.0035	2247 ± 44	113
32.2	e,osc,ov	557	226	0.41	0.00004 ± 0.00001	0.0006	2.383 ± 0.129	0.1479 ± 0.0009	2322 ± 11	97
33.1	e,osc,rp	188	73	0.39	0.00000 ± 0.00001	0.0000	2.341 ± 0.089	0.1609 ± 0.0027	2466 ± 29	93
34.1	m,osc,rp	266	231	0.87	0.00794 ± 0.00053	0.1117	1.966 ± 0.092	0.1813 ± 0.0131	2665 ± 125	100
35.1	m,osc,ov	346	57	0.17	0.00006 ± 0.00004	0.0008	2.508 ± 0.111	0.1510 ± 0.0055	2357 ± 64	92
36.1	m,osc,rp	294	153	0.52	0.00017 ± 0.00003	0.0024	1.821 ± 0.066	0.2081 ± 0.0051	2891 ± 40	98
37.1	m,osc,ov	321	286	0.89	0.00001 ± 0.00001	0.0001	2.027 ± 0.086	0.1929 ± 0.0006	2767 ± 5	93
38.1	e,osc,ov	179	122	0.68	0.00000 ± 0.00002	0.0000	1.733 ± 0.058	0.2190 ± 0.0028	2973 ± 21	99
39.1	m,osc,ov	225	154	0.68	0.00005 ± 0.00002	0.0007	2.527 ± 0.106	0.1514 ± 0.0057	2362 ± 65	91
40.1	m,osc,ov	80	46	0.58	0.00018 ± 0.00009	0.0026	1.989 ± 0.068	0.1772 ± 0.0034	2627 ± 32	100
243506 metaquartzite - southern Inglefield Land (map 77°58'N 70°55'W - collected 1978)										
1.1	e,osc,rp	83	53	0.64	0.00000 ± 0.00008	0.0000	1.821 ± 0.099	0.1900 ± 0.0159	2742 ± 144	103
2.1	m,osc,ov	182	83	0.45	0.00006 ± 0.00004	0.0009	2.098 ± 0.122	0.1677 ± 0.0036	2535 ± 37	99
3.1	m,osc,ov	148	111	0.75	0.00008 ± 0.00004	0.0012	1.882 ± 0.066	0.1891 ± 0.0014	2735 ± 12	100
4.1	m,osc,ov	230	121	0.52	0.01484 ± 0.00050	0.2088	2.386 ± 0.110	0.1572 ± 0.0086	2426 ± 96	93
5.1	m,osc,ov	290	147	0.51	0.00020 ± 0.00003	0.0028	2.036 ± 0.100	0.1850 ± 0.0015	2698 ± 13	96
6.1	e,osc,rp	137	50	0.36	0.01015 ± 0.00061	0.1428	2.462 ± 0.103	0.1749 ± 0.0108	2605 ± 107	84
7.1	m,osc,ov	343	75	0.22	0.01753 ± 0.00025	0.2467	2.625 ± 0.114	0.1692 ± 0.0048	2550 ± 48	82
8.1	e,osc,rp	181	42	0.23	0.01338 ± 0.00032	0.1883	2.662 ± 0.130	0.2160 ± 0.0067	2951 ± 51	70
9.1	e,osc,ov	213	122	0.57	0.00309 ± 0.00027	0.0435	2.695 ± 0.117	0.1565 ± 0.0058	2419 ± 64	84
10.1	m,osc,ov	115	158	1.37	0.00000 ± 0.00002	0.0000	1.603 ± 0.077	0.2507 ± 0.0022	3189 ± 14	98
11.1	m,osc,ov	137	69	0.51	0.00009 ± 0.00005	0.0013	2.175 ± 0.130	0.1753 ± 0.0019	2609 ± 19	94
12.1	e,osc,rp	886	80	0.09	0.04845 ± 0.00045	0.6817	6.477 ± 0.863	0.1800 ± 0.0123	2653 ± 118	35
13.1	m,osc,ov	276	138	0.50	0.00011 ± 0.00004	0.0016	2.118 ± 0.090	0.1808 ± 0.0031	2660 ± 28	94
14.1	m,osc,ov	346	133	0.39	0.00026 ± 0.00003	0.0037	2.239 ± 0.077	0.1594 ± 0.0010	2449 ± 10	97
15.1	m,osc,ov	41	19	0.46	0.00613 ± 0.00102	0.0862	2.585 ± 0.167	0.1337 ± 0.0174	2146 ± 247	98
15.2	e,osc,ov	39	21	0.54	0.00292 ± 0.00053	0.0411	2.411 ± 0.117	0.1587 ± 0.0108	2442 ± 120	92
16.1	e,osc,rp	105	66	0.63	0.00186 ± 0.00026	0.0261	2.298 ± 0.090	0.1647 ± 0.0042	2504 ± 44	93
17.1	e,osc,rp	147	119	0.81	0.01834 ± 0.00093	0.2580	2.688 ± 0.113	0.1554 ± 0.0187	2406 ± 220	85
18.1	e,osc,rp	397	96	0.24	0.02527 ± 0.00094	0.3555	5.113 ± 0.584	0.1710 ± 0.0184	2568 ± 192	45
19.1	e,osc,rp	229	140	0.61	0.01741 ± 0.00081	0.2449	2.609 ± 0.125	0.1778 ± 0.0145	2633 ± 142	79
20.1	m,osc,rp	173	34	0.20	0.00594 ± 0.00027	0.0836	2.495 ± 0.086	0.1459 ± 0.0052	2298 ± 62	95
21.1	m,osc,rp	212	110	0.52	0.02681 ± 0.00085	0.3773	3.575 ± 0.162	0.1542 ± 0.0185	2393 ± 220	67
22.1	e,osc,rp	92	50	0.54	0.00163 ± 0.00026	0.0229	2.162 ± 0.115	0.1611 ± 0.0052	2467 ± 55	99
23.1	e,osc,rp	129	64	0.49	0.00056 ± 0.00010	0.0078	2.149 ± 0.090	0.1641 ± 0.0019	2499 ± 19	99
24.1	m,osc,ov	169	70	0.41	0.00304 ± 0.00023	0.0427	2.431 ± 0.098	0.1510 ± 0.0043	2358 ± 49	94
25.1	e,osc,ov	329	129	0.39	0.01184 ± 0.00098	0.1666	3.107 ± 0.266	0.2220 ± 0.0187	2995 ± 142	60
26.1	m,osc,ov	67	102	1.53	0.00099 ± 0.00016	0.0139	1.996 ± 0.088	0.1726 ± 0.0037	2583 ± 36	101
27.1	m,osc,ov	193	99	0.51	0.00748 ± 0.00024	0.1052	2.241 ± 0.092	0.1698 ± 0.0051	2555 ± 51	93
28.1	m,osc,rp/ov	98	69	0.70	0.00059 ± 0.00011	0.0083	2.233 ± 0.089	0.1613 ± 0.0025	2469 ± 26	97
29.1	m,osc,ov	108	74	0.68	0.00012 ± 0.00005	0.0017	2.064 ± 0.090	0.1624 ± 0.0019	2480 ± 19	103
30.1	m,osc,rp	220	101	0.46	0.01506 ± 0.00080	0.2119	3.061 ± 0.179	0.1358 ± 0.0145	2175 ± 199	84
30.2	e,osc,rp	180	74	0.41	0.00763 ± 0.00059	0.1074	2.435 ± 0.142	0.1622 ± 0.0119	2479 ± 130	90
31.1	m,osc,rp	74	56	0.75	0.00106 ± 0.00015	0.0150	2.095 ± 0.127	0.1676 ± 0.0030	2534 ± 30	99
32.1	m,osc,ov	141	73	0.52	0.00018 ± 0.00004	0.0025	2.044 ± 0.095	0.1613 ± 0.0016	2469 ± 17	104
33.1	e,osc,ov	409	52	0.13	0.02609 ± 0.00081	0.3671	3.631 ± 0.498	0.0837 ± 0.0185	1286 ± 504	122
243510 metapelite (metamorphic zircons only, map 77°58'N 70°55'W - collected 1978)										
1.1	e,hd,ov	511	14	0.03	0.00011 ± 0.00003	0.0016	2.845 ± 0.107	0.1181 ± 0.0010	1927 ± 15	101
2.1	e,hd,ov	500	54	0.11	0.00001 ± 0.00001	0.0001	2.957 ± 0.122	0.1177 ± 0.0008	1922 ± 12	98
3.1	e,hd,ov	543	49	0.09	0.00001 ± 0.00001	0.0001	3.009 ± 0.125	0.1179 ± 0.0006	1924 ± 9	96
4.1	e,hd,ov	637	118	0.18	0.00010 ± 0.00003	0.0016	2.870 ± 0.169	0.1195 ± 0.0015	1949 ± 22	99
5.1	e,hd,ov	583	35	0.06	0.00003 ± 0.00001	0.0005	3.006 ± 0.119	0.1171 ± 0.0005	1913 ± 8	97
6.1	e,hd,ov	399	19	0.05	0.00000 ± 0.00000	0.0000	2.814 ± 0.090	0.1187 ± 0.0006	1936 ± 9	101
7.1	e,hd,ov	713	135	0.19	0.00001 ± 0.00001	0.0001	3.055 ± 0.125	0.1182 ± 0.0010	1930 ± 15	95
8.1	e,hd,ov	759	60	0.08	0.00002 ± 0.00002	0.0004	3.039 ± 0.151	0.1163 ± 0.0009	1901 ± 14	97

Labels	Morphology	U ppm	Th ppm	Th/U	204Pb/206Pb	f206	238U/206Pb corrected	207Pb/206Pb corrected	207Pb/206Pb date Ma (1σ)	conc.
Central terrane										
440314 paragneiss - northeastern Inglefield Land (GPS 78°57.49'N 66°27.72'W - collected 1999)										
1.1	m,osc,p	177	172	0.97	0.00005 ± 0.00002	0.0008	2.715 ± 0.124	0.1286 ± 0.0009	2079 ± 12	97
2.1	e,osc,eq/p	216	104	0.48	0.00007 ± 0.00004	0.0010	2.700 ± 0.166	0.1230 ± 0.0012	2000 ± 17	102
3.1	e,osc,p	247	81	0.33	0.00005 ± 0.00002	0.0008	2.724 ± 0.107	0.1232 ± 0.0012	2003 ± 17	101
4.1	e,osc,p	182	63	0.34	0.00010 ± 0.00006	0.0015	2.948 ± 0.121	0.1201 ± 0.0034	1957 ± 51	96
5.1	e,osc,p	317	165	0.52	0.00007 ± 0.00004	0.0011	3.063 ± 0.169	0.1217 ± 0.0012	1982 ± 17	92
6.1	e,osc,p	301	85	0.28	0.00010 ± 0.00004	0.0016	2.797 ± 0.104	0.1223 ± 0.0012	1990 ± 17	99
7.1	e,osc,p	270	115	0.43	0.00014 ± 0.00003	0.0022	2.795 ± 0.118	0.1217 ± 0.0012	1981 ± 18	100
8.1	e,osc,p	433	169	0.39	0.00003 ± 0.00002	0.0005	2.807 ± 0.102	0.1222 ± 0.0007	1988 ± 10	99
9.1	m,osc,p	132	60	0.46	0.00027 ± 0.00013	0.0041	2.819 ± 0.172	0.1244 ± 0.0035	2020 ± 51	97
10.1	e,osc,p	242	164	0.68	0.00008 ± 0.00003	0.0013	2.728 ± 0.113	0.1223 ± 0.0016	1989 ± 23	101
11.1	e,osc,p	183	92	0.51	0.00009 ± 0.00003	0.0014	2.951 ± 0.124	0.1225 ± 0.0011	1993 ± 17	94
12.1	e,osc,p	142	72	0.51	0.00001 ± 0.00002	0.0001	2.777 ± 0.131	0.1224 ± 0.0014	1991 ± 20	100
13.1	e,osc,p	208	110	0.53	0.00008 ± 0.00004	0.0012	2.656 ± 0.118	0.1209 ± 0.0018	1970 ± 26	105
14.1	e,osc,p	437	107	0.24	0.00053 ± 0.00009	0.0080	3.256 ± 0.278	0.1162 ± 0.0030	1899 ± 46	91
15.1	e,osc,p	359	104	0.29	0.00009 ± 0.00003	0.0013	2.610 ± 0.166	0.1270 ± 0.0021	2057 ± 29	102
16.1	m,osc,p	372	90	0.24	0.00008 ± 0.00004	0.0011	3.060 ± 0.135	0.1178 ± 0.0013	1924 ± 20	95
17.1	m,osc/h,ov	117	42	0.36	0.00023 ± 0.00009	0.0035	2.732 ± 0.117	0.1160 ± 0.0019	1895 ± 30	106
18.1	m,osc,p	279	112	0.40	0.00002 ± 0.00004	0.0003	2.888 ± 0.103	0.1212 ± 0.0009	1974 ± 14	97
19.1	e,osc,p	296	126	0.42	0.00093 ± 0.00016	0.0141	3.397 ± 0.475	0.1091 ± 0.0029	1784 ± 49	93
19.2	m,osc,p	431	985	2.29	0.00009 ± 0.00003	0.0013	2.755 ± 0.159	0.1263 ± 0.0013	2046 ± 18	98
20.1	m,osc,eq/p	329	186	0.57	0.00004 ± 0.00001	0.0005	2.772 ± 0.113	0.1238 ± 0.0017	2012 ± 24	99
21.1	e,osc,p	415	195	0.47	0.00023 ± 0.00004	0.0035	3.064 ± 0.166	0.1221 ± 0.0019	1987 ± 28	92
22.1	e,osc,p	332	99	0.30	0.00013 ± 0.00007	0.0019	3.030 ± 0.128	0.1194 ± 0.0015	1947 ± 23	94
23.1	e,osc,p	270	169	0.63	0.00007 ± 0.00004	0.0010	3.014 ± 0.107	0.1192 ± 0.0018	1944 ± 27	95
24.1	m,osc,eq/p	117	55	0.47	0.00005 ± 0.00004	0.0008	2.872 ± 0.192	0.1181 ± 0.0024	1928 ± 36	100
25.1	m,osc,p	440	195	0.44	0.00005 ± 0.00002	0.0008	2.947 ± 0.154	0.1222 ± 0.0010	1989 ± 14	95
26.1	m,osc,ov	457	207	0.45	0.00488 ± 0.00018	0.0738	2.667 ± 0.089	0.1259 ± 0.0040	2042 ± 58	101
27.1	m,osc,p	310	205	0.66	0.00014 ± 0.00003	0.0022	2.833 ± 0.108	0.1228 ± 0.0020	1998 ± 29	98
28.1	m,osc,p	555	310	0.56	0.00006 ± 0.00001	0.0009	2.922 ± 0.121	0.1208 ± 0.0006	1967 ± 9	97
29.1	m,osc,p	254	124	0.49	0.00010 ± 0.00003	0.0016	2.678 ± 0.100	0.1225 ± 0.0009	1994 ± 13	103
30.1	e,osc,p	301	483	1.60	0.00004 ± 0.00003	0.0006	2.949 ± 0.097	0.1246 ± 0.0009	2024 ± 12	93
440321 paragneiss - central Inglefield Land (GPS 787°46.30'N 68°55.27'W - collected 1999)										
1.1	e,osc,eq	266	202	0.76	0.00004 ± 0.00003	0.0005	2.944 ± 0.158	0.1198 ± 0.0011	1954 ± 17	97
2.1	e,osc,eq/p	259	116	0.45	0.00004 ± 0.00002	0.0007	2.697 ± 0.097	0.1239 ± 0.0013	2013 ± 18	101
3.1	e,osc,p/eq	238	162	0.68	0.00019 ± 0.00005	0.0029	2.840 ± 0.110	0.1195 ± 0.0024	1948 ± 37	100
4.1	e,osc,fr	77	45	0.57	0.00003 ± 0.00004	0.0005	2.836 ± 0.154	0.1236 ± 0.0025	2008 ± 37	97
5.1	osc,eq	401	101	0.25	0.00058 ± 0.00015	0.0088	3.803 ± 0.384	0.1172 ± 0.0033	1913 ± 52	79
6.1	m,osc,eq	452	557	1.23	0.00009 ± 0.00004	0.0013	2.897 ± 0.153	0.1233 ± 0.0009	2005 ± 13	95
7.1	m,osc,eq	448	327	0.73	0.00004 ± 0.00004	0.0007	2.886 ± 0.127	0.1243 ± 0.0010	2019 ± 15	95
8.1	e,osc,p	242	173	0.71	0.00006 ± 0.00004	0.0010	2.758 ± 0.097	0.1214 ± 0.0014	1977 ± 20	101
9.1	m,osc,eq	236	207	0.88	0.00016 ± 0.00005	0.0024	2.688 ± 0.100	0.1208 ± 0.0014	1967 ± 20	104
10.1	m,osc,eq	241	189	0.78	0.00000 ± 0.00002	0.0000	2.719 ± 0.120	0.1232 ± 0.0008	2002 ± 12	101
11.1	e,osc,p	187	138	0.74	0.00009 ± 0.00004	0.0014	3.026 ± 0.175	0.1240 ± 0.0014	2015 ± 19	91
12.1	m,osc,eq	315	279	0.89	0.00005 ± 0.00003	0.0008	2.804 ± 0.120	0.1211 ± 0.0009	1972 ± 13	100
13.1	m,osc,eq	310	281	0.90	0.00003 ± 0.00002	0.0004	2.853 ± 0.129	0.1222 ± 0.0009	1988 ± 13	97
14.1*	r+c,eq	394	116	0.29	0.00022 ± 0.00006	0.0034	3.404 ± 0.416	0.1136 ± 0.0017	1857 ± 27	89
14.2	r,hd,eq	684	25	0.04	0.00002 ± 0.00003	0.0003	3.191 ± 0.472	0.1176 ± 0.0024	1920 ± 37	92
14.3	r,hd,eq	1732	10	0.01	0.00001 ± 0.00000	0.0001	2.738 ± 0.142	0.1180 ± 0.0004	1927 ± 7	104
14.4	c,osc,eq	147	113	0.77	0.00004 ± 0.00005	0.0006	2.894 ± 0.235	0.1249 ± 0.0019	2027 ± 27	94
15.1	m,osc,p	355	143	0.40	0.00014 ± 0.00005	0.0021	2.596 ± 0.139	0.1214 ± 0.0013	1977 ± 19	106
16.1	m,osc,eq	419	408	0.97	0.00002 ± 0.00001	0.0003	2.701 ± 0.091	0.1227 ± 0.0011	1995 ± 16	102
17.1	m,osc,eq	647	634	0.98	0.00003 ± 0.00001	0.0004	2.837 ± 0.140	0.1193 ± 0.0017	1946 ± 26	100
18.1	m,osc,eq	403	329	0.82	0.00006 ± 0.00003	0.0009	3.051 ± 0.130	0.1204 ± 0.0010	1962 ± 15	93
19.1	m,osc,eq	354	321	0.91	0.00020 ± 0.00006	0.0030	2.814 ± 0.138	0.1236 ± 0.0017	2008 ± 25	98
20.1	e,osc,p	216	88	0.41	0.00009 ± 0.00003	0.0013	2.480 ± 0.107	0.1349 ± 0.0015	2163 ± 20	101
21.1	m,osc,p	358	314	0.88	0.00003 ± 0.00001	0.0004	2.900 ± 0.161	0.1203 ± 0.0011	1961 ± 16	97
22.1	osc,eq	711	157	0.22	0.00007 ± 0.00002	0.0011	2.637 ± 0.184	0.1200 ± 0.0008	1956 ± 12	106
23.1	e,osc,eq	288	195	0.68	0.00019 ± 0.00005	0.0029	2.782 ± 0.193	0.1203 ± 0.0019	1960 ± 29	101
24.1	m,osc,p	447	323	0.72	0.00031 ± 0.00006	0.0048	2.929 ± 0.164	0.1210 ± 0.0012	1971 ± 17	96
25.1	e,osc,p	186	104	0.56	0.00014 ± 0.00008	0.0022	3.129 ± 0.209	0.1203 ± 0.0018	1960 ± 27	91
26.1	m,h,eq	474	413	0.87	0.00003 ± 0.00002	0.0005	2.749 ± 0.127	0.1231 ± 0.0009	2001 ± 13	100
27.1	m,osc,eq	1045	94	0.09	0.00009 ± 0.00002	0.0013	2.708 ± 0.129	0.1193 ± 0.0010	1946 ± 15	104
425522 orthogneiss - northeastern Inglefield Land (GPS 79°03.62'N 66°08.24'W - collected 1995)										
1.1	e,osc,p	698	170	0.24	0.00056 ± 0.00005	0.0085	3.285 ± 0.072	0.1176 ± 0.0009	1920 ± 14	89
2.1	e,osc,p	132	45	0.34	0.00028 ± 0.00010	0.0042	2.822 ± 0.072	0.1211 ± 0.0027	1972 ± 40	99
3.1	e,osc,p	209	84	0.40	0.00032 ± 0.00008	0.0050	2.804 ± 0.061	0.1199 ± 0.0018	1954 ± 26	101
4.1	e,osc,p	333	138	0.42	0.00005 ± 0.00002	0.0008	2.894 ± 0.118	0.1190 ± 0.0006	1941 ± 9	99
5.1	e,osc,p	443	176	0.40	0.00022 ± 0.00003	0.0034	2.956 ± 0.110	0.1195 ± 0.0013	1949 ± 20	96
6.1	e,osc,p	465	146	0.31	0.00011 ± 0.00002	0.0017	2.859 ± 0.137	0.1190 ± 0.0005	1942 ± 8	100
425542 orthopyroxene quartz diorite - Hiawatha pluton (GPS 78°52.37'N 66°36.85'W - collected 1995)										

Labels	Morphology	U ppm	Th ppm	Th/U	204Pb/206Pb	f206	238U/206Pb corrected	207Pb/206Pb corrected	207Pb/206Pb date Ma (1σ)	conc.
1.1	e,osc,p	230	99	0.43	0.00033 ± 0.00008	0.0050	2.771 ± 0.059	0.1179 ± 0.0016	1924 ± 25	103
2.1	e,osc,p	145	40	0.28	0.00045 ± 0.00011	0.0068	2.864 ± 0.067	0.1191 ± 0.0020	1943 ± 31	99
3.1	e,osc,p	166	53	0.32	0.00048 ± 0.00010	0.0074	2.924 ± 0.073	0.1171 ± 0.0021	1913 ± 33	99
4.1	e,osc,p	740	125	0.17	0.00016 ± 0.00003	0.0024	2.909 ± 0.160	0.1200 ± 0.0011	1957 ± 16	97
5.1	e,osc,p	211	64	0.30	0.00005 ± 0.00002	0.0008	2.657 ± 0.088	0.1197 ± 0.0012	1952 ± 18	106
6.1	e,osc,p	433	153	0.35	0.00608 ± 0.00036	0.0926	3.471 ± 0.174	0.1041 ± 0.0061	1698 ± 113	96
7.1	e,osc,p	264	98	0.37	0.00013 ± 0.00009	0.0019	2.631 ± 0.087	0.1198 ± 0.0016	1953 ± 24	106
8.1	e,osc,p	389	76	0.20	0.00010 ± 0.00003	0.0016	2.823 ± 0.077	0.1199 ± 0.0012	1954 ± 18	100
9.1	e,osc,p	286	93	0.33	0.00008 ± 0.00003	0.0012	3.186 ± 0.138	0.1200 ± 0.0011	1957 ± 16	90
10.1	e,osc,p	654	253	0.39	0.00095 ± 0.00005	0.0145	2.605 ± 0.159	0.1193 ± 0.0011	1945 ± 16	108
425623 granite - Hiawatha Gletscher (GPS 78°48.26'N 67°16.57'W - collected 1995)										
1.1	e,osc,p	333	179	0.54	0.00014 ± 0.00006	0.0021	2.941 ± 0.065	0.1170 ± 0.0015	1911 ± 23	99
2.1	e,osc,p	329	174	0.53	0.00014 ± 0.00003	0.0021	3.002 ± 0.059	0.1166 ± 0.0009	1905 ± 14	97
3.1	e,osc,p	373	222	0.60	0.00008 ± 0.00005	0.0012	2.947 ± 0.062	0.1177 ± 0.0017	1921 ± 27	98
4.1	e,h/osc,p,fr	361	208	0.58	0.00003 ± 0.00001	0.0005	2.873 ± 0.108	0.1180 ± 0.0007	1926 ± 11	100
5.1	e,h/osc,p,fr	363	209	0.58	0.00002 ± 0.00002	0.0002	2.953 ± 0.134	0.1156 ± 0.0011	1889 ± 16	100
6.1	e,osc,p	586	456	0.78	0.00005 ± 0.00001	0.0007	3.192 ± 0.121	0.1182 ± 0.0007	1929 ± 11	91
7.1	e,h,p,fr	377	283	0.75	0.00114 ± 0.00012	0.0173	2.766 ± 0.097	0.1173 ± 0.0021	1915 ± 33	104
8.1	e,osc,eq/p	373	234	0.63	0.00032 ± 0.00003	0.0049	2.810 ± 0.094	0.1168 ± 0.0007	1908 ± 11	103
425562 monzogranite - Humboldt pluton (GPS 79°03.36'N 65°55.87'W - collected 1995)										
1.1	e,osc,p	238	63	0.26	0.00622 ± 0.00031	0.0953	2.679 ± 0.069	0.1175 ± 0.0055	1919 ± 87	107
2.1	e,osc,p	292	167	0.57	0.00083 ± 0.00015	0.0127	2.950 ± 0.076	0.1201 ± 0.0025	1958 ± 37	96
3.1	e,osc,p	112	69	0.61	0.00204 ± 0.00030	0.0312	3.013 ± 0.078	0.1149 ± 0.0057	1878 ± 93	98
4.1	m,osc,eq/p	2186	111	0.05	0.00001 ± 0.00000	0.0001	2.844 ± 0.095	0.1176 ± 0.0008	1921 ± 12	101
5.1	e,osc,p	208	78	0.37	0.00036 ± 0.00028	0.0056	2.738 ± 0.200	0.1194 ± 0.0045	1948 ± 68	103
6.1	m,osc,p	167	65	0.39	0.00047 ± 0.00018	0.0072	3.091 ± 0.165	0.1163 ± 0.0035	1900 ± 54	95
7.1	e,osc,p	273	109	0.40	0.00053 ± 0.00015	0.0080	3.265 ± 0.166	0.1190 ± 0.0028	1941 ± 43	89
8.1	e,osc,p	489	152	0.31	0.00056 ± 0.00012	0.0086	2.754 ± 0.119	0.1174 ± 0.0027	1917 ± 43	104
9.1	e,osc,p	1950	98	0.05	0.00699 ± 0.00074	0.1069	3.227 ± 0.177	0.1129 ± 0.0149	1847 ± 259	94
10.1	m,osc,eq/p	2362	184	0.08	0.00072 ± 0.00012	0.0109	5.440 ± 0.407	0.1043 ± 0.0033	1703 ± 59	64
425571 syenite - Wulff structure (GPS 79°03.28'N 67°14.40'W - collected 1995)										
1.1	e,osc,p	985	302	0.31	0.00008 ± 0.00002	0.0012	2.861 ± 0.055	0.1176 ± 0.0011	1921 ± 17	101
2.1	e,osc,p	1462	445	0.30	0.00007 ± 0.00001	0.0011	3.074 ± 0.078	0.1169 ± 0.0010	1909 ± 15	95
3.1	e,osc,p	759	187	0.25	0.00006 ± 0.00002	0.0009	3.037 ± 0.074	0.1180 ± 0.0008	1926 ± 12	95
4.1	e,osc,p	655	128	0.20	0.00009 ± 0.00002	0.0013	3.056 ± 0.083	0.1148 ± 0.0009	1877 ± 14	97
425583 orthogneiss (late granite) - Minturn complex (GPS 78°32.98'N 68°09.05'W - collected 1995)										
1.1	e,osc,p	192	77	0.40	0.00028 ± 0.00006	0.0050	3.421 ± 0.083	0.1064 ± 0.0019	1738 ± 33	95
2.1	inherited core	243	48	0.20	0.00073 ± 0.00008	0.0130	2.131 ± 0.068	0.1780 ± 0.0062	2635 ± 59	94
3.1	e,osc,p	176	64	0.36	0.00111 ± 0.00016	0.0199	5.753 ± 0.133	0.1054 ± 0.0028	1721 ± 50	60
4.1	e,osc,p	626	51	0.08	0.00378 ± 0.00014	0.0675	3.379 ± 0.076	0.1099 ± 0.0033	1798 ± 56	93
4.2	e,osc,p	153	80	0.53	0.00009 ± 0.00020	0.0015	3.390 ± 0.103	0.1063 ± 0.0034	1737 ± 59	96
5.1	e,osc,p	219	77	0.35	0.00003 ± 0.00004	0.0005	3.325 ± 0.122	0.1070 ± 0.0026	1749 ± 45	97
6.1	e,osc,p	56	19	0.34	0.00001 ± 0.00005	0.0002	3.722 ± 0.146	0.1071 ± 0.0025	1751 ± 43	88
7.1	e,osc,p	464	171	0.37	0.00001 ± 0.00006	0.0002	3.255 ± 0.088	0.1074 ± 0.0011	1756 ± 19	98
8.1	e,osc,p	143	65	0.45	0.00006 ± 0.00018	0.0009	3.051 ± 0.092	0.1054 ± 0.0031	1721 ± 55	106
9.1	e,osc,p	204	96	0.47	0.00003 ± 0.00015	0.0004	3.229 ± 0.104	0.1073 ± 0.0024	1754 ± 41	99
425627 granitoid - Force Bugt (GPS 78°33.25'N 71°44.61'W - collected 1995)										
1.1	osc,p,fr	493	173	0.35	0.00011 ± 0.00004	0.0018	3.682 ± 0.070	0.1074 ± 0.0009	1756 ± 16	88
1.2	osc,p,fr	432	163	0.38	0.00007 ± 0.00003	0.0011	3.185 ± 0.026	0.1063 ± 0.0007	1737 ± 12	101
1.3	osc,p,fr	475	98	0.21	0.00010 ± 0.00004	0.0016	4.567 ± 0.060	0.1023 ± 0.0009	1666 ± 16	77
1.4	osc,p,fr	431	167	0.39	0.00011 ± 0.00007	0.0017	3.252 ± 0.042	0.1057 ± 0.0016	1727 ± 28	100
1.5	osc,p,fr	472	176	0.37	0.00006 ± 0.00005	0.0010	3.413 ± 0.033	0.1065 ± 0.0010	1740 ± 16	95
2.1	c-inh	550	144	0.26	0.00012 ± 0.00002	0.0019	2.376 ± 0.047	0.1573 ± 0.0046	2427 ± 51	93
3.1	c-inh	283	131	0.46	0.00025 ± 0.00004	0.0039	2.602 ± 0.069	0.1381 ± 0.0010	2204 ± 13	95
3.2	c-inh	343	192	0.56	0.00004 ± 0.00005	0.0007	2.566 ± 0.068	0.1375 ± 0.0010	2196 ± 13	97
3.3	c-inh	327	183	0.56	0.00003 ± 0.00004	0.0005	2.420 ± 0.063	0.1375 ± 0.0010	2195 ± 13	102
4.1	c-inh	679	231	0.34	0.00004 ± 0.00001	0.0006	3.152 ± 0.063	0.1162 ± 0.0006	1899 ± 9	94
5.1	c-inh	1576	313	0.20	0.01126 ± 0.00027	0.1759	10.590 ± 0.361	0.0585 ± 0.0315	548 ± 2047	106
6.1	c-inh	969	158	0.16	0.00002 ± 0.00001	0.0003	3.221 ± 0.071	0.1146 ± 0.0006	1873 ± 9	93
7.1	c-inh	795	110	0.14	0.00003 ± 0.00001	0.0005	2.928 ± 0.055	0.1159 ± 0.0010	1894 ± 16	100
8.1	c-inh	863	154	0.18	0.00712 ± 0.00022	0.1112	4.951 ± 0.427	0.1271 ± 0.0380	2058 ± 653	58
425793 granite dyke - Hiawatha Gletscher (GPS 78°48.04'N 67°15.59'W - collected 1995)										
1.1	e,osc,p	341	683	2.01	0.0004 ± 0.0002	0.0068	3.346 ± 0.256	0.1101 ± 0.0033	1801 ± 56	94
2.1	e,osc,p	416	536	1.29	0.0055 ± 0.0003	0.0860	4.897 ± 0.321	0.1086 ± 0.0048	1776 ± 82	68
3.1	e,osc,p	1016	1067	1.05	0.0022 ± 0.0005	0.0335	2.350 ± 0.991	0.1051 ± 0.0102	1715 ± 190	133
4.1	e,osc,p	346	560	1.62	0.0027 ± 0.0003	0.0426	3.916 ± 0.207	0.1156 ± 0.0054	1890 ± 86	78
5.1	e,osc,p	323	504	1.56	0.0007 ± 0.0001	0.0114	4.286 ± 0.254	0.1082 ± 0.0026	1769 ± 45	76
6.1	e,osc,p	432	803	1.86	0.0002 ± 0.0001	0.0026	3.528 ± 0.220	0.1102 ± 0.0011	1802 ± 19	89
7.1	e,osc,p	485	654	1.35	0.0003 ± 0.0001	0.0045	5.119 ± 0.397	0.1034 ± 0.0017	1685 ± 31	68
8.1	e,osc,p	803	1151	1.43	0.0011 ± 0.0001	0.0166	4.391 ± 0.305	0.1076 ± 0.0014	1759 ± 24	75
9.1	e,osc,p	369	597	1.62	0.0034 ± 0.0003	0.0526	4.884 ± 0.462	0.1000 ± 0.0086	1623 ± 169	74
10.1	e,osc,p	485	746	1.54	0.0001 ± 0.0000	0.0008	4.740 ± 0.225	0.1083 ± 0.0013	1770 ± 22	70

Labels	Morphology	U ppm	Th ppm	Th/U	204Pb/206Pb	f206	238U/206Pb corrected	207Pb/206Pb corrected	207Pb/206Pb date Ma (1σ)	conc.
425794 late granitoid, cut by 425793 (GPS 78°48.04'N 67°15.59'W- collected 1995)										
1.1	e,hd,p,fr	4223	439	0.10	0.01089 ± 0.00021	0.1701	8.534 ± 0.883	0.0890 ± 0.0039	1405 ± 87	51
2.1	m,hd,p,fr	10056	3372	0.34	0.00236 ± 0.00006	0.0369	9.099 ± 0.890	0.0772 ± 0.0010	1126 ± 26	60
Northern terrane										
312632 granitic gneiss - Victoria Fjord (map 81°31'N 44°45'W - collected 1984)										
1.1	osc,p	1470	429	0.29	0.00003 ± 0.00001	0.0003	1.549 ± 0.034	0.2831 ± 0.0004	3380 ± 2	95
1.2	osc,p	1002	355	0.35	0.00005 ± 0.00001	0.0006	1.627 ± 0.033	0.2813 ± 0.0008	3370 ± 5	92
2.1	osc,p	1037	45	0.04	0.00087 ± 0.00003	0.0105	2.670 ± 0.057	0.2472 ± 0.0012	3167 ± 8	65
3.1	hb,rex,p	3283	191	0.06	0.00001 ± 0.00000	0.0002	1.599 ± 0.044	0.2664 ± 0.0004	3285 ± 2	95
3.2	hd,rex,p	3471	200	0.06	0.00095 ± 0.00004	0.0114	9.011 ± 0.276	0.1174 ± 0.0007	1917 ± 11	35
3.3	hd,rex,p	7783	1204	0.15	0.00052 ± 0.00002	0.0063	12.408 ± 0.469	0.0778 ± 0.0007	1143 ± 18	44
4.1	osc,p	541	44	0.08	0.00021 ± 0.00002	0.0025	1.977 ± 0.056	0.2691 ± 0.0010	3301 ± 6	80
5.1	hb,rex,p	2802	157	0.06	0.00003 ± 0.00000	0.0003	1.649 ± 0.033	0.2622 ± 0.0003	3260 ± 2	94

analysis code; x.y = grain.site number. Those shown in **bold** used to calculate weighted mean ages.
grain habit; p=prism (aspect ratio >2), eq/p=stubby prism (aspect ratio<2), eq=equant, ov =oval, rp=rounded prism, fr=fragment, a
analysed site; e=end or edge, m=middle, r=overgrowth, c=core, c-inh=inherited core
CL imagery; osc=oscillatory finescale zoning, h=homogeneous, hd=dark in CL images
dates and f206=percentage of 206Pb that is common, based on measured 204Pb and
Cumming and Richards (1975) model Pb composition for likely age of rock

Table 2. Sm-Nd isotopic data from the Inglefield Mobile Belt.

Sample	Rock type	Zircon U/Pb age protolith (T, Ma)[a]	Zircon U/Pb age inheritance (Ma)	Sm	Nd	Sm/Nd	$^{147}Sm/^{144}Nd$[b]	$^{143}Nd/^{144}Nd$	+/-2σ	ε_{Nd} (0)	$^{143}Nd/^{144}Nd$ (T)	ε_{Nd} (T)[c]	T_{CHUR} (Ma)	T_{DM1}[d] (Ma)	T_{DM2}[e] (Ma)
Etah Group supracrustal rocks															
425748	*garnet-biotite schist (Sunrise Pynt S. Belt)*			2.980	14.37	0.2074	0.1253	0.511551	11	-21.2			2312	2573	2750
425727	*sillimanite-garnet paragneiss (central IMB)*			8.875	55.24	0.1606	0.0971	0.511479	6	-22.6			1769	2032	2181
Etah Group meta-igneous complex															
425536	*banded amphibolite*			2.428	11.19	0.2171	0.1312	0.511882	8	-14.7			1755	2135	2340
425542	*opx-qtz diorite, Hiawatha pluton*	1949		2.895	15.02	0.1927	0.1165	0.511711	6	-18.1	0.510217	2.00	1757	2078	2253
425571	*syenite, Wulff structure*	1920		2.349	9.854	0.2384	0.1441	0.512043	23	-11.6	0.510222	1.37	1720	2180	2422
425574	*syenite*			4.955	25.37	0.1953	0.1181	0.511713	8	-18.0			1788	2110	2287
425579	*opx diorite*			4.811	23.19	0.2074	0.1254	0.511816	8	-16.0			1752	2107	2299
425594	*opx diorite*			3.665	19.98	0.1834	0.1109	0.511627	7	-19.7			1790	2089	2254
425623	*granite, Hiawatha Gletscher*	1915		12.89	110.6	0.1166	0.0704	0.511079	8	-30.4	0.510191	0.63	1876	2080	2199
Late granitoids															
425530	*granite*			0.769	6.123	0.1256	0.0759	0.511127	32	-29.5			1901	2110	2233
425552	*foliated granite*			8.942	49.89	0.1793	0.1083	0.511547	17	-21.3			1876	2155	2315
425558	*porphyroblastic granite*			6.446	37.54	0.1717	0.1038	0.511502	14	-22.2			1858	2127	2281
425583	*orthogneiss (late granite), Minturn complex*	1752	c. 2650	3.828	20.31	0.1885	0.1139	0.511614	8	-20.0	0.510301	-1.37	1880	2174	2342
425793	*granite dyke*	1783		12.48	94.90	0.1315	0.0795	0.510512	7	-41.5	0.509580	-14.72	2748	2875	2981

[a] Age determined by U-Pb SHRIMP geochronology

[b] $^{147}Sm/^{144}Nd$ reproducible to ± 0.3%

[c] ε_{Nd} values are reported relative to CHUR, using $^{143}Nd/^{144}Nd = 0.512638$, $^{147}Sm/^{144}Nd = 0.1967$.

[d] T_{DM1} is calculated depleted mantle model (intercept) age using the equation of DePaolo (1981).

[e] T_{DM2} is calculated depleted mantle model (intercept) age using a linearly depleting mantle (Goldstein et al., 1984).